Vol. 65 • No. 12

December 2022

Microwave Journal

horizon house®

Founded in 1958

mwjournal.com

Picoprobe®

Picoprobe elevates probe cards to a higher level…

(…110 GHz to be exact.)

Since 1981, GGB Industries, Inc., has blazed the on-chip measurement trail with innovative designs, quality craftsmanship, and highly reliable products. Our line of custom microwave probe cards continues our tradition of manufacturing exceptional testing instruments.

Through unique modular design techniques, hundreds of low frequency probe needles and a variety of microwave probes with operating frequencies from DC to 40, 67, or even 110 GHz can be custom configured to your layout.

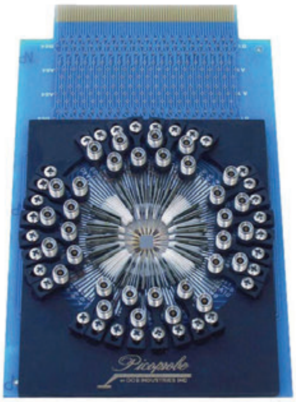

Our patented probe structures provide the precision and ruggedness you require for both production and characterization testing. And only Picoprobe® offers the lowest loss, best match, low inductance power supplies, and current sources on a single probe card.

Our proven probe card design technology allows full visibility with inking capability and ensures reliable contacts, even when probing non-planar structures.

Not only do you get all the attractive features mentioned, but you get personal, professional service, rapid response, and continuous product support--all at an affordable price so your project can be completed on time and within budget.

Typical Specs	10GHz	20GHz	40GHz
Insertion Loss	0.6 dB	0.8 dB	1.3 dB
Return Loss	22 dB	18 dB	15 dB

For technical assistance, custom product designs, or off-the-shelf delivery,call GGB Industries, Inc., at (239) 643-4400.

GGB INDUSTRIES, INC. • P.O. BOX 10958 • NAPLES, FL 34101

Telephone (239) 643-4400 • Fax (239) 643-4403 • E-mail email@ggb.com • www.picoprobe.com

EVERY BLOCK... COVERED!

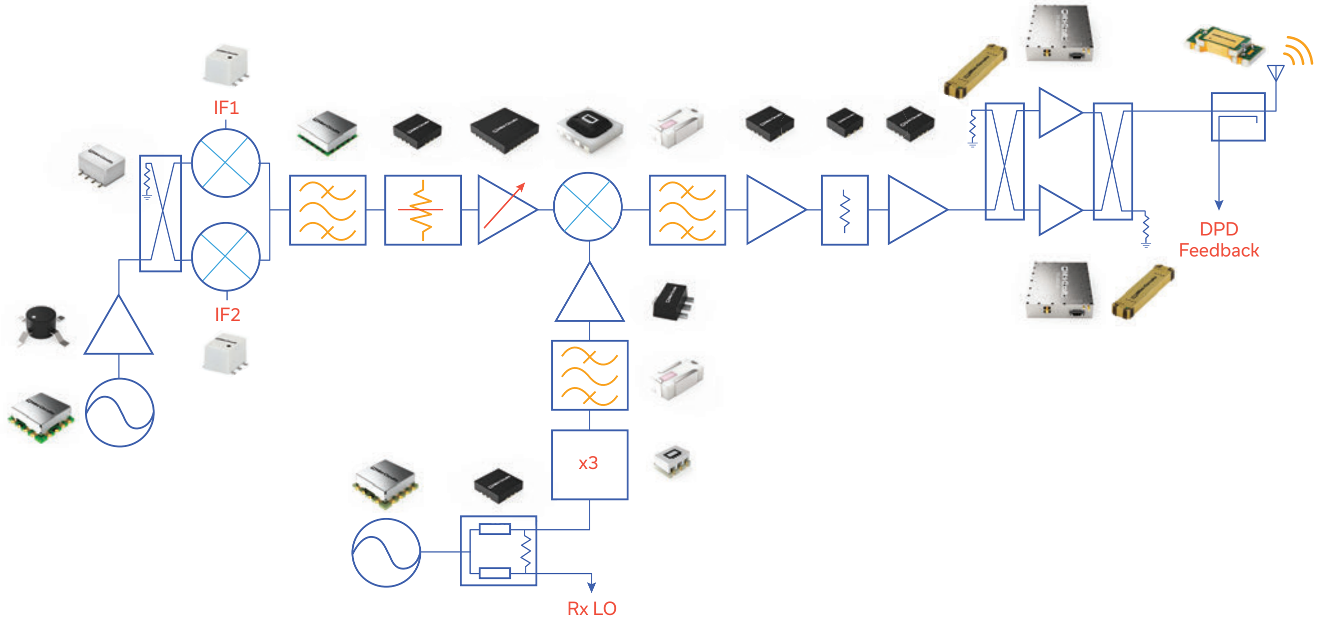

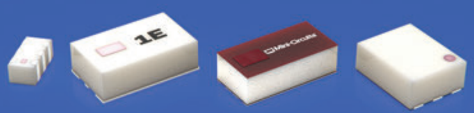

LTCC Passives

750+ Models

- **Couplers**: DC to 7.2 GHz
- **Filters:** Passbands to 40 GHz, Stopbands to 58 GHz
- **Power Splitters**: 600 MHz to 6.5 GHz
- **Transformers & Baluns**: 200 MHz to 18 GHz

MMICs

700+ Models in Die or SMT

- **Amplifiers**: DC to 50 GHz
- **Control Products**: DC to 45 GHz
- **Frequency Conversion**: RF & LO to 65 GHz
- **Passives**: DC to 50 GHz
- **Reflectionless Filters**: Passbands to 40 GHz

AND MORE

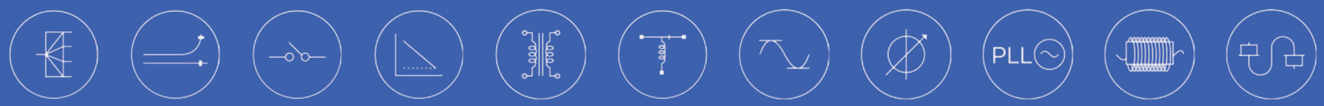

The Industry's Broadest Technology Portfolio From DC to mmWave

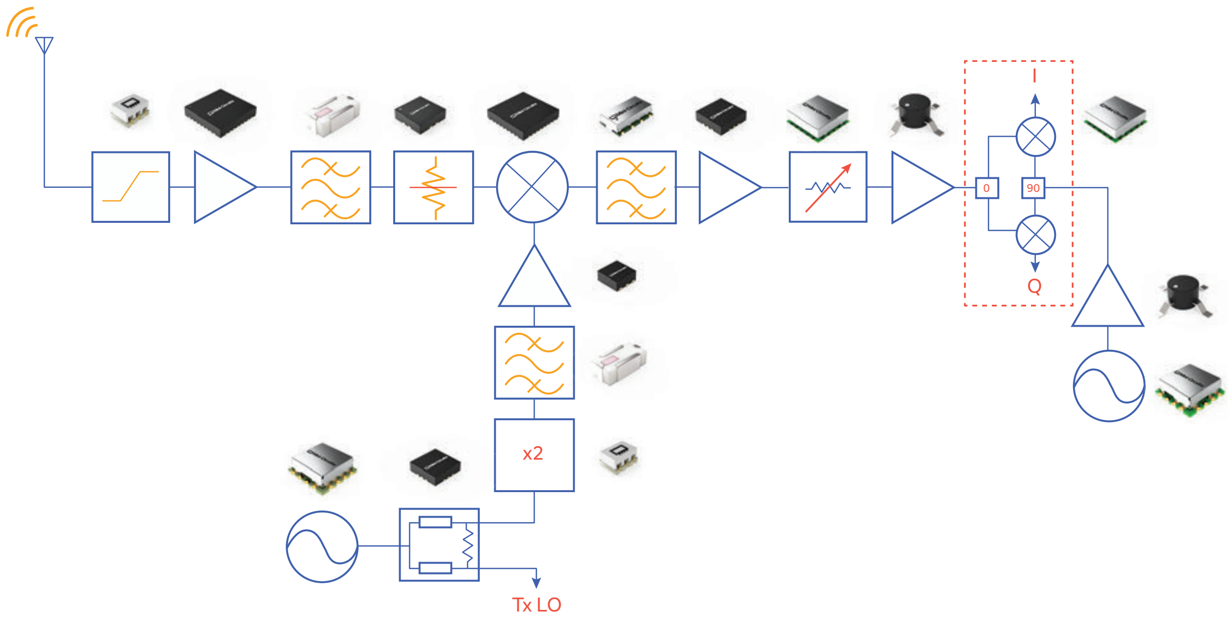

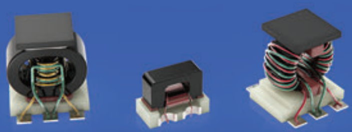

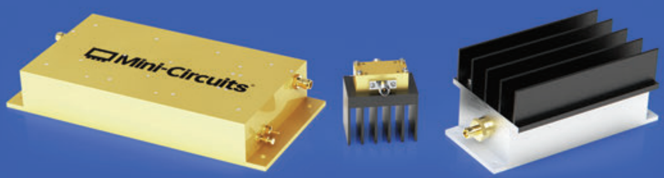

Magnetic Core & Wire

10k+ Models

- **Directional Couplers**: 1 MHz to 6 GHz
- **Power Splitters**: DC to 18 GHz
- **Transformers & Baluns**: 0.004 MHz to 11 GHz

Amplifier Modules

270+ Models

- **Power**: Up to 250W
- **Medium Power**: Up to 95 GHz
- **Low Noise**: Up to 85 GHz
- **Low Phase Noise**: -173 dBc/Hz @ 10kHz

Mini-Circuits®


apitech™
We help you navigate the complexities of wireless test
From guidance to gear, get there with APITech
For more information vist:
apitech.com/wireless-test

RF-LAMBDA
THE LEADER OF RF BROADBAND SOLUTIONS
BROADBAND SSPA / EMC BENCHTOP
SOLID STATE POWER AMPLIFIER
0.1-22GHZ
ULTRA BROADBAND SSPA
RFLUPA01M22GA
4W 0.1-22GHZ
RFLUPA0218GB
20W 1-19GHZ
300W 6-18GHZ SOLID STATE BROADBAND
400W 8-11GHZ
SOLID STATE BROADBAND
0.1-6GHZ VHZ,
UHF, L, S, C BAND
RFLUPA02G06GC
100W 2-6GHZ
RFLUPA0706GD
30W 0.7-6GHZ
MADE IN USA
6-18GHZ C, X, KU BAND
RFLUPA08G11GA
50W 8-11GHZ
RFLUPA0618GD
60W 6-18GHZ
RFLUPA06G12GB
25W 6-12GHZ
18-50GHZ K, KA, V BAND
RFLUPA18G47GC
2W 18-47GHZ
RFLUPA27G34GB
15W 27-34GHZ
RFLUPA47G53GA2
10W 47-53GHZ
RFLUPA27G34GB
30W 18-40GHZ
BENCHTOP RF MICROWAVE SYSTEM POWER AMPLIFIER
RAMP00G06GA- 30W 0.01-6GHZ
RAMP39G48GA- 4W 39-48GHZ
RAMP01G22GA- 8W 1-22GHZ
RAMP27G34GA- 8W 27-34GHZ
www.rflambda.com
sales@rflambda.com
1-888-976-8880
1-972-767-5998
San Diego, CA, US
Carrollton, TX, US
Ottawa, ONT, Canada
Frankfurt, Germany

Microwave Journal

CONTENTS

December 2022
Vol. 65 • No. 12
Government & Military Electronics
mwjournal.com

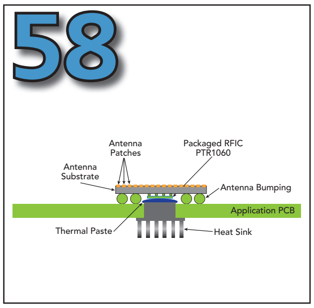

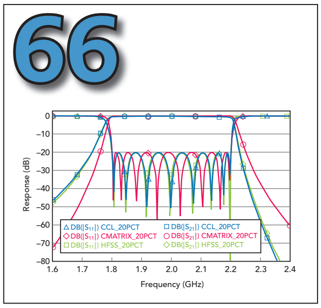

online spotlight

Look for this month's exclusive article online at mwjournal.com

Critical Role of the Conductance Parameter in the Channel Response of a Power Line Cable

Ashraf Sheria and Arnold S. de Beerb

Editor's Note

Cover Feature

Technical Features

Application Note

2022 Editorial Index

A complete listing of 2022 Microwave Journal articles, organized by subject and indexed alphabetically by author, can be found at mwjournal.com/edindex2022.

65 YEARS OF PUBLISHING EXCELLENCE

Microwave Journal CONTENTS

mwjournal.com

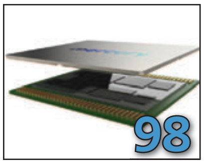

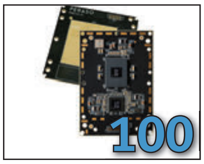

Product Features

Tech Briefs

Departments

Microwave Journal (USPS 396-250) (ISSN 0192-6225) is published monthly by Horizon House Publications Inc., 685 Canton St., Norwood, MA 02062. Periodicals postage paid at Norwood, MA 02062 and additional mailing offices.

POSTMASTER: Send address corrections to Microwave Journal, PO Box 1028, Lowell, MA 01853 or e-mail mwj@e-circ.net.com. Subscription information: (978) 671-0446. This journal is issued without charge upon written request to qualified persons working in the RF & microwave industry. Other subscriptions are: domestic, $120.00 per year, two-year subscriptions, $185.00; foreign, $200.00 per year, two-year subscriptions, $370.00; back issues (if available) and single copies, $10.00 domestic and $20.00 foreign. Claims for missing issues must be filed within 90 days of date of issue for complimentary replacement.

STAFF

Publisher: Carl Sheffres
Associate Publisher: Michael Hallman
Editorial Director: Patrick Hindle
Editor: Gary Lerude
Managing Editor: Jennifer DiMarco
Associate Technical Editor: Cliff Drubin
Editorial & Media Specialist: Kelley Roche
Associate Editor: Emma Lutjen
Multimedia Staff Editor: Barbara Walsh
Electronic Marketing Manager: Chris Stanfa
Senior Digital Content Specialist: Lauren Tully
Digital Content Specialist: Vincent Carrabino
Audience Development Manager: Carol Spach
Director of Production & Distribution: Edward Kiessling
Art Director: Janice Levenson
Graphic Designer: Ann Pierce

EUROPE
Office Manager: Nina Plesu

CORPORATE STAFF
CEO: William M. Bazzy
President: Ivar Bazzy
Vice President: Jared Bazzy

EXECUTIVE EDITORIAL OFFICE
685 Canton Street, Norwood, MA 02062
Tel: (781) 769-9750
FAX: (781) 769-5037
e-mail: mwj@mwjournal.com

EUROPEAN EDITORIAL OFFICE
16 Sussex Street, London SW1V 4RW, England
Tel: Editorial: +44 207 596 8730 Sales: +44 207 596 8740
FAX: +44 207 596 8749

SUBSCRIPTION SERVICES
Send subscription inquiries and address changes to:
Tel: (978) 671-0446
e-mail: mwj@e-circ.net

www.mwjournal.com

Printed in the USA

Microwave Journal ONLINE .COM

E-LEARNING CENTER

Insights into High Power Solid State Combining in L, S and C Band

Sponsored by: Empower RF Systems 1/25

Catch *Frequency Matters*, the industry update from *Microwave Journal*, microwavejournal.com/FrequencyMatters

WHITE PAPERS

NSI-MI AMETEK — Using a Higher-Order Basis Function based Method of Moments Analysis for Designing Compact Antenna Test Ranges

ar — Multi-Tone Testing Theory & Practice

cadence — In-Design Thermal Analysis for MMIC and RF PCB Power Applications

ROHDE & SCHWARZ Make ideas real — The Electric Drivetrain Evolution from Past to Future

Look for additional content from:

ROHDE & SCHWARZ Make ideas real

Wireless Telecom Group

Executive Interviews

Peter Waldow, co-founder and CEO of **IMST**, describes the company's wide product and market focus, including its work in EM simulation, radar, IoT radios and smart cities.

Bruce Lancaster, CEO of **Wilson Electronics**, talks about leadership, the market for the company's cellular and IoT products and its approach to improving 5G's mmWave coverage.

Join Us Online

Follow us
@Pathindle
@MWJGary
@MWJEditor

Join us at the RF and Microwave Community

Become a fan at facebook.com/microwavejournal

Visit us @ mwjournal.com

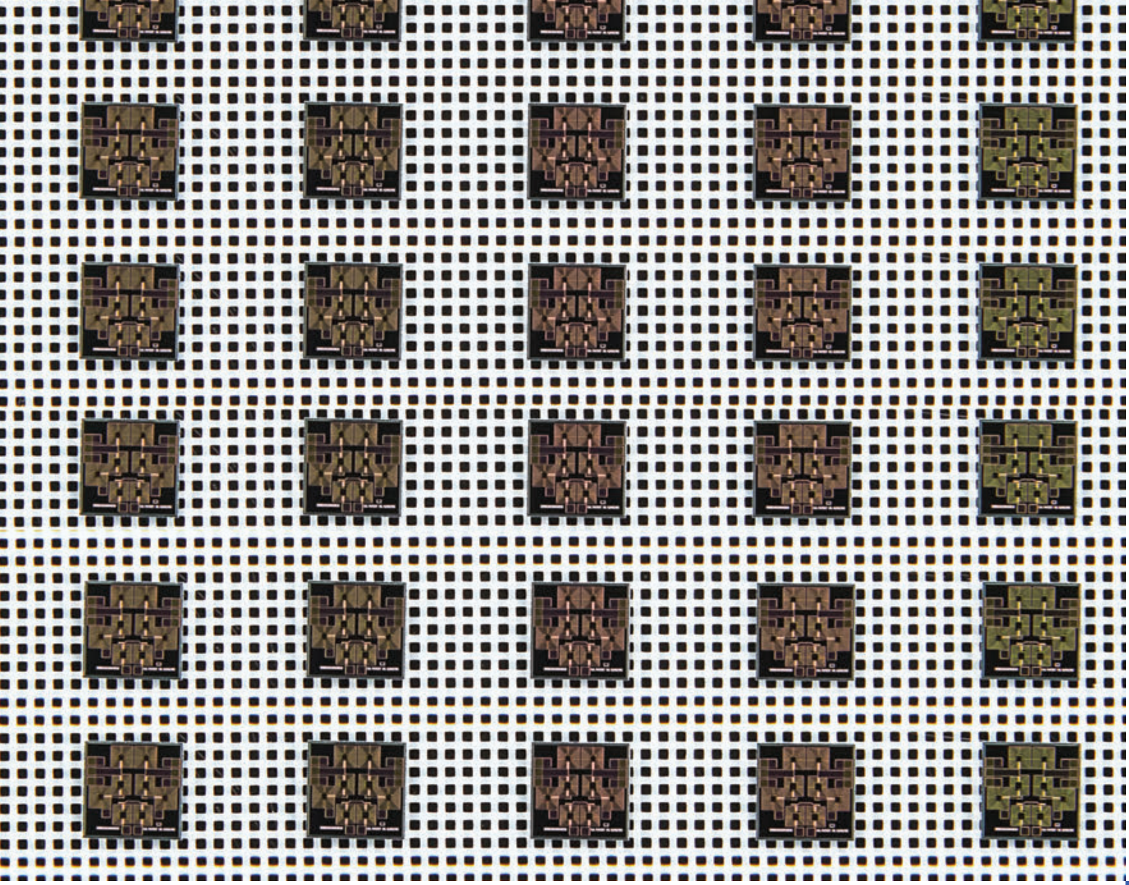

STAY CONNECTED TO COMING EVENTS

MARK YOUR CALENDAR

DECEMBER

12-15
IEEE MAPCON 2022
Bangalore, India
www.ieeemapcon.org

JANUARY

5-8
CES
Las Vegas, Nev. & Online
www.ces.tech

21-26
IPC APEX EXPO
San Diego, Calif.
www.ipcapexexpo.org

22-25
ARFTG
Las Vegas, Nev.
www.arftg.org

22-25
Radio Wireless Week
Las Vegas, Nev.
www.radiowirelessweek.org

31-2/2
DesignCon
Santa Clara, Calif.
www.designcon.com/en/home.html

FEBRUARY

13-14
TOP Conference
London, U.K.
https://topconference.com

27-3/2
MWC Barcelona
Barcelona, Spain
www.mwcbarcelona.com

MARCH

4-11
IEEE Aerospace Conference
Big Sky, Mont.
www.aeroconf.org

13-16
Satellite 2023
Washington, DC
www.satshow.com

20-23
GOMACTech
San Diego, Calif.
www.gomactech.net

28-30
EMV
Stuttgart, Germany
https://emv.mesago.com/stuttgart/en.html

Call for Papers Deadlines

1/15	RFIC 2023
3/19	EuMW 2023
5/1	AMTA 2023

Online Panel

1/18

Additive Manufacturing and 3D Printing Technologies for RF/Microwave Applications

FOR DETAILS VISIT MWJOURNAL.COM/EVENTS

A Privilege and an Honor

Gary Lerude, *Microwave Journal Editor*

I hate goodbyes. I'd rather quietly fade away, just as the alpenglow gradually gives way to the starlight. I wasn't given that option, so rather than leaving a blank page, I find myself writing a farewell. While I have loved my role with *Microwave Journal*, I'm yearning for more space in my life, a pause in the incessant cadence of work. I want time for other interests. After all, it has been 47 years since I started my career.

When I received my undergraduate degree, my goal was to start a career as an audio engineer, designing loudspeakers, microphones or power amplifiers. However, the economy was in recession and job interviews with consumer electronics companies didn't yield offers. The defense market was strong, though, and my first job led to RF/microwave and a fascinating and fulfilling career nurtured by this technology. I've had the privilege of working at four iconic firms: Texas Instruments, M/A-COM, TriQuint and *Microwave Journal*. I've contributed to semiconductors and subsystems for defense and commercial markets through many roles: design, program management, product management, marketing, business development and, finally, editor.

Not too many have the opportunity to contribute to a transformational change in technology. In my case, it was the development and commercialization of GaAs MMICs, beginning with their qualification and adoption in military systems—phased array radars have always been the Holy Grail—then "crossing the chasm" to cell phones, Wi-Fi and communications links. Along the way, I've learned about manufacturing, six sigma, business, acquisitions and leadership. I've had the privilege of seeing much of the world, developing a global perspective and friendships in many places.

My path would not have been possible without those who opened doors, mentored and challenged me. To them I am deeply grateful, as well as to my many colleagues: it has been an honor to meet and work with so many bright and dedicated individuals who make this industry what it is—vital to our lives and, economically, the healthiest it has ever been.

Throughout my career, my desk has always had a stack of *Microwave Journals*, each issue full of interesting and relevant articles to be read. While the IEEE journals track the advancement of technology, they miss the evolution of the markets and the companies that serve them. *Microwave Journal* is the closest we have to an archive of the industry, stretching back to 1958. Joining the editorial team was a serendipitous opportunity, a privilege to spend the past eight years contributing to this legacy, helping authors and companies tell their stories so they are preserved for coming generations.

Microwave Journal in all its forms—the magazine, Frequency Matters, webinars, podcasts, eBooks, conferences—is produced by an incredible team of smart, dedicated, fun, humble folks. It's an honor to work with each person on the team. In this era of trade magazines being squeezed for profits until they disappear, I want to acknowledge the Bazzy family for their long-term commitment and leadership, providing the opportunity for us to do what we love to do.

I leave you in good hands. Eric Higham is assuming my role and brings deep knowledge of the industry from his years at Strategy Analytics, covering advanced semiconductors and the defense market. He and I met when I joined M/A-COM, and I have always respected his technical insight and approachable manner. He will be a good fit at *Microwave Journal*.

Thank you for the privilege of showing up in your mailbox and on your screens. Keep doing the good work you're doing. ■


ANALOG DEVICES
AHEAD OF WHAT'S POSSIBLE™
Power for your world.
Simplify your designs by leveraging ADI's highly integrated power solutions.
Integrated Solutions
Local Design Support
Easy to Use Tools
Find your competitive advantage at
analog.com/power

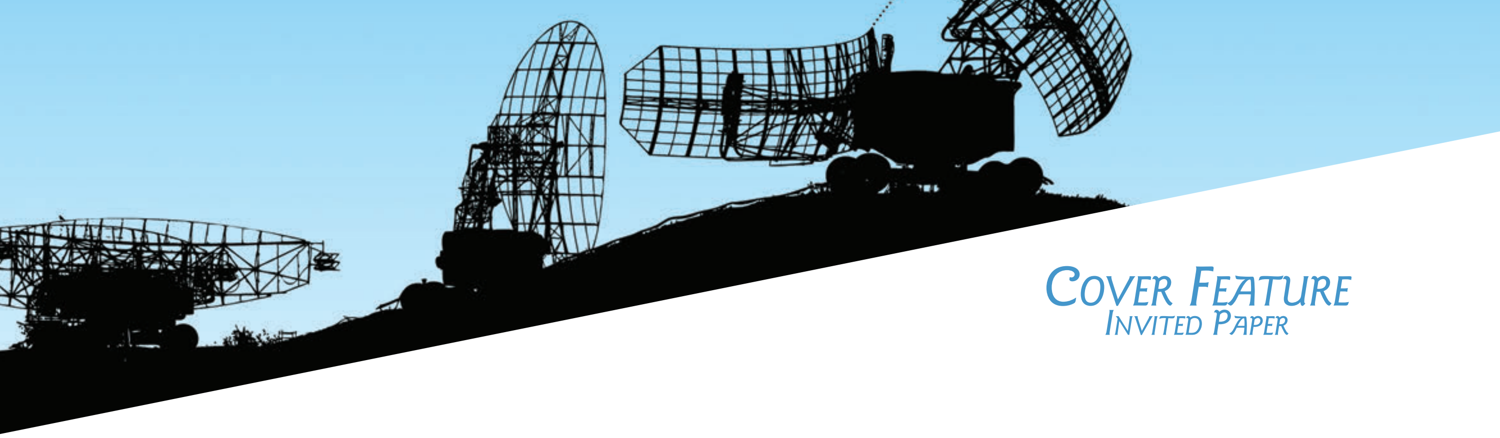

Software-Defined Direct RF Simultaneous Sampling Multi-Band/Service Transceiver

Nicolas Chantier and Julien Cochard
Teledyne e2v Semiconductors, France

Microwave RF transceiver system development (L- through Ka-Band) is rapidly changing as new hardware becomes available. Significant advances in analog-to-digital converters (ADCs), digital-to-analog converters (DACs), system on chip (SoC) and system in package (SiP) technologies, requiring varying degrees of corresponding software, create a daunting set of variables for today's engineers.[2] In addition, expanding market applications requiring simultaneous processing of multiple microwave RF bands to provide multiple services, such as ground penetrating radar, navigation and satcom, while adhering to SWaP-C constraints, requires next-generation planning and partnering. Newly developed L- through Ka-Band ADCs, DACs and mixed signal systems in packages (MiXiP SiPs), including SoC field-programmable gate arrays (FPGAs), solve these problems.[1] They are completely software controlled, enabling simultaneous sampling for multi-band and multi-service operations.

RF transceivers have traditionally employed a heterodyne architecture (see ***Figure 1***). A transmitted (Tx) or received (Rx) analog RF signal is derived from a DAC or digitized by an ADC through a mixer (up-converted for Tx or down-converted for Rx) with a local oscillator (LO). The derived Tx and Rx signals are "In-Direct" to the RF and are called the intermediate frequency (IF) signals.

IF signals (Tx or Rx) are the sum or difference of the RF and LO signals (RF = IF + LO or IF = RF - LO).

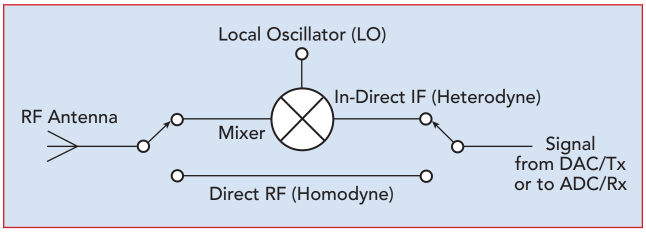

Fig. 1 **Conceptual difference between heterodyne and homodyne transceivers.**

The heterodyne architecture is generally designed for a single frequency band and single service. The advantages of the heterodyne architecture are low-cost, mature implementations, available narrowband components and hardware switchable reconfigurations. The disadvantages are that it is hardware constrained, single band (narrow), single service and limited to sequential sampling/operations.

Some microwave RF transceivers use a homodyne direct RF architecture (see Figure 1).[5] Direct RF eliminates the need for mixing (or up/down frequency conversion) and processes the Tx and Rx signals directly in the appropriate RF band required for the service operation. Effectively, direct RF looks like a wire between the antenna from the DAC/Tx or to the ADC/Rx.

The evolution from heterodyne

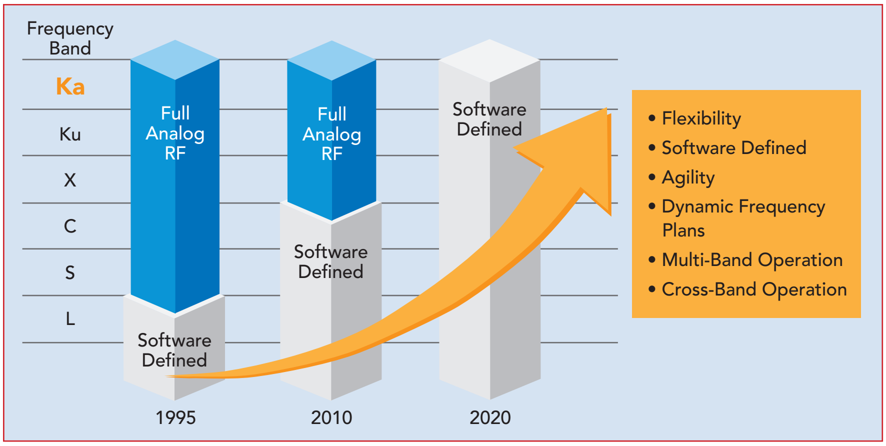

Fig. 2 Evolution to software defined radio from L- to Ka-Band.

to homodyne transceiver development enabled by advancements in both hardware and software, is shown in ***Figure 2***. Over this time, the greater the processing bandwidth of the hardware, along with software development, has incrementally reduced transceiver analog hardware to the point that the transceiver simply becomes a software-defined radio.

Teledyne e2v now offers a direct RF simultaneous sampling multi-band/service transceiver for conversion up to Ka-Band.[1] This single chain transceiver can convert L- through Ka-Band simultaneously (not sequentially) for multi-service operations. This direct RF conversion approach requires that the Tx/Rx module be as close to the antenna as possible, along with all the required circuitry for digital frequency conversion, beam steering, modulation and demodulation functions.

Optimal noise and frequency performance is realized without up-/down-conversion and insertion losses are reduced with no combiner/splitters required. For frequency planning, once the hardware implementation is set (e.g., data converters and filters), the only design variable in the system (other than software reconfigurations) is the sample clock frequency. A completely software-defined system allows for continuous dynamic software reconfigurations, ultimately using AI technology.

TRANSCEIVER APPLICATIONS AND IMPLEMENTATIONS

Microwave transceivers include both Tx and Rx functions within the same module using either heterodyne or homodyne architectures. Transceivers either operate in half-duplex or full-duplex modes. Half-duplex means that Tx and Rx functions must alternate in time, while full-duplex allows the system to transmit and receive data simultaneously.

Figure 3 shows various satellite applications operating in different RF bands.[3] Traditionally, transceivers were designed as separate systems per application per RF band. This resulted in one investment per single band per service (for Figure

Fig. 3 Individual transceiver development per service and band.

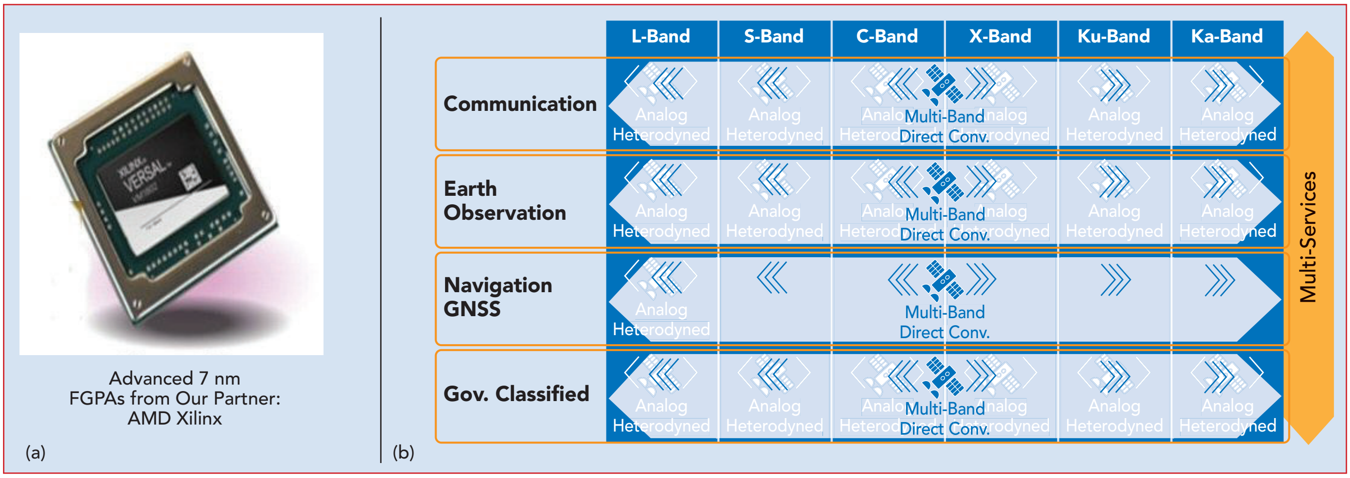

Fig. 4 Advanced FPGA devices (a) allow unprecedented signal processing capabilities, enabling waveform management of multiple services simultaneously from one system/one investment (b).

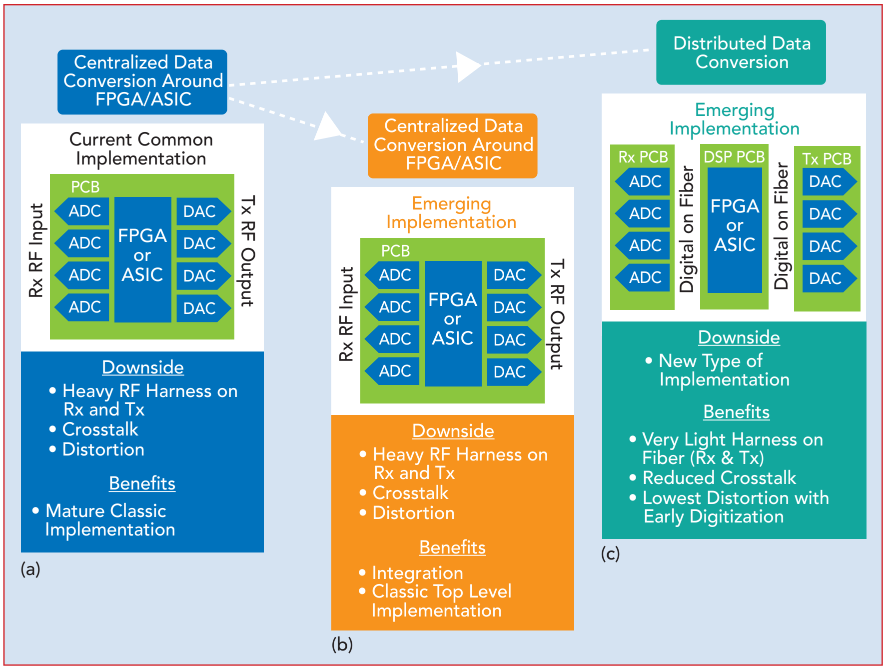

Fig. 5 Transceiver Partitioning: MCM (a), SoC (b), SiPs + SoC (c).

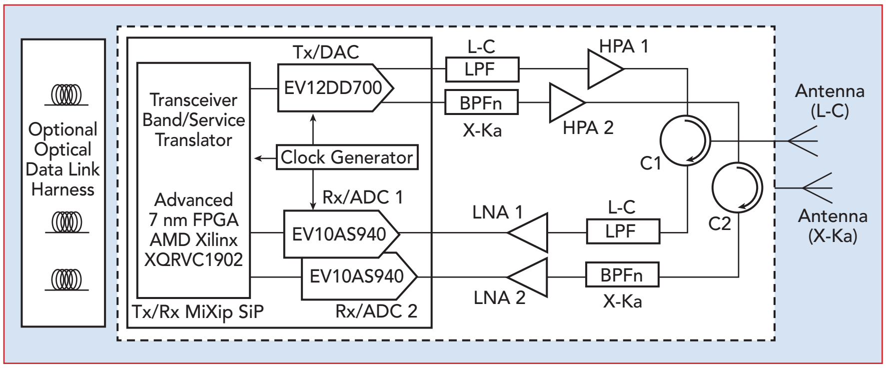

Fig. 6 Software-defined direct RF simultaneous sampling transceiver.

3, this could represent 19 individual investments and developments/deployments). To maximize functionality (multi-band and multi-service) and minimize development costs, switchable transceiver channels can sequentially switch analog and digital channel functionality with delay times in-between.

Today's direct RF transceiver developments are efficiently designed for multi-band performance per service (see ***Figure 4***). Unfortunately, multi-band operation may be limited, such as L- and C- or X- and Ku-Bands, depending on the ADCs and DACs that are available. Whether multi-service operation can be fully realized generally depends on digital modulator/demodulator processing and computation speeds. Digital data routing can also be a significant impediment.

Enabling waveform management of multiple services simultaneously as shown in Figure 4 is accomplished with this new direct RF simultaneous sampling multi-band/service transceiver. It simultaneously (not sequentially) processes multiple bands (L- through Ka-Band) as well as multiple services. This is accomplished using Teledyne e2v's Ka-Band capable ADCs and DACs in conjunction with AMD Xilinx's advanced 7 nm FPGA XQRVC1902 digital engine packaged together using MiXiP SiP technology.

A multi-band/service microwave transceiver, besides requiring ultra-high performance components, requires cutting edge packaging and interconnect technology to partition the system in ways that minimize analog and digital interference.[2] ***Figure 5*** shows several transceiver


CAES
PIONEERING ADVANCED ELECTRONICS

partitioning techniques: 1) common single multi-chip module with centralized data around the FPGA that minimizes digital routing, 2) SoC and 3) SiPs interconnected with optical digital fiber that place the ADCs and DACs near the antenna while isolating the digital functions from the analog.

Technique 1 has been used for decades but requires complex routing of analog signals for both the ADCs and DACs. Of course, as operational system frequencies increase, analog signal routing becomes problematic.

Technique 2 uses an SoC, which requires monolithic process technology and device geometries that must accomplish both the microwave analog and digital functions necessary for the transceiver. This is very difficult, expensive and requires extreme development timeframes.

Technique 3 combines the best of both techniques 1 and 2 but requires optical data link drive capabilities and is not offered by Teledyne e2v. It lends itself particularly to the use of separate transmitters and receivers connected to separate antennas.

DIRECT RF SIMULTANEOUS SAMPLING MULTI-BAND/ SERVICE TRANSCEIVER ARCHITECTURE

Figure 6 is the block diagram of a software-defined direct RF simultaneous sampling transceiver in a single, contained, transceiver antenna module (TAM) connected directly to the antennas for L- through Ka-Band service/operations. At the core of the TAM is the Tx/Rx MiXiP SiP which houses Teledyne e2v's EV12DD700 (DAC), two EV10AS940 (ADCs) and AMD Xilinx's XQRVC1902 7 nm FPGA digital engine. The TAM also includes auxiliary components such as lowpass filters (LPFs), bandpass filters/multi-band (n) pass filters (BPFns), low noise amplifiers (LNAs), high-power amplifiers (HPAs) and circulators.[1,2,5]

Packaging and partitioning of the TAM depends on the required service frequency bands, power transmission levels, physical dimensions and thermal requirements of each auxiliary component. For example, it may be optimal to have the MiXiP SiP, LNAs, LPFs and BPFns on a single PCB directly connected to the HPAs and circulators, which would in-turn connect to the antennas.

The advantages of a TAM that uses the L- through Ka-Band operational MiXiP SiP core is that the system is no longer hardware constrained. With the DAC, ADCs and FPGA MiXiP SiP's ability to operate up to Ka-Band and with the system contained within a single SiP package, developers need only select from a vast array of auxiliary components to meet system performance requirements.

Once the auxiliary components are selected, the TAM becomes completely software-defined (dynamically software reconfigurable) with simultaneous sampling, handovers and seamless connectivity. Once the TAM hardware implementation is set, the only design vari-

RF-LAMBDA

MADE IN USA

THE LEADER OF RF BROADBAND SOLUTIONS

EMC Broadband RF Power Amplifier

High Power Solid State

HUNDREDS IN STOCK

FAST SHIPPING

FREQUENCY UP TO 90GHZ

POWER UP TO 2KW CW

REMC06G18GG

6-18GHZ 300W

- AUTOMATIC BUILT IN SELF CALIBRATION AND BIAS ADJUSTMENT.
- OVER TEMPERATURE, CURRENT, INPUT POWER PROTECTION.
- VSWR MEASUREMENT AND OPEN CIRCUIT PROTECTION.
- USER FRIENDLY CONTROL INTERFACE.
- REMOTE ETHERNET CONTROL AND FIRMWARE UPDATE.
- HIGH POWER EFFICIENCY AND LIGHTWEIGHT.

RAMP42G47GA 42-47GHZ 8W

RAMP18G40GB-U 18-40G 20W

RAMP05M80GC 0.5-80GHZ

REMC02G06GE 2-6GHZ 500W

REMC08G11GE 8-11GHZ 400W

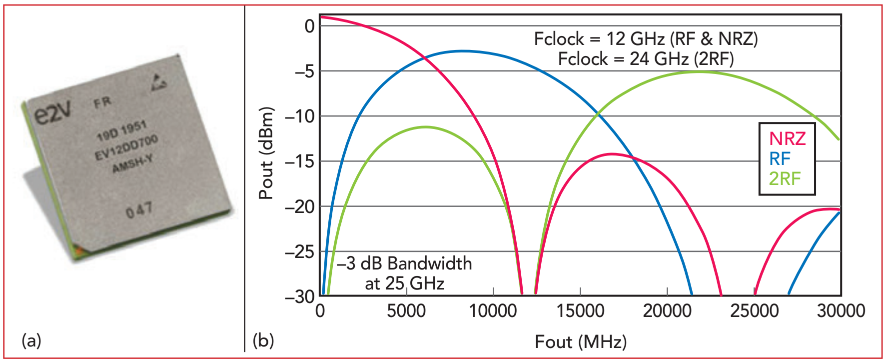

Fig. 7 EV12DD700 (a) and amplitude versus output frequency (b).

able in the system (besides software reconfigurations) is the sample clock frequency. The simultaneous sampling multi-band and multi-service operational capabilities of the TAM provide users with greater system-level resilience, independence of local/terrestrial/space EM infrastructures and automatic switching, which also enables other functions such as system monitoring, encryption operations and antenna blockage avoidance.[3]

Transmitter DAC

The EV12DD700 is a Ka-Band capable, radiation-tolerant, dual current-steering, 12-bit DAC with conversion rates up to 12 GSps. It can synthesize signals at frequencies over 21 GHz without up-conversion (see ***Figure 7***). It embeds digital features like interpolation, digital up-conversion, direct digital synthesis, chirp, beamforming, beam hopping and ultra-fast frequency hopping.[1,2,8]

The sinc(x) = sin(x)/x DAC output response can be compensated through the anti-sinc feature (A-SINC). In addition to the classical non-return-to-zero output mode (NRZ), the DAC cores have an embedded RF mode and a 2RF mode requiring a clock at twice the speed of other modes. These output modes enable the DAC to directly synthetize frequencies up to 21+ GHz without an external up-converter for operation up to and including Ka-Band.

Figure 8 shows the spectral output of the device when simultaneously transmitting L- and C-Bands (DAC Channel A (NRZ mode)) and X- and Ku-Bands (DAC Channel B (RF mode)) output signals.

Receiver ADC

The EV10AS940 is a 10-bit Ka-Band capable single channel ADC enabling sample rates up to 12.8 GSps. It also features digital down-conversion (DDC) and frequency hopping (FH) capabilities with multiple digital channels by integration of multiple numerically controlled oscillators. Other extensive digital features are included as well (see ***Figure 9***).

Its high analog input bandwidth (35 GHz) makes it the best choice

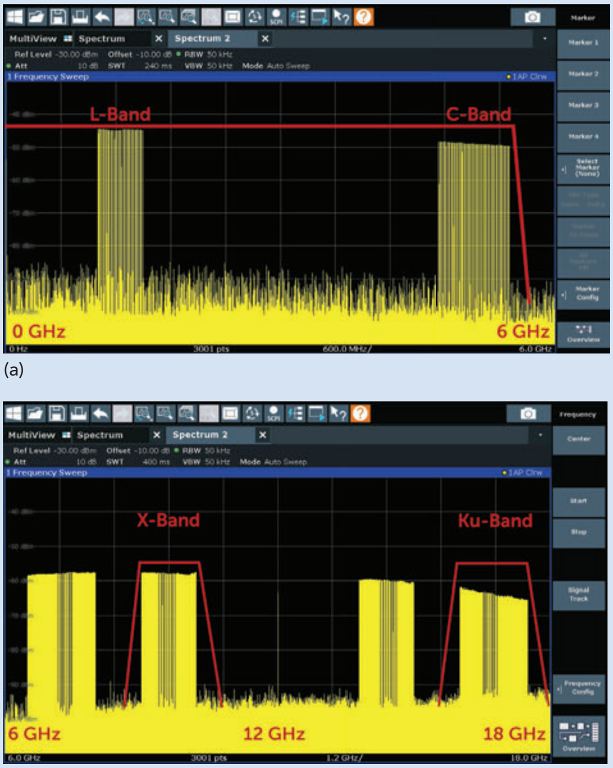

(a)
(b)

Fig. 8 **EV12DD700 simultaneous output: L- and C-Bands (a), X- and Ku-Bands (b).**

for direct RF Ka-Band architectures, eliminating any requirements to integrate dedicated mixers. Power consumption is as low as 2.5 W. It also features 11 ESIstream serial links that operate synchronously with the sampling clock to achieve deterministic data transfer.

- Direct Conversion to Ka-Band 35 GHz Analog Input Bandwidth (–3 dB)
- Up to 12.8 GSPS Data Rate
- Power Consumption: 2.5 W
  Ultra-Low Power Consumption per GSPS: 0.2 W/GSPS
- ENOB @ Fin = 25 GHz: 6.8 Bits
- Space, Military, Industrial Grade

Part: EV10A940
Nb of Channels: 1
Fs Max: 12.8 GSPS
Direct Conversion: Up to Ka-Band
Qual Grade: Commercial, Industrial, Military, Space

Extensive Digital Features
DDC from 2 to 1024
X4 NCO Allow Multi-Channel Management
Fast Frequency Hopping
Beamforming/Digital Delay
Automatic Background Calibration
Easy Multi-Chip Synchronization

Fig. 9 **EV10AS940 performance and features.**

DDC functionality has multiple options for decimation rates with up to four independent NCOs to support FH in multi-band operation. Coherent FH is possible due to multiple phase accumulators on each NCO and deterministic dedicated hopping trigger I/Os. Digital integer and fractional delays enable beamforming for use in phased array applications.

Other features include back-

ground and temperature calibration, temperature monitoring, DDC with decimation ratios from 2 to 1024, 4 DDC channels, dedicated FH I/Os, deterministic FH with return to zero, continuous and coherent modes, ESIstream 62/64b, high speed serial link (HSSL) reach selection and HSSL impedance control (2 × 50 Ω ± 20 percent).

Table 1 shows spurious free dynamic range (SFDR) and ***Table 2*** shows noise power ratio (NPR), which are helpful in assessing the ADC's multi-band/multi-tone performance capabilities.

Tx/Rx MiXiP SiP

Figure 10 shows the Tx/Rx MiXiP SiP core of the TAM which houses the EV12DD700, 2 EV10AS940s and the XQRVC1902. The complete MiXiP SiP transceiver has a compact form factor outline of 63 × 50 mm with a SiP ball matrix of 52 × 47 mm. The SiP (substrate patent pending) is pre-built using rad-tolerant DAC and ADCs with known reliability.

The ADCs also have single-ended inputs which are extremely helpful when selecting LNA drivers and eliminating the need for any transformer/balun requirements. Of course, the MiXiP positions the XQRVC1902 are next to the DAC and ADCs, thereby minimizing digital routing and reducing interference.

The AMD Xilinx VC1902 (7 nm) is a Versal-based AI core and adapt compute acceleration platform (ACAP) AI inference engine. Versal AI cores offer

TABLE 1

DYNAMIC PERFORMANCE

SFDR (Single Tone)		
f_{in} (GHz)	dBFS	SFDR (dBc)
1.1	-1	40
	-3	45
	-6	50
6.7	-1	40
	-3	45
	-6	49
15.6	-1	40
	-3	45
	-6	50
28.2	-1	43
	-3	47
	-6	50
34.5	-1	—
	-3	—
	-6	41
40.5	-1	—
	-3	—
	-6	32

TABLE 2

NPR @ -14 DB LOADING FACTOR
(with 5.1 GHz pattern width, 50 MHz notch located at sampling frequency/4)

Parameter	Typical (dB)
1st Nyquist	35.5
2nd Nyquist	35.0
3rd Nyquist	35.0
4th Nyquist	34.5
5th Nyquist	34.0
6th Nyquist	33.5
7th Nyquist	33.0

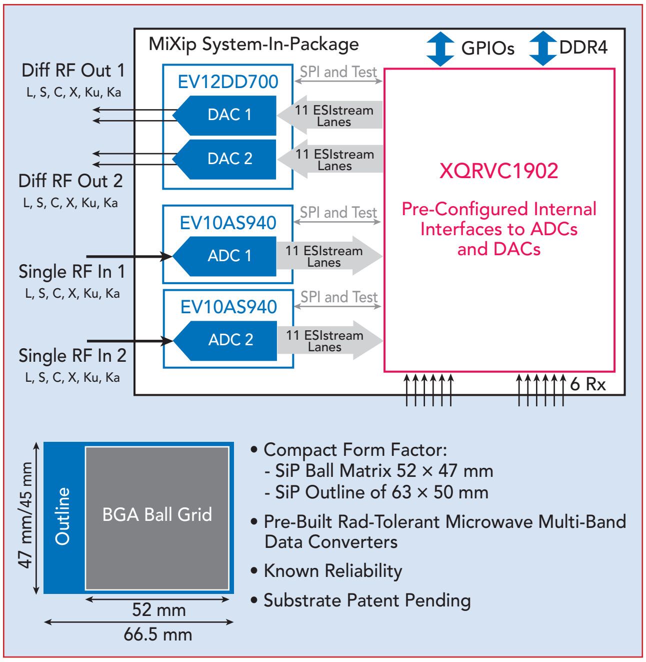

Fig. 10 **Tx/Rx MiXiP SiP core for a TAM design.**

breakthrough AI inference that deliver over 100x greater performance than server-class CPUs.

The Versal ACAP is a comprehensive SoC that combines CPUs, DSPs, I/O and RAM control along with programmable hardware logic. The XQRVC1902 enables the Tx/Rx MiXiP SiP to have dynamic frequency planning and to be software controllable, flexible, multiband, multi-service and able to crossband (receive multiple bands while simultaneously transmitting other bands).

TAM Auxiliary Components

To fully implement a software-defined direct RF simultaneous sampling multi-band/service transceiver operating from L- through Ka-Band, each system component is a key enabler. Besides using the Ka-Band capable Tx/Rx MiXiP, every other system component must be evaluated and understood from a simultaneous sampling multi-band performance perspective as well.[6,7]

For example, six simultaneous Tx/Rx RF bands/tones will be processed by the antennas, HPAs, LNAs, filters and circulators. Traditionally, these components are evaluated by varying single tones and/or two-tone tests. What is required now, however, is a multi-band performance evaluation mindset for each component.

This is where NPR testing might prove useful. NPR testing is typically thought of in terms of the "quietness" of a specific band within a multi-band system. Noise and intermodulation distortion products of other bands will fall into a specific band. Therefore, NPR testing may prove helpful in assessing auxiliary components' multi-band/multi-tone performance capabilities. Some considerations for selecting TAM auxiliary components are:

Antennas and Operating Frequencies/Polarizations

If all Tx and Rx signals are in same plane, use linear polarized antennas; if not, use circular polarization.

www.islinc.com

THE FUTURE OF
ADVANCED VIRTUAL RF FLIGHT TEST
IN CONTESTED/CONGESTED ENVIRONMENTS

The future RF environment for many advanced RF applications is both congested and possibly contested. Emulating this environment in field tests can be very costly and, in some cases, not feasible. ISL's RF Digital Engineering family of tools (RFView®) can greatly facilitate the entire life-cycle of advanced RF systems from development through sustainment for radar, electronic warfare (EW), ELINT, and other advanced RF applications. With ISL's RFView® hardware-in-the-loop (HWIL) solution, for the first time, actual flight hardware can be integrated into the high-fidelity mod&sim environment via RF analog or digital interface.

www.islinc.com/rfview

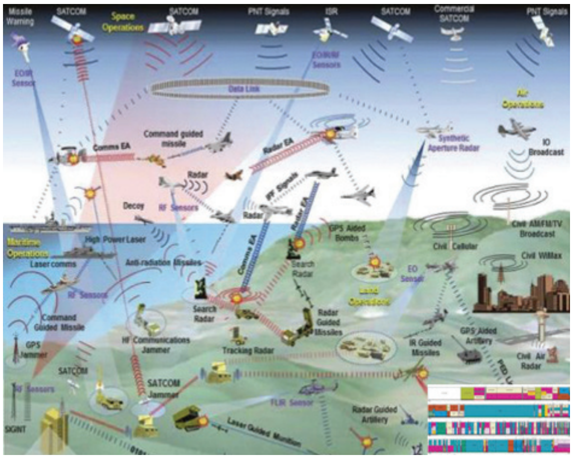

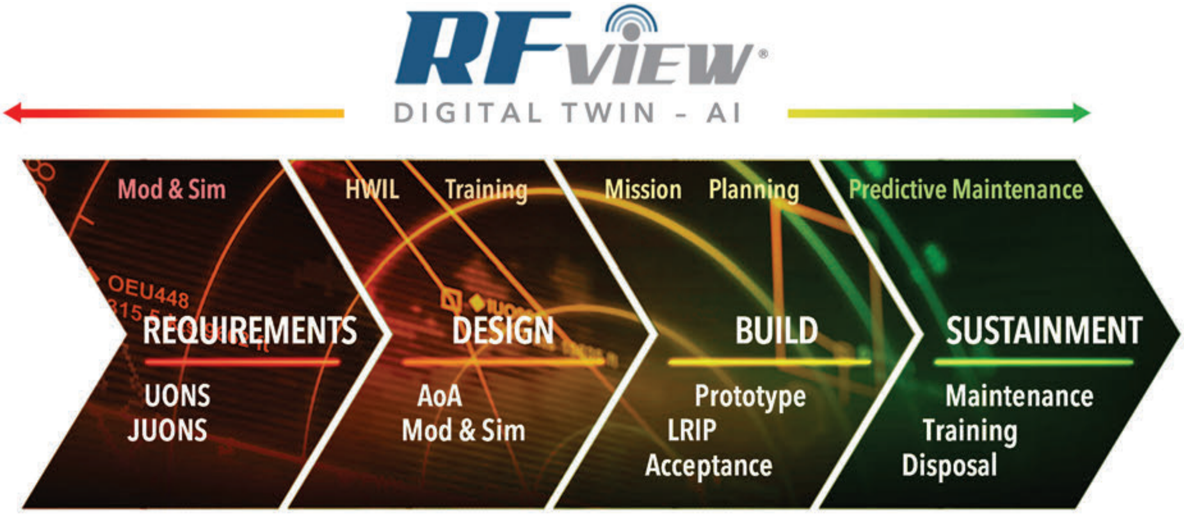

RFView®'s family of digital engineering tools support the entire product lifecycle from requirements and analysis-of-alternatives (AoAs), through design/protypting, test & evaluation (T&E), training, mission planning and sustainment. RFView® also provides a state-of-the art synthetic training environment for advanced AI machine learning (AI/ML) applications.

RFview® MODELING & SIM | RFview® HWIL | RFview® TRAINING | RFview® AI

RFVIEW® PHYSICS-BASED MOD&SIM ⟶ RFVIEW® HWIL (RTEMES) = AFRL SBIR SUCCESS STORY

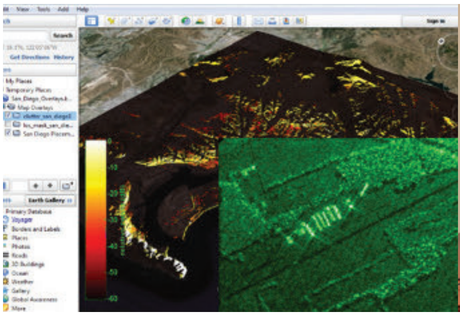

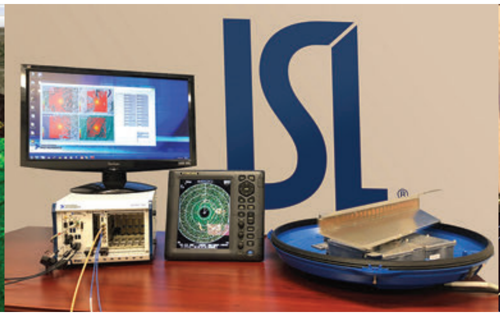

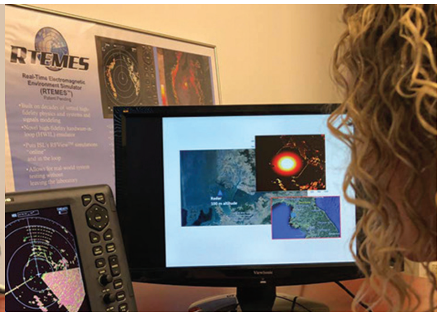

Wideband (circular polarized) antennas are generally provided by defense/satcom suppliers and a few commercial suppliers.

Wideband antenna design requires tradeoffs between antenna gain, antenna size, multi-beam capability, beamforming/shaping and steerability. Note that Ka-Band bandwidths are 4× larger than lower bands and therefore use multiple focused spot beams for frequency reuse operations that allow for Tx/Rx of different signals simultaneously at the same frequency.[4]

Ka-Band is susceptible to adverse weather conditions and therefore requires alternate/additional bands for seamless operation. It also has a greater number of orbital slots and capability for high capacity/density with smaller steerable beams. Ka-Band is resilient, using high data rates without degradation on smaller terminals and employs smaller antenna sizes than other bands (approximately ¼ size).

HPA

The HPA converts low-power RF signals (from the DAC) into high-power signals that drive the transmit antenna. Required specifications include gain, power output, output drive configuration (e.g., Class A, AB), bandwidth, efficiency, linearity (low signal compression at rated output), input/output impedance matching and heat dissipation. Each HPA component must be evaluated and understood from a multi-band simultaneous sampling performance perspective (as previously noted).

LNA

The LNA converts and amplifies very low-power RF signals from the antenna without significantly degrading signal to noise ratio and drives the receiver ADC. Required specifications include gain, noise figure, bandwidth, linearity, gain flatness, stability, input/output impedance matching and maximum RF input. An RF LNA must be low noise, high gain and have a sufficiently large intermodulation compression point (IP3 and P1db). An RF LNA must be protected by a power limiter to recover from large input signal transients that can occur during duplex switching (from Tx to Rx transitions).

Circulators/Switches (Duplexers)

RF duplexers enable bidirectional signal transmission through a single path (isolating the receiver from the transmitter and permitting them to share the same antenna). RF circulators enable full-duplex transceiver operations (transmitting and receiving at the same time with a single shared antenna over various frequencies). Ports are connected through waveguide transmission lines as well as microstrip line or coaxial cables. Specifications include frequency range, insertion loss, return loss, isolation, rotation and maximum power handling.

Waveguides/Filters

Waveguides are hollow metal pipes used as transmission lines connecting the transmitter and receiver to the antenna and the ge-


RELIABLE SOLUTIONS
FOR TOP PRIORITY
MISSIONS
Low Current
Fuses
Active
Antennas
EC646
Hi-Rel Ceramic
Capacitors
KYOCERA
AVX
WWW.KYOCERA-AVX.COM

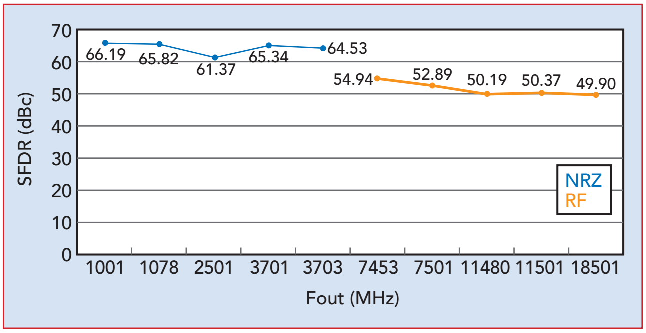

Fig. 11 EV12DD700 SFDR versus frequency.

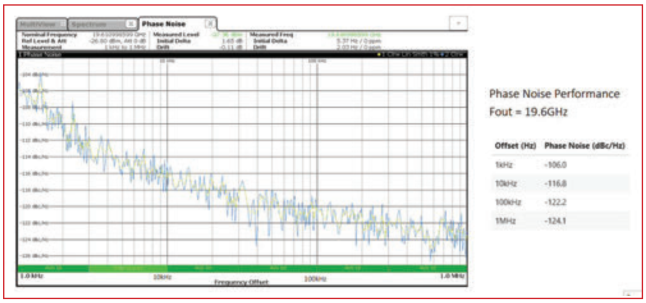

Fig. 12 EV12DD700 phase noise.

ometry of the waveguide structure can also serve as a filter to determine which frequencies are passed and which are rejected.

Clock Generator

The clock generator is an electronic oscillator that produces clock signals for use in synchronizing system-level operations. The clock generator must be programmable and provide enough drive for multiple copies to be distributed throughout the system. Specifications include frequency range, programmability, power drive, phase noise and jitter.

Optical Digital Harness

An optical optical digital harness may also be useful. It electrically isolates the system interconnections and enables further antenna digitization and weight reduction.

MEASURED PERFORMANCE

Figures 11 and ***12*** show SFDR and phase noise performance of the EV12DD700 DAC.

Figures 13 and ***14*** show SFDR and uncalibrated/calibrated performance of the EV10AS940 ADC.

CONCLUSION

Microwave RF transceiver developers face design challenges for simultaneous sampling, multi-band and multi-service systems while adhering to SWaP-C constraints. In addition, the continuous release of next-generation ADCs, DACs and FPGAs impact hardware development plans driving frequent redesign.

Now, however, Tx and Rx data conversion components can achieve L- through Ka-Band capabilities and advanced SiP assembly technologies place the FPGA within the same package. These advances enable Teledyne e2v's Tx/Rx MiXiP SiP design for microwave RF transceiver systems with software-de-

Nxbeam

Ka-Band Power

27 TO 31 GHz

Maximized performance for linear power applications

GaN MMIC's to 40W

Nxbeam's suite of Ka-band PA MMICs offers customers an unparalleled combination of power, gain, and efficiency with proven reliability.

PRODUCTS:
NPA2001-DE
NPA2002-DE
NPA2003-DE
NPA2030-DE

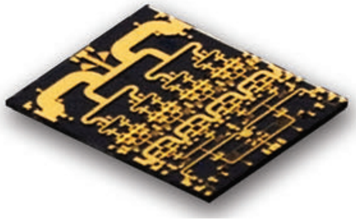

Packaged MMICs to 35W

Nxbeam offers its Ka-band MMICs in leaded flange packages for easier system integration

PRODUCTS:
NPA2001-FL
NPA2002-FL
NPA2003-FL
NPA2030-FL

Module Products to 60W

For higher levels of power and integration, Nxbeam offers modules that combine multiple Nxbeam MMICs to achieve higher performance in an easy-to-use form factor. Custom designs available

PRODUCTS:
NPM2001-KW
NPM2002-KW
NPM2003-KW

fined flexibility and multi-band/multi-service capability. Teledyne e2v's advanced MixSiP SiP design gives TAM designers the highest performance (up to Ka-Band) and value through a software-defined direct RF simultaneous sampling multi-band/multi-service transceiver. ■

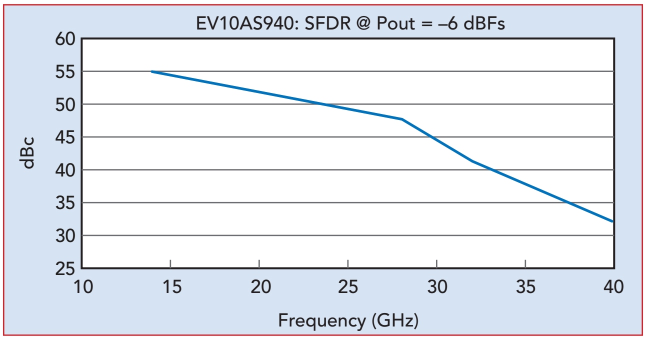

Fig. 13 EV10AS940 SFDR versus frequency.

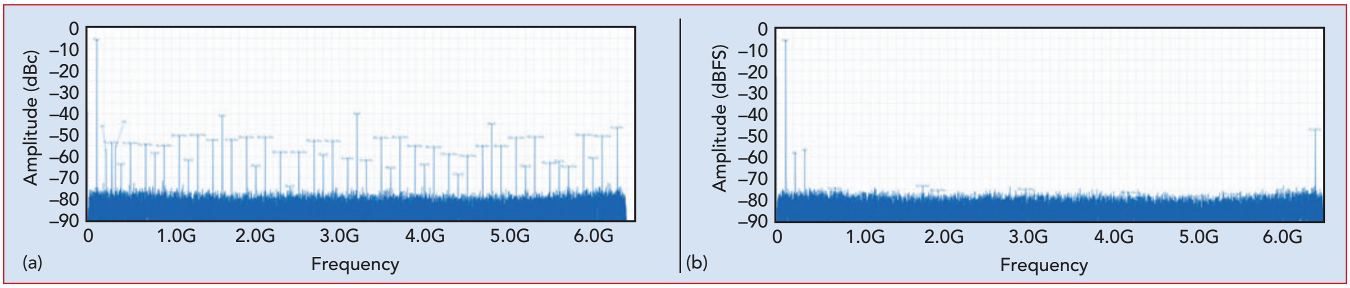

Fig. 14 EV10AS940 frequency performance uncalibrated (a) versus calibrated (b).

References

1. S. Lischi, R. Massini, R. Pilard, D. Stagliano and N. Chantier, "Feasibility Study of a Fully-Digital Multi-Band SAR System operating at L, C, X and Ku Bands," *7th Workshop on RF and Microwave Systems, Instruments & Sub-systems + 5th Ka-band Workshop*, May 2022.
2. F. Deviere, N. Seller and J. Rohou, "Making History: Advanced System in a Package Technologies Enable Direct RF Conversion," White Paper, *Microwave Journal*, Vol. 64, No. 1, January 2021.
3. B. Dunbar and S. Caldwell, "9.0 Communications," *National Aeronautics and Space Administration*, March 2022.
4. R. Cohen-Hirsch, "Why Ka-Band Best Supports the Modern Miliary Mission," *MilsatMagazine*, September 2015.
5. T. O'Farrell, R. Singh, Q. Bai, K. L. Ford, R. Langley, M. Beach, E. Arabi, C. Gamlath and K. A. Morris, "Tunable, Concurrent Multi-band, Single Chain Radio Architecture for Low Energy 5G-Rans," *IEEE 85th Vehicular Technology Conference (VTC Spring)*, June 2017.
6. S. Amin, P. Handel and D. Ronnow, "Characterization and Modeling of RF Amplifiers with Multiple Input Signals," *Conference: Swedish Microwave Days*, March 2016.
7. X. Yang, S. Li and F. Li, "Fourth-Order Nonlinear Distortion to the Power Spectrum of RF Amplifiers," The Journal of Engineering: *The Institute of Engineering and Technology*, Vol. 2022, No. 1, January 2022, pp. 53–63.
8. A. Patyuchenko, M. Younis, S. Huber, F. Bordoni and G. Krieger, "Design Aspects and Performance Estimation of the Reflector Based Digital Beam-Forming SAR System," *Conference: International Radar Symposium (IRS)*, April 2009.

MI-WAVE®

Millimeter Wave Products Inc.

Millimeter Wave
Products & Solutions

Millimeter Wave Products, Inc. is a global leader of millimeter wave and microwave technology, components, and assemblies. Our capabilities range from custom designed systems to large volume production within the 7-325 GHz spectrum.

Our products are the foundation of many of the devices and applications that are changing and enhancing everyday lives around the world.

We work with a wide variety of clients across many industries globally providing everything from standard products to research, design & building custom designed assemblies.

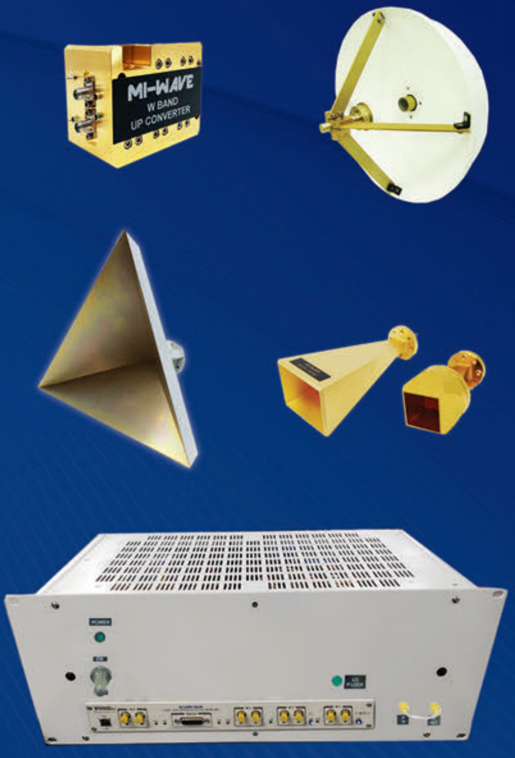

- Commercial
- Defense
- Telecommunications
- Space

www.MIWV.com

MADE IN USA

TEL: 727-563-0034 - EMAIL: SALES@MIWV.COM

2007 GANDY BLVD N, SUITE 1310, ST. PETERSBURG, FL

RF Amplifiers and Sub-Assemblies for Every Application

Delivery from Stock to 2 Weeks ARO from the catalog or built to your specifications!

- Competitive Pricing & Fast Delivery
- Military Reliability & Qualification
- Various Options: Temperature Compensation, Input Limiter Protection, Detectors/TTL & More
- Unconditionally Stable (100% tested)

ISO 9001:2000 and AS9100B CERTIFIED

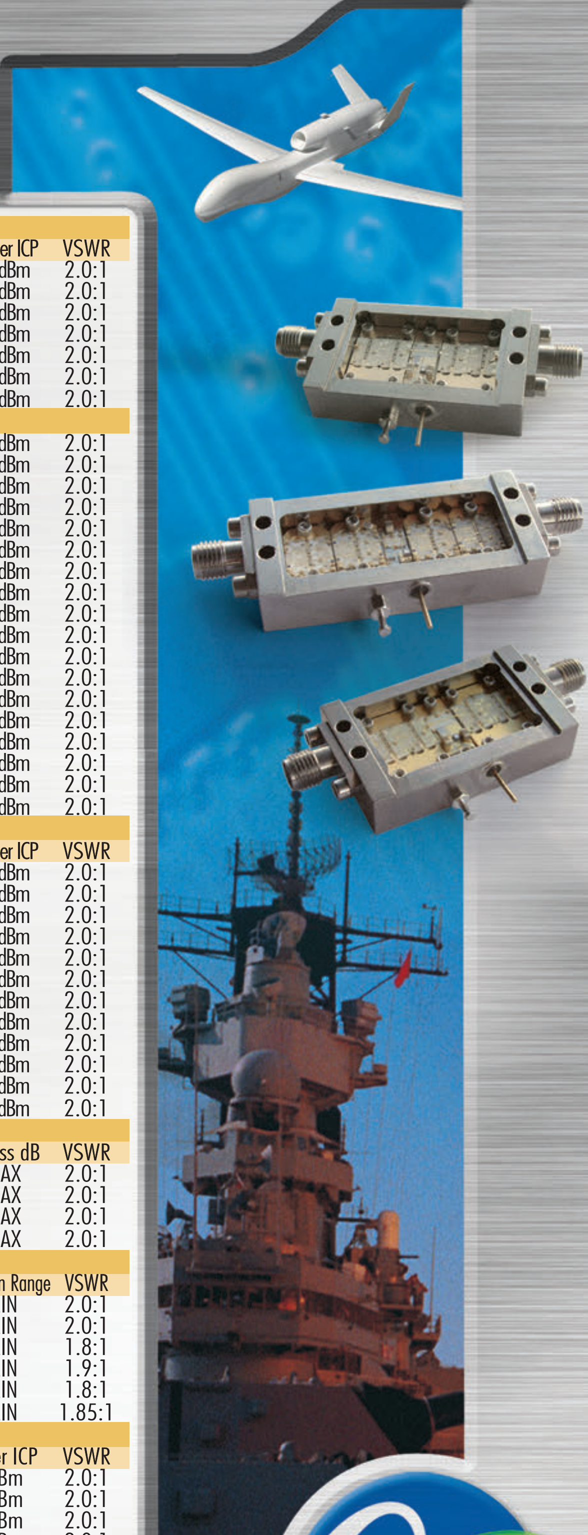

OCTAVE BAND LOW NOISE AMPLIFIERS

Model No.	Freq (GHz)	Gain (dB) MIN	Noise Figure (dB)	Power-out @ P1-dB	3rd Order ICP	VSWR
CA01-2110	0.5-1.0	28	1.0 MAX, 0.7 TYP	+10 MIN	+20 dBm	2.0:1
CA12-2110	1.0-2.0	30	1.0 MAX, 0.7 TYP	+10 MIN	+20 dBm	2.0:1
CA24-2111	2.0-4.0	29	1.1 MAX, 0.95 TYP	+10 MIN	+20 dBm	2.0:1
CA48-2111	4.0-8.0	29	1.3 MAX, 1.0 TYP	+10 MIN	+20 dBm	2.0:1
CA812-3111	8.0-12.0	27	1.6 MAX, 1.4 TYP	+10 MIN	+20 dBm	2.0:1
CA1218-4111	12.0-18.0	25	1.9 MAX, 1.7 TYP	+10 MIN	+20 dBm	2.0:1
CA1826-2110	18.0-26.5	32	3.0 MAX, 2.5 TYP	+10 MIN	+20 dBm	2.0:1

NARROW BAND LOW NOISE AND MEDIUM POWER AMPLIFIERS

Model No.	Freq (GHz)	Gain (dB) MIN	Noise Figure (dB)	Power-out @ P1-dB	3rd Order ICP	VSWR
CA01-2111	0.4 - 0.5	28	0.6 MAX, 0.4 TYP	+10 MIN	+20 dBm	2.0:1
CA01-2113	0.8 - 1.0	28	0.6 MAX, 0.4 TYP	+10 MIN	+20 dBm	2.0:1
CA12-3117	1.2 - 1.6	25	0.6 MAX, 0.4 TYP	+10 MIN	+20 dBm	2.0:1
CA23-3111	2.2 - 2.4	30	0.6 MAX, 0.45 TYP	+10 MIN	+20 dBm	2.0:1
CA23-3116	2.7 - 2.9	29	0.7 MAX, 0.5 TYP	+10 MIN	+20 dBm	2.0:1
CA34-2110	3.7 - 4.2	28	1.0 MAX, 0.5 TYP	+10 MIN	+20 dBm	2.0:1
CA56-3110	5.4 - 5.9	40	1.0 MAX, 0.5 TYP	+10 MIN	+20 dBm	2.0:1
CA78-4110	7.25 - 7.75	32	1.2 MAX, 1.0 TYP	+10 MIN	+20 dBm	2.0:1
CA910-3110	9.0 - 10.6	25	1.4 MAX, 1.2 TYP	+10 MIN	+20 dBm	2.0:1
CA1315-3110	13.75 - 15.4	25	1.6 MAX, 1.4 TYP	+10 MIN	+20 dBm	2.0:1
CA12-3114	1.35 - 1.85	30	4.0 MAX, 3.0 TYP	+33 MIN	+41 dBm	2.0:1
CA34-6116	3.1 - 3.5	40	4.5 MAX, 3.5 TYP	+35 MIN	+43 dBm	2.0:1
CA56-5114	5.9 - 6.4	30	5.0 MAX, 4.0 TYP	+30 MIN	+40 dBm	2.0:1
CA812-6115	8.0 - 12.0	30	4.5 MAX, 3.5 TYP	+30 MIN	+40 dBm	2.0:1
CA812-6116	8.0 - 12.0	30	5.0 MAX, 4.0 TYP	+33 MIN	+41 dBm	2.0:1
CA1213-7110	12.2 - 13.25	28	6.0 MAX, 5.5 TYP	+33 MIN	+42 dBm	2.0:1
CA1415-7110	14.0 - 15.0	30	5.0 MAX, 4.0 TYP	+30 MIN	+40 dBm	2.0:1
CA1722-4110	17.0 - 22.0	25	3.5 MAX, 2.8 TYP	+21 MIN	+31 dBm	2.0:1

ULTRA-BROADBAND & MULTI-OCTAVE BAND AMPLIFIERS

Model No.	Freq (GHz)	Gain (dB) MIN	Noise Figure (dB)	Power-out @ P1-dB	3rd Order ICP	VSWR
CA0102-3111	0.1-2.0	28	1.6 Max, 1.2 TYP	+10 MIN	+20 dBm	2.0:1
CA0106-3111	0.1-6.0	28	1.9 Max, 1.5 TYP	+10 MIN	+20 dBm	2.0:1
CA0108-3110	0.1-8.0	26	2.2 Max, 1.8 TYP	+10 MIN	+20 dBm	2.0:1
CA0108-4112	0.1-8.0	32	3.0 MAX, 1.8 TYP	+22 MIN	+32 dBm	2.0:1
CA02-3112	0.5-2.0	36	4.5 MAX, 2.5 TYP	+30 MIN	+40 dBm	2.0:1
CA26-3110	2.0-6.0	26	2.0 MAX, 1.5 TYP	+10 MIN	+20 dBm	2.0:1
CA26-4114	2.0-6.0	22	5.0 MAX, 3.5 TYP	+30 MIN	+40 dBm	2.0:1
CA618-4112	6.0-18.0	25	5.0 MAX, 3.5 TYP	+23 MIN	+33 dBm	2.0:1
CA618-6114	6.0-18.0	35	5.0 MAX, 3.5 TYP	+30 MIN	+40 dBm	2.0:1
CA218-4116	2.0-18.0	30	3.5 MAX, 2.8 TYP	+10 MIN	+20 dBm	2.0:1
CA218-4110	2.0-18.0	30	5.0 MAX, 3.5 TYP	+20 MIN	+30 dBm	2.0:1
CA218-4112	2.0-18.0	29	5.0 MAX, 3.5 TYP	+24 MIN	+34 dBm	2.0:1

LIMITING AMPLIFIERS

Model No.	Freq (GHz)	Input Dynamic Range	Output Power Range Psat	Power Flatness dB	VSWR
CLA24-4001	2.0 - 4.0	-28 to +10 dBm	+7 to +11 dBm	+/- 1.5 MAX	2.0:1
CLA26-8001	2.0 - 6.0	-50 to +20 dBm	+14 to +18 dBm	+/- 1.5 MAX	2.0:1
CLA712-5001	7.0 - 12.4	-21 to +10 dBm	+14 to +19 dBm	+/- 1.5 MAX	2.0:1
CLA618-1201	6.0 - 18.0	-50 to +20 dBm	+14 to +19 dBm	+/- 1.5 MAX	2.0:1

AMPLIFIERS WITH INTEGRATED GAIN ATTENUATION

Model No.	Freq (GHz)	Gain (dB) MIN	Noise Figure (dB)	Power-out @ P1-dB	Gain Attenuation Range	VSWR
CA001-2511A	0.025-0.150	21	5.0 MAX, 3.5 TYP	+12 MIN	30 dB MIN	2.0:1
CA05-3110A	0.5-5.5	23	2.5 MAX, 1.5 TYP	+18 MIN	20 dB MIN	2.0:1
CA56-3110A	5.85-6.425	28	2.5 MAX, 1.5 TYP	+16 MIN	22 dB MIN	1.8:1
CA612-4110A	6.0-12.0	24	2.5 MAX, 1.5 TYP	+12 MIN	15 dB MIN	1.9:1
CA1315-4110A	13.75-15.4	25	2.2 MAX, 1.6 TYP	+16 MIN	20 dB MIN	1.8:1
CA1518-4110A	15.0-18.0	30	3.0 MAX, 2.0 TYP	+18 MIN	20 dB MIN	1.85:1

LOW FREQUENCY AMPLIFIERS

Model No.	Freq (GHz)	Gain (dB) MIN	Noise Figure dB	Power-out @ P1-dB	3rd Order ICP	VSWR
CA001-2110	0.01-0.10	18	4.0 MAX, 2.2 TYP	+10 MIN	+20 dBm	2.0:1
CA001-2211	0.04-0.15	24	3.5 MAX, 2.2 TYP	+13 MIN	+23 dBm	2.0:1
CA001-2215	0.04-0.15	23	4.0 MAX, 2.2 TYP	+23 MIN	+33 dBm	2.0:1
CA001-3113	0.01-1.0	28	4.0 MAX, 2.8 TYP	+17 MIN	+27 dBm	2.0:1
CA002-3114	0.01-2.0	27	4.0 MAX, 2.8 TYP	+20 MIN	+30 dBm	2.0:1
CA003-3116	0.01-3.0	18	4.0 MAX, 2.8 TYP	+25 MIN	+35 dBm	2.0:1
CA004-3112	0.01-4.0	32	4.0 MAX, 2.8 TYP	+15 MIN	+25 dBm	2.0:1

CIAO Wireless can easily modify any of its standard models to meet your "exact" requirements at the Catalog Pricing.

Visit our web site at **www.ciaowireless.com** for our complete product offering.

Ciao wireless

Ciao Wireless, Inc. 4000 Via Pescador, Camarillo, CA 93012

Tel (805) 389-3224 Fax (805) 389-3629 sales@ciaowireless.com

DefenseNews

Cliff Drubin, Associate Technical Editor

Raytheon Missiles & Defense Uses Warfighter Feedback to Improve Counter-UAS Solutions

In partnership with the U.S. Army's Integrated Fires and Rapid Capabilities Office, Raytheon Missiles & Defense, a Raytheon Technologies business, showcased the capabilities of the Low, slow, small-unmanned aircraft system (UAS) Integrated Defeat System (LIDS), during the U.S. Army summer test period.

LIDS is a U.S. Army-developed counter-UAS solution. It integrates the Ku-Band Radio Frequency Sensor (KuRFS) and the Coyote® family of effectors, both made by Raytheon Missiles & Defense, with Northrop Grumman's Forward Area Air Defense Command and Control system and an electronic warfare system made by Syracuse Research Corporation.

LIDS (Source: Raytheon Missiles and Defense)

Building off the performance of the 2021 summer test period and incorporating direct input from warfighters operating the systems, Raytheon Missiles & Defense used real-world data to enhance the systems and further improve performance and dependability. During the tests, LIDS detected and defeated drones and drone swarms varying in size, maneuverability and range, validating those updates and reaffirming the effectiveness of the solution.

"The ability to rapidly integrate warfighter feedback and data-informed updates into these proven systems allows us to continually enhance this critical capability against real and emerging threats," said Tom Laliberty, president of land warfare and air defense at Raytheon Missiles & Defense. "The successful performance of Coyote and KuRFS during the summer test period proves LIDS gives warfighters around the globe a competitive advantage."

Revolutionizing Radar Signal Processing

Radar systems have seen many technology improvements in apertures (antennas) and associated hardware and software since the nascent operational versions in World War II. What has not changed significantly over the decades, however, is that radars still use linear signal processing between the aperture and the detector. In the 1940s, linear radar signal processing used vacuum tubes and analog circuits, while current radars accomplish linear signal processing digitally with microchips and software.

With the Beyond Linear Processing (BLiP) program, DARPA's goal is to improve radar performance by applying innovative signal processing methods. BLiP will leverage high-power computer processing to explore new, non-linear and iterative signal processing techniques that could lead to lighter, smaller and less expensive—but equally capable—radar systems. If successful, BLiP would enable the same radar performance achieved on large platforms today on much smaller sea, air and ground platforms.

BLiP will address the current immaturity of non-linear and iterative signal processing methods. Over the course of the two-year program, end-to-end radar signal processing chains will be developed, analyzed, implemented and tested—initially through non-real-time laboratory testing and culminating in real-time implementation and full-scale field testing using an operational National Weather Service radar. Key technical challenges for BLiP will be the development, understanding, optimization of the signal processing chain and the practical aspects of implementing BLiP algorithms using real-time, high performance processing.

DOD Continues to Advance Hypersonic Capabilities

The Navy Strategic Systems Programs and the Army Hypersonic Project Office (AHPO) successfully conducted the second High Operational Tempo for Hypersonics flight campaign recently. This flight campaign was executed by Sandia National Laboratories (SNL) from the NASA Wallops Flight Facility. This test will be used to inform the development of the Navy's Conventional Prompt Strike (CPS) and the Army's Long Range Hypersonic Weapon offensive hypersonic strike capability. The CPS and AHPO programs are on track to support the first fielding of a hypersonic capability to the Army in fiscal year 2023. The Missile Defense Agency (MDA) took part in the campaign to gather data for its work developing systems that will defend against hypersonic weapons.

One precision sounding rocket launch was conducted containing hypersonic experiments from partners, including CPS, MDA, AHPO, the Joint Hypersonic Transition Office, SNL, Johns Hopkins University/Applied Physics Laboratory, MITRE, Oak Ridge National Laboratory and several defense contractors. A second sounding rocket completed the campaign. These rockets contained experimental payloads that provided data on the performance of materials and systems in a realistic hypersonic environment.

During weapon system development, precision sounding rocket launches fill a critical gap between

For More Information Visit mwjournal.com for more defense news.

ground testing and full system flight testing. These launches enable frequent and regular flight testing opportunities to support rapid maturation of offensive and defensive hypersonic technologies. The data collected from the latest sounding rocket campaign will drive warfighting capability improvements for both Navy and Army to ensure continued battlefield dominance.

The Navy and Army will continue to work in close collaboration to leverage joint testing opportunities and routinely share data with the MDA that supports its work on hypersonic defenses.

L3Harris Reveals New Handheld Radio Module Enabling Worldwide Communications for Warfighters

L3Harris Technologies unveiled its Iridium Distributed Tactical Communications Systems (DTCS) mission module at AUSA's Annual Meeting and Exposition, enabling push-to-talk voice and data for warfighters worldwide.

The mission module connects the L3Harris AN/PRC-163 multi-channel handheld tactical radio to the U.S. Space Force's DTCS network, providing warfighters in the field secure voice and data communication without having to carry a separate Iridium satellite radio.

Harris Radio (Source: L3Harris)

"This new capability enables warfighters to stay connected anywhere on the battlefield and provides commanders extraordinary versatility exercising command and control," said Ed Zoiss, president of space and airborne systems at L3Harris. "The ability to stay connected in virtually any situation allows for better planning and responsive execution of missions."

Warfighters armed with the AN/PRC-163 and DTCS mission module can now communicate using any combination of satellite communications, mobile ad-hoc network or line-of-sight modes even in situations when one or more connection methods are not available. Small, power efficient and easy to use, the mission module attaches directly to the AN/PRC-163, or through a tethered cable, and controlled from the radio's existing control panel.

The mission module, a part of the Assured Reach family of communications technologies, complements L3Harris' Falcon® radio product line, delivering networked communications to more than 700,000 U.S. and allied users around the world.

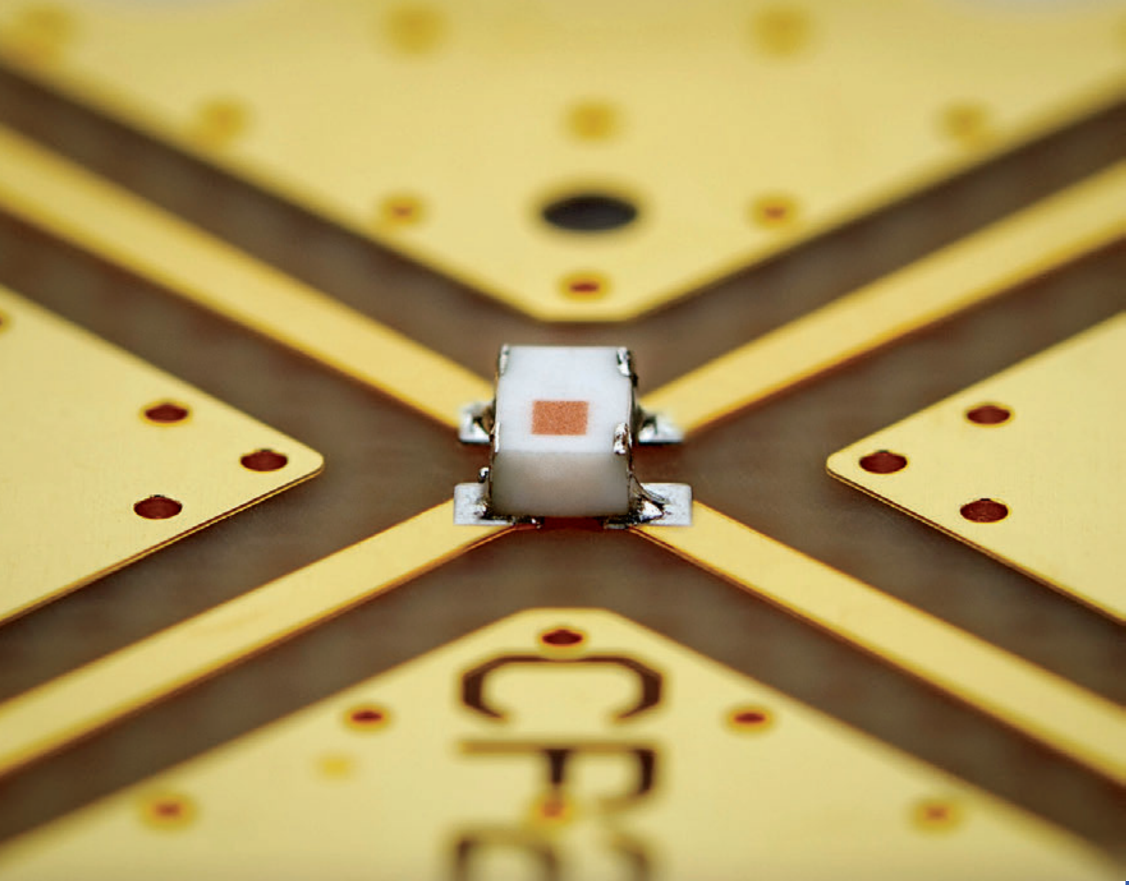

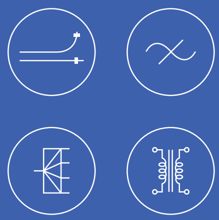

INDUSTRY-LEADING DESIGN

LTCC Products

The World's Broadest Portfolio

- 750+ in-stock models
- Custom designs with fast turnaround
- Superior RF performance
- Package sizes as small as 0202

Mini-Circuits®

Ericsson's Largest Consumer Study Shows 5G is Already Paving Way to the Metaverse

As 5G uptake in many parts of the world bridges the milestone from early adopters to mass adoption, major new Ericsson research underlines consumers' growing commitment to 5G and their expectations on next-generation uses cases.

Called "5G: The Next Wave," the Ericsson ConsumerLab report addresses the impact 5G has had on early adopter consumers since launching in various countries, as well as gauging the intention of non-5G subscribers to take up the technology—and their related expectations. The report forecasts that at least 30 percent of smartphone users intend to take up a 5G subscription within the next year.

The mix of Ericsson tracking data covering 5G launches since 2019, and the new consumer survey, has enabled Ericsson ConsumerLab to identify six key trends impacting the next wave of 5G adoption.

The report covers the behavioral changes triggered by the bundling of digital services into 5G plans by communications service providers—particularly the increased use of enhanced video and augmented reality (AR) apps.

> 5G is driving increased use of enhanced video and AR.

The report also addresses the speed of mainstream 5G adoption, whether consumer demands are being met and 5G-related changes in smartphone behavior—and their impact on network traffic.

More than 49,000 consumers in 37 countries were interviewed in the research—the largest global 5G-related consumer survey in the industry to date and the largest consumer survey conducted by Ericsson on any topic. The survey scope is representative of the opinions of about 1.7 billion consumers worldwide, including 430 million 5G subscribers.

The report forecasts that 5G consumers with experience of using extended reality (XR) functionality are likely to be the first to embrace future devices as they are more positive about the potential of mixed-reality glasses. Half of 5G users who already use XR-related services weekly think that AR apps will move from smartphones to XR headsets within the next two years, compared to one-third of 4G consumer who hold this view.

5G – the Next Wave Report: Six Key Trends:

- 5G adoption to be inflation resilient: At least 510 million consumers across 37 markets are likely to take up 5G in 2023
- The demanding next wave of users: The next wave of 5G users have high expectations on 5G performance, especially network coverage, compared to early adopters—who care about new innovative services enabled by 5G
- Perceived 5G availability is emerging as the new satisfaction benchmark among consumers. Geographical coverage, indoor/outdoor coverage and congregation hot-spot coverage are more important to building a user perception than population coverage
- 5G is pushing up usage of enhanced video and AR. Over the past two years, time spent on AR apps by 5G users has doubled to two hours per week
- 5G monetization models are expected to evolve: Six in 10 consumers expect 5G offerings to move beyond more data volume and speeds to on-demand tailored network capabilities for specific needs.

5G adoption is setting the path to the metaverse. 5G users on average are already spending one hour more per week in metaverse-related services than 4G users. They also expect two hours of more video content will be consumed weekly on mobile devices, 1.5 hours of which will be on AR/VR glasses by 2025.

Smart Poles to Become a Key Deployment Framework for Urban Infrastructure

Smart poles are multi-functional aggregation points for smart urban infrastructure, built on top of smart streetlights and connected utility poles. According to ABI Research, by 2030, the installed base of smart poles will exceed 10.8 million globally, with system revenues amounting to US$60 billion.

"The relevance of smart poles for smart cities is huge. They offer an efficient, scalable and modular framework for deploying the whole spectrum of smart urban infrastructure, ranging from 5G small cells and Wi-Fi hotspots to surveillance and traffic cameras, signage and information displays, air quality and flood monitoring solutions, and charging points for two- and four-wheel vehicles, drones and handsets including renewable energy generation," said Dominique Bonte, vice president end markets and verticals at ABI Research. "However, the main driver behind smart pole deployments is the need for cellular network densification in the form of 5G and future 6G small cells and the use of mmWave radio spectrum. As such, the telco ecosystem is expected to at least partially fund the additional smart cities functionality embedded in smart poles."

Typical barriers slowing down smart pole adoption include issues related to co-ownership and management (design, maintenance, backhaul cost sharing), conflicting priorities and agendas, sensor data privacy concerns, and the lack of awareness of city govern-

For More Information Visit mwjournal.com for more commercial market news.

ments about the many benefits offered by smart poles in terms of cost savings, deployment time, scaling opportunities and future-proof modularity. Consequently, deployments are only expected to gather momentum toward the end of this decade.

Key vendors in the smart pole ecosystem include Ubicquia, Verizon, Huawei, Signify, Nokia/LuxTurrim5G, and ELKO EP, next to a range of smart streetlight suppliers venturing into smart pole technologies. Main initiatives include the EU's Humble Lamppost Project and deployments by the Seoul Metropolitan Government, Los Angeles, Munich and Leuven. Also cities in China (Shenzhen, Hangzhou) and India (Bhopal, New Delhi and Indore) have implemented smart pole projects.

5G FWA Subscriptions Will Reach 58M by 2026

In the short term, 5G Fixed Wireless Access will progress without capacity constraints, but steady growth in the long term depends on network capacity, spectrum and resource optimization.

Fixed Wireless Access (FWA) allows mobile network operators (MNOs) to reuse the existing mobile infrastructure to offer faster and more affordable broadband services. FWA using 4G has already been deployed by MNOs worldwide, but it is often unable to provide the speed that can compete with wired broadband connections. With 5G, FWA can offer fiber-like speed due to the improved spectral efficiency with advanced antenna technologies, making it a competitive alternative to wired broadband solutions. According to ABI Research, worldwide 5G FWA will reach 58 million subscriptions in 2026. In the near term, the United States is driving the number of 5G FWA connections with major operators aggressively expanding their FWA business.

"MNOs can launch 5G FWA services to boost revenues by using their spare network capacity in the short term. However, in the long term, 5G FWA depends on sufficient network capacity and spectrum and the optimization of network resources," explained Fei Liu, 5G & mobile network infrastructure industry analyst at ABI Research. "An FWA user can consume 40x more network resources than a mobile user. Therefore, MNOs need to conduct a proper market assessment and detailed plan to understand the required capacity in their targeted markets and how many FWA subscribers they can truly support."

The strategy to offer 5G FWA varies with MNOs targeting different markets. The main strategies include 5G FWA for last-mile connectivity, 5G FWA for business, 5G FWA to connect the unconnected, 5G FWA as a value-added service and 5G FWA as a backup for fixed broadband.

Around the **Circuit**

Barbara Walsh, Multimedia Staff Editor

MERGERS & ACQUISITIONS

Renesas Electronics Corp. announced that it has completed the acquisition of **Steradian Semiconductors Private Limited**. Headquartered in Bengaluru, India, Steradian is a start-up founded in 2016 and provides radar solutions that enable highly accurate object recognition and power efficiency in a small chip. Radar is a vital technology for advanced driver assistance system, which uses a complex combination of various sensors in vehicles to detect objects. Renesas plans to capitalize on the high growth opportunities the automotive radar market offers, by expanding its automotive product portfolio with Steradian's radar technology and extending its reach in the radar market.

Microwave Vision Group (MVG); global service provider in antenna measurements, radar and RCS testing solutions; has acquired **Singularis Solutions**, an electro-mechanical engineering firm based in Philadelphia which specializes in design, integration, manufacturing and testing of complex systems. The two companies had collaborated on several projects over the years which not only supported the decision well, but also led to a quick and smooth acquisition process. Final agreements were signed in October. This acquisition reflects MVG's momentum and ambition for growth in the North American aerospace and defense sector.

COLLABORATIONS

Frontier Precision, a large U.S. distributor of geospatial and unmanned solutions, and **Synspective**, a synthetic aperture radar (SAR) satellite data and solutions provider, announced a new distribution partnership for their SAR-based solutions across North America. Synspective develops and operates high frequency, high-resolution SAR satellites to provide high-quality data set and solution services. The company has already succeeded in putting three satellites into targeted orbit. And, by 2023, it will have six satellites in orbit, bringing them closer to a planned constellation of 30 satellites around 2026.

Qualcomm Technologies and **Vodafone** have joined forces to develop, test and integrate next-generation 5G distributed units and radio units with massive MIMO capabilities, ultimately to deliver the commercial deployment of Open RAN in Europe. This builds on the companies' previous commitment in April 2021 to develop technical blueprints that will help equipment suppliers build 5G networks of the future using Open RAN technology. Qualcomm Technologies and Vodafone are developing 5G Open RAN Infrastructure solutions powered by the Qualcomm X100 5G RAN Accelerator Card and the high performance Qualcomm QRU100 5G RAN Platform.

NEW STARTS

Quantic PMI; designer and manufacturer of RF/microwave components, integrated modules and subsystems; announced that it would be consolidating its East Coast Operations under one state-of-the-art facility at 7309-A Grove Road, Frederick, Md. Some features of this facility are components and sub-assembly manufacturing, hybrid assembly, engineering and test departments, QA/QC, sales, marketing and executive offices and three conference rooms (production, engineering and S&M). The consolidation will provide additional manufacturing space, increased capacity and a much-needed space for expansion of Quantic PMI product offering and services.

ACHIEVEMENTS

CEVA, a licensor of wireless connectivity and smart sensing technologies and co-creation solutions, and **ASR Microelectronics**, a wireless semiconductor company, announced that shipments of ASR wireless IoT chips powered by CEVA's IPs have surpassed 100 million units. This monumental milestone was achieved in less than two years since ASR's first CEVA-powered chips were introduced. CEVA's RivieraWaves Bluetooth and Wi-Fi IP platforms provide comprehensive solutions for the integration of Bluetooth and/or Wi-Fi connectivity into any IC or SoC design. Each platform consists of a hardware modem, baseband controller or MAC, plus a feature-rich software protocol stack.

Ericsson has successfully achieved a peak data rate of more than 1 Gbps for a single user device in a recent 5G Standalone field trial. The trial was done over a live Citizen's Broadband Radio Service (CBRS) multi-operator, neutral host capable network at the company's North American headquarters in Plano, Texas. The OnGo Alliance coordinated the interoperability of the CBRS ecosystem. The network where this trial took place is supported by a 5G core network as part of the 5G Distributed Innovation Network at Ericsson's facility in North Texas.

Qorvo® announced recognition by **Raytheon Technologies** with their Premier Award for performance and overall excellence in technology & innovation and collaboration and also by **BAE Systems Inc.**'s electronic systems sector with a Silver Tier Award for exceptional performance and contributions to supply chain success. The Premier Award is an annual recognition platform under the Raytheon Technologies Performance+ Program, designed to honor suppliers that have provided superior performance and exceptional value to Raytheon Technologies in one of the four key categories: cost competitiveness, technology & innovation, business management/customer service and collaboration.

The **U.S. Army**'s AN/TPQ-53 (Q-53) Multi-Mission Radar integrated with an Army command and control system was successfully demonstrated in Yuma, Ariz. During the demonstration, it provided tracking data to

For More Information For up-to-date news briefs, visit mwjournal.com

GOLD STANDARD

8 to 15 GHZ DRO / SDRO series

FEATURES:
- ► *Exceptional Phase Noise*
- ► *Lead Free RoHS Compliant*
- ► *Patented Technology*

Applications:
Radar, Test Equipment, 5G, Frequency Synthesizer

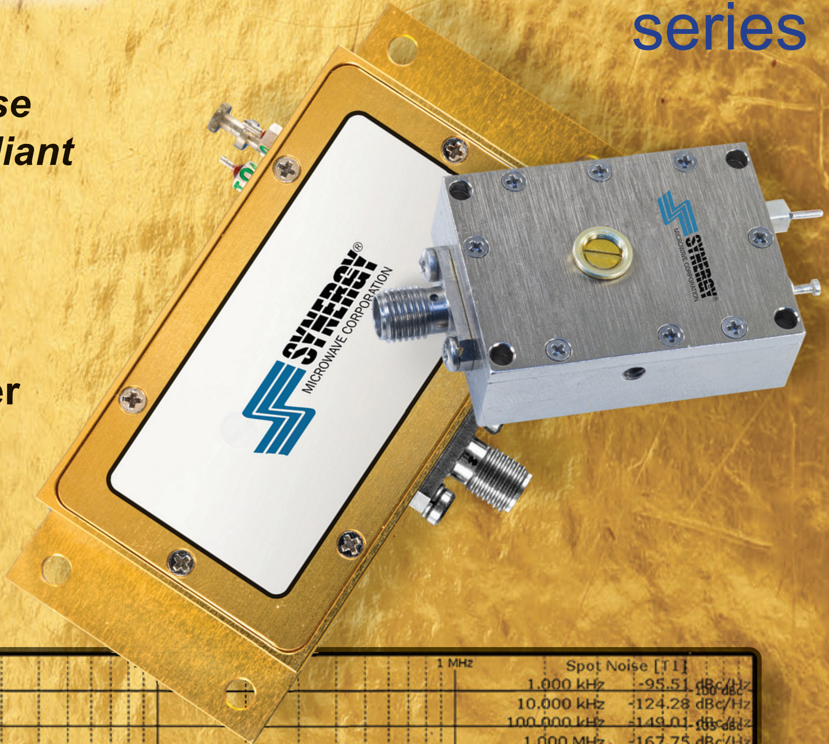

SDRO Series
0.75" x 0.75 x 0.53"

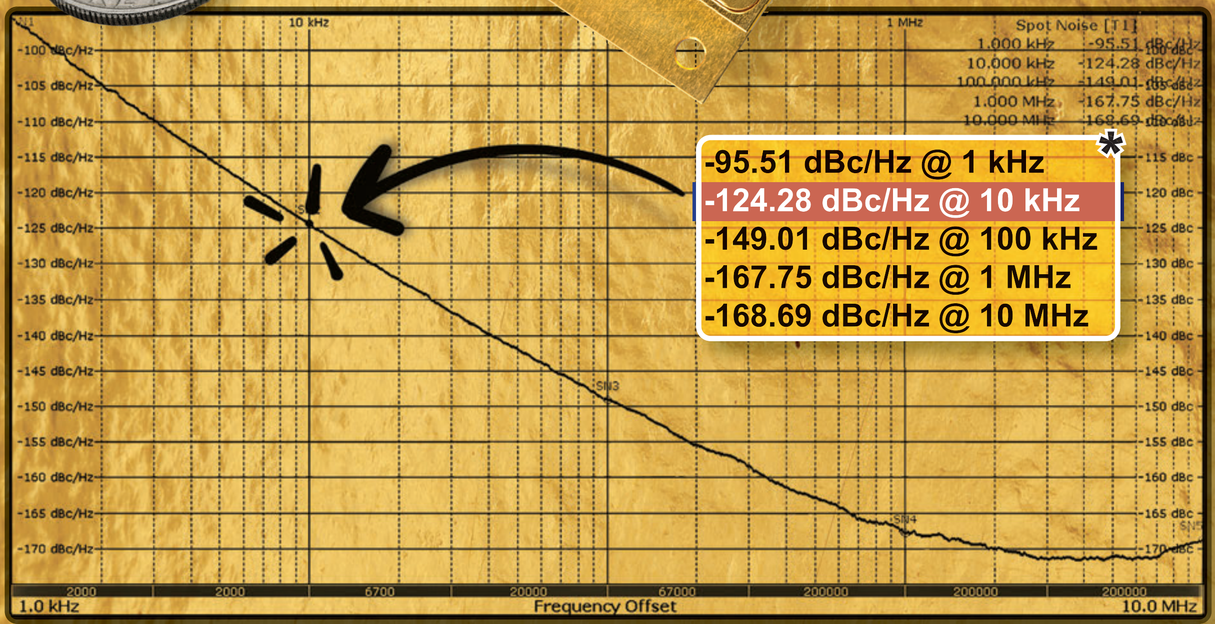

*Typical For 10 GHz RF Output

Talk To Us About Your Custom Requirements.

SYNERGY® MICROWAVE CORPORATION
Phone: (973) 881-8800 | Fax: (973) 881-8361
E-mail: sales@synergymwave.com | Web: www.synergymwave.com
Mail: 201 McLean Boulevard, Paterson, NJ 07504

launch a counter unmanned aerial system (C-UAS) defeat system. The rapidly deployable Q-53 radar, which is ideal for the C-UAS mission, is developed and manufactured by Lockheed Martin in Syracuse, N.Y. During the exercise, the Q-53 integrated with the Forward Area Air Defense Command and Control system to serve as the primary fire control source for the Coyote Block 2 C-UAS defeat system during testing in Yuma.

CONTRACTS

The Commonwealth's Capability Acquisition and Sustainment Group (CASG) has selected **EM Solutions** to carry out Introduction into Service and Support Services for the Royal Australian Navy's existing fleet of Cobra maritime satellite communications (satcom) terminals for a period of three years, through to August 2025. The contract, which is initially valued at approximately $25.7 million, gives CASG the ability to purchase additional terminals as needed to meet requirements for new ship builds and for the provision of enhanced satcom capabilities to existing ships. In recent years, EM Solutions' Cobra terminals have been purchased and installed through various individual ADF project offices.

Elbit Systems Ltd. has announced that it was awarded a contract valued at approximately $25 million from the **Finnish Ministry of Defence** to supply radio communications systems to the Finnish Army. The contract will be executed over a two-year period. Under the contract, Elbit Systems will supply advanced secured radio communications systems that enable enhanced tactical command and fire control and are backward compatible with analog radio equipment that is currently in use by the Finnish Army. Military radio communications solutions of Elbit Systems have been selected to date by several European and NATO countries including Sweden, Germany, Switzerland, the Netherlands, Canada, Spain and others.

IQE plc, a supplier of compound semiconductor wafer products and advanced material solutions, announced the signing of a multi-year agreement with **Advanced Wireless Semiconductor Company (AWSC)**, for the supply of epiwafers for wireless applications. AWSC, a leader in the field of compound semiconductor wafer fabrication, has been a partner of IQE for over 20 years. This three-year supply agreement covers epitaxial wafers spanning a range of AWSC's wireless products, including those which enable 4G and 5G mobile handsets and Wi-Fi products. The agreement provides IQE with diversification opportunities into mass market power amplifier products.

PEOPLE


▲ *Steve Shpock*

Steve Shpock, who has been serving as vice president and general manager of Stellant's Williamsport, Pa., operations, has been appointed COO for **Stellant Systems Inc.** In this new role, Shpoc will continue to report directly to Stellant's Chief Executive Officer Paul Russell and will oversee and drive operational performance across all Stellant engineering and manufacturing facilities in Torrance, Calif., Williamsport, Pa., and Folsom, Calif. With over 35 years of experience in the RF and microwave business, Shpock has held positions of increasing technical and management responsibility with L3Harris, Vitec Group, Thales, Cobham and CPI.


▲ *Henrik Tölander*

SweGaN AB, manufacturer of custom-made GaN-on-SiC epitaxial wafers for an extensive range of devices used in telecom, satellite, defense and power electronics, announced it has added a new role to its executive team. Newly appointed chief operating officer, **Henrik Tölander**, joined SweGaN on October 31. The new management role supports the company's ambitious growth strategy to serve explosive global market demand and follows the company's recently completed Series A financing round.


▲ *John Vesey*

ETL Systems, a global manufacturer and distributor of critical RF equipment for satellite ground stations and RF components, has appointed **John Vesey** as business development director. Vesey brings more than 30 years of industry experience to ETL Systems, having previously worked as

Around the **Circuit**

vice president of Sojitz Corporation of America. During this time, Vesey oversaw product development, manufacturing and operations, as well as business development and sales, working closely with industry leaders such as OneWeb, Telesat and Inmarsat.

▲ *Harish Krishnaswamy*

Sivers Semiconductors AB has appointed **Harish Krishnaswamy**, co-founder of and former CTO at MixComm, as managing director (MD) of Sivers Wireless. Krishnaswamy will also join the management team of Sivers. **Mike Noonen**, former interim MD of Sivers Wireless and U.S. president, will continue as an adviser to Sivers. Sivers Wireless has two development units. The one in the U.S., which has been run by Harish Krishnaswamy, will now be run by **Arun Natarajan**, former vice president of RF technology at MixComm and professor in electrical and computer engineering at Oregon State University.

▲ *Igor Faleichik*

▲ *Jim McCoy*

Indium Corp. announced two new additions to its Engineered Solder Materials (ESM) team—**Igor Faleichik**, senior product specialist and **Jim McCoy**, product specialist. Faleichik assumes responsibility for creating, driving and supporting initiatives to grow his product lines, with a focus on the connector and RF infrastructure markets for ESM. He researches and analyzes customer and market data for his respective products to understand market trends and technical inflection points. McCoy is responsible for researching and aligning customer needs with product capabilities to facilitate current and prospective business within the ESM segment.

REP APPOINTMENT

Altum RF, a supplier of high performance RF to mmWave semiconductor solutions for next-generation markets and applications, announced a sales representative agreement with **NWN Inc.**, covering customers located in Northern California, Northern Nevada and Oregon. Founded in 1994 with headquarters in San Jose, Calif., NWN specializes in technical knowledge of RF, mmWave, microwave, frequency control and analog components. NWN also has expertise and solid relationships in the commercial advanced technology, semiconductor tool, networking components, test and measurement, military and aerospace markets.

INVITED PAPER

mmWave CMOS Integration Enables Fixed Wireless Access in Unlicensed Bands

Carl De Ranter and Khaled Khalaf
Pharrowtech, Leuven, Belgium

The pandemic marked a turning point for the broadband industry, leaving network providers struggling to meet rising consumer demand. While the digital divide is not a new phenomenon, its negative impact on both individuals and society increased because of COVID-19. Governments and operators across the world are responding, working to deploy robust infrastructure that delivers super-fast broadband connectivity, but we are still a long way from achieving this goal, with 50 percent of the world's population without reliable connectivity.

Existing network technologies like twisted pair and coax cannot provide the required capacity, while fiber to the home (FTTH) deployments are often unfeasible because they are prohibitively expensive and slow to deploy. Fixed wireless access (FWA) technology, on the other hand, is an attractive solution to the challenge of delivering connectivity to rural and other underserved areas. FWA can fill the Gbps broadband need where fiber is not commercially or logistically viable, bringing Gbps speeds to the home with a total cost of ownership less than half of FTTH.[1]

While the mid-band spectrum below 6 GHz provides range, the mmWave bands provide capacity. 5G FWA uses the 30 to 300 GHz frequency range, corresponding to wavelengths spanning 1 to 10 mm. mmWave technology is an essential component of 3GPP's 5G standards, as it enables the multi-Gbps data rates promised by 5G. While most mmWave usage is centered on the licensed spectrum bands used by the tier 1 operators, the unlicensed band in the 60 GHz range is currently underused and can extend broadband networks to rural and other underserved areas.

60 GHz provides high speed and low latency internet connectivity, making it an attractive and efficient choice for last mile access. 60 GHz FWA enables employees and businesses to remain productive via a high performance and reliable network and can help connect a world of people via the "metaverse" and other extended reality technologies that require high speed, low latency internet access. The opportunity for 60 GHz is large, and the FWA industry is in the process of realizing its potential.


Portable Handheld Field Solutions
Expand your signal analysis capabilities
to 6G Research, Development & Deployment
90 GHz to 220 GHz and Beyond
M08H4BDC
90 GHz to 140 GHz
M06H6BDC
110 GHz to 170 GHz
M05H6BDC
140 GHz to 220 GHZ
Innovation in Millimeter Wave Solutions
www.omlinc.com
(408) 779-2698
OML

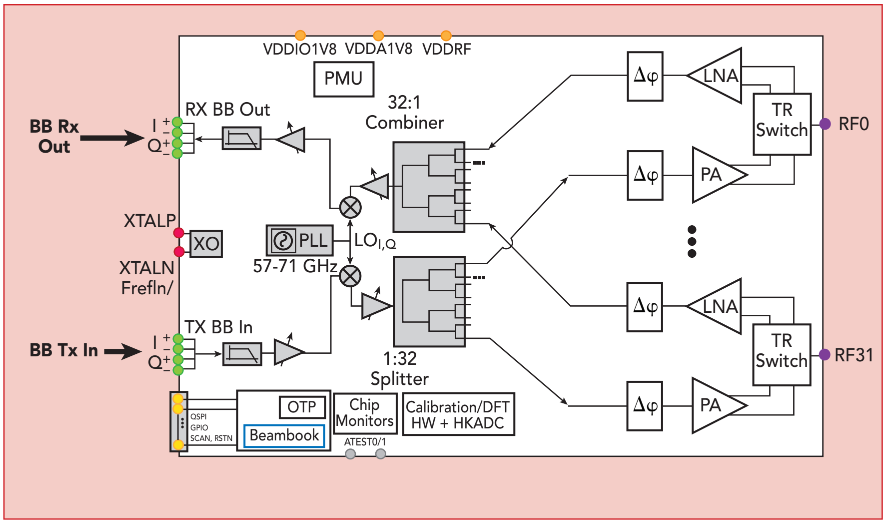

▲ Fig. 1 PTR1060 IC block diagram.

60 GHZ CMOS

Pharrowtech, an imec-backed fabless semiconductor and antenna provider, designs and develops hardware and software for next-generation wireless applications. Responding to the 60 GHz FWA opportunity, Pharrowtech is commercializing a fully integrated CMOS beamforming transceiver and phased array antenna. Based on 15 years of R&D at imec, Pharrowtech's founder, Wim Van Thillo, saw a lack of cost-effective options for the mmWave phased arrays required by FWA systems. Based on the belief that CMOS is the most cost-effective semiconductor technology for FWA, Pharrowtech was launched to commercialize a CMOS-based transceiver. Based on its R&D and prototypes, the company has raised €21 million to scale the RFICs into production.

The core intellectual property developed at imec was a transceiver for the unlicensed 57 to 71 GHz band designed in mature 28 and 40 nm CMOS process nodes. The transceiver architecture is based on the 802.11ay standard. Compared to 5G New Radio, the 802.11ay architecture yields a lower complexity modem and software design, resulting in lower system cost. (Based on its commercial potential and the need for more spectrum, the 60 GHz band has been added to 3GPP Release 17.)

The first product released by Pharrowtech, the PTR1060, is a packaged transceiver with 32-way beamformer and transmit (Tx)/receive (Rx) switching, fabricated in CMOS (see ***Figure 1***). The RFIC covers 57 to 71 GHz and supports channel bandwidths to 4.32 GHz. The transceiver uses a direct conversion architecture to minimize the circuitry and reduce calibration complexity. A universal I/Q analog I/O was chosen to interface with commercially available baseband ICs for digital signal processing.

High-resolution phase shifters in the beamformer provide 1 degree phase resolution, which is useful for large arrays. Supporting 1024 beam book entries, a full 90 × 90-degree antenna field of view (FoV), defined as ±3 dB per direction, can be covered with less than 3-degree beam steering resolution. The PTR1060 integrates a powerful, flexible high speed digital control block supporting both standard (Q-)SPI and a proprietary HSCL digital interface for fast beam steering, AGC and Tx/Rx switching. A wideband phase-locked loop (PLL) was designed together with the LO path in a way to provide immunity to power amplifier (PA) pulling. The digital I/O runs from a standard 1.8 V supply, while the main supply voltage of 0.9 V is provided by the on-chip power management unit (PMU) or, alternatively, a dedicated external supply. An on-board oscillator using a low-cost crystal provides a 40 or 45 MHz reference clock.

By choosing CMOS, a large, cost-effective SRAM has been integrated on the IC. It stores separate beam

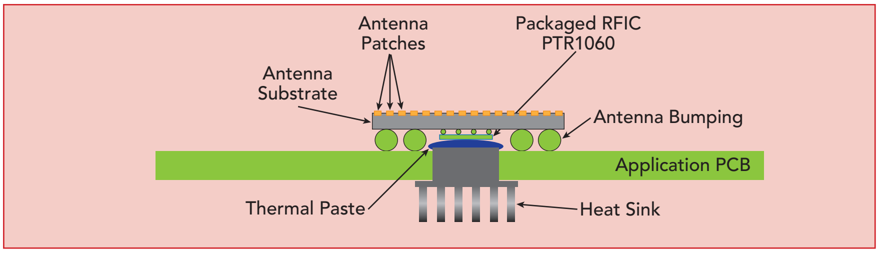

Fig. 2 **Cross-section of PTM1060 and antenna substrate mounting on a PCB.**

book entries for Tx and Rx, supports fast gain switching for transmit while ensuring 11ay timing-compliant AGC control, with 0.5 dB gain steps for the Rx chain. Programmable baseband filters are included in both the Rx and Tx paths, avoiding the need for external anti-aliasing filters in the Rx chain or reconstruction filters in the Tx chain. The sub-channel frequency tuning capability of the integrated frequency synthesizer provides sub-channelization options for dense 3GPP deployments in the unlicensed 60 GHz band.

Pharrowtech's transceiver is encapsulated in a BGA package with a standard 500 µm ball pitch. The packaged IC can be integrated with an antenna (the PTM1060 antenna module) by mounting it on a substrate containing an 8 × 8 patch antenna. The RFIC is flip-chip mounted to the antenna substrate, with the backside of the die exposed for efficient thermal management. In a system, the antenna-RFIC module is mounted to a system printed circuit board (PCB) with an integral thermal heat sink for the RFIC (see ***Figure 2***). To help users evaluate the RFIC in lab or field environments, Pharrowtech has developed an evaluation kit using this same approach, where the PTM1060 is mounted on a reference PCB.

The 8 × 8 patch antenna array provides 20 dBi net gain and a beamwidth of 16 degrees, achieving a 90-degree azimuth × 60-degree elevation FoV with 6 dB combined azimuth/elevation scan loss at the edges, i.e., 3 dB per direction. The array uses two patches per antenna element and is fabricated on substrate material with less than 0.1 dB/mm loss. The array substrate uses the standard 800 µm ball pitch.

LINK PERFORMANCE

The performance of a 60 GHz link using the CMOS transceiver with a customized array antenna at each end has been simulated (see ***Figure 3***). The figure shows the results of a Matlab estimate of link range versus choice of 802.11ay modulation and coding, defined as the MCS level. The simulation uses the RFIC and antenna module performance parameters to calculate the available Tx output power and Rx sensitivity, considering the signal properties at the selected MCS level and the effective beam power and sensitivity across the beam FoV. The simulation combines both beam cases and the effects of rain (assuming rain zone K) on path loss. For each modulation

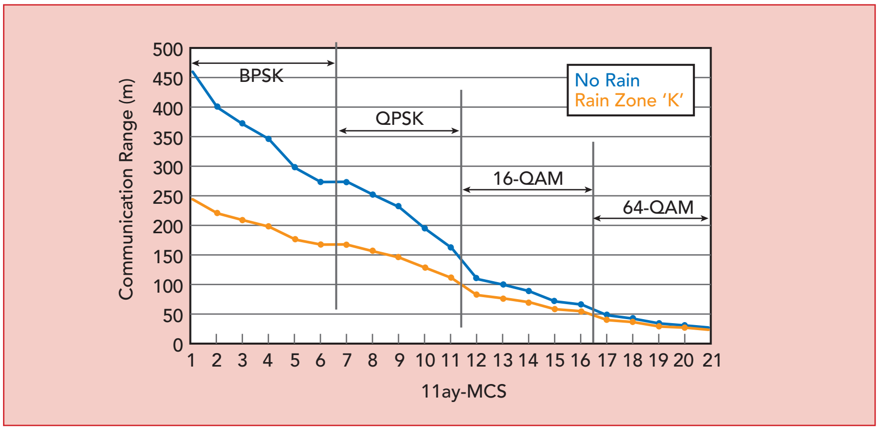

Fig. 3 **Predicted link performance.**


Our Creativity
has no Competition
All Roads
lead to
Exodus,
another Industry First!
AMP4066B-LC
26.5-40.0GHz, 200W
3674 E. Sunset Road, Suite 100
Las Vegas, Nevada 89120 USA
Tel : 1-702-534-6564
Fax : 1-702-441-7016
Email : sales@exoduscomm.com
EXODUS ADVANCED COMMUNICATIONS
Reliability is the answer
www.exoduscomm.com

depth, the PA back-off is increased from the 1 dB compression point to generate the curves shown in the plot. For a 1 Gbps data rate (MCS 3), a range of greater than 150 m is expected during rainy conditions in rain zone K; it increases to more than 300 m for the ideal channel conditions at boresight. At MCS 12, a data rate greater than 3 Gbps can reach a range greater than 100 m at boresight.

CMOS VS. SIGE BICMOS

Pharrowtech's RFIC is on par with the best performing SiGe BiCMOS transceiver RFICs, providing approximately 40 dBm EIRP, yet with a smaller antenna substrate or half the DC power consumption compared to the existing SiGe products: typically, 5 W DC power consumption in Tx mode. With a 60 GHz carrier, it has phase noise of -99 dBc at 1 MHz offset. The Pharrowtech RFIC has 32 active paths, double the number available from commercial SiGe BiCMOS products, and a beam table size of 1024 × 2 entries for Tx and Rx, larger than any other RFIC currently available. Comparing the die areas of the RFICs on the market, the CMOS transceiver is smallest. CMOS' main supply voltage of 0.9 V, 1.8 V for I/O is lower than the supply required by SiGe RFICs: 1.65 to 3.3 V for the main PA supply.

The design of such a complex mmWave beamforming transceiver requires a rigorous design and verification methodology. First, all system functions must be included in the design to ensure straightforward system development: the signal path, local oscillator subsystems, crystal oscillator and system reference clock generation, start-up circuits such as power-on-reset and digital clock enable, power management, generic and custom digital control interfaces, calibration and self-test provisions. To ensure faultless operation of the integrated system, each block must be finalized with high confidence in the silicon's performance before the final layout is delivered to the foundry for manufacturing.

The intrinsic difficulty of working at 60 GHz requires more elaborate 3D electromagnetic (EM) modeling and co-simulation than used with sub-6 GHz designs. In pre-tape-out design and verification, the mmWave models include all the coupling effects of the package, antenna substrate and PCB. To avoid lengthy and costly design and layout iterations, these effects must be considered from the start of the design; they cannot be left to a verification check at the end.

Pharrowtech has a team with multiple decades of experience designing products verified to the high standards necessary for both performance and reliability. By following this structured design and verification methodology and elaborate EM modeling using leading simulation tools, the team yielded a fully functional PTR1060 prototype on the first pass, and the first samples met customer expectations.

SUMMARY

Clearly, connectivity is pivotal to maintain societal and commercial cohesiveness in a post pandemic world. The global demand for broadband internet will only increase, so operators must adopt technologies to meet this need. FWA can provide broadband service with less construction and for a much lower cost than fiber. However, certain implementation challenges must be addressed. A CMOS integration will help reduce implementation costs and system complexity while a tested antenna array module will lower a customer's technical expertise needed to add mmWave connectivity. No doubt mmWave CMOS will increase the capabilities of FWA, helping to meet the demands of a new generation of high data rate wireless networks. ■

Reference

1. S. Weston, "5G FWA could 'Halve the Cost' of Rural Full-fibre Rollout," *IT-Pro*, July 2021, Web: www.itpro.co.uk/mobile/5g/360354/5g-fwa-could-halve-the-cost-of-rural-full-fibre-rollout-says-three.


SM4234
SM4477

Fully Predictive Combline Filter Modeling

Daniel Swanson
DGS Associates, LLC, Boulder, Colo.

The purpose of this work is to point out some of the more subtle points of combline filter design. These issues vary depending on the technology used to realize the filter. While these issues may be well-known to practitioners of the same generation as the author, they may not be well understood by the current generation of engineers, students and academics. Our goal is to find simulation and design methods which fully predict the performance of the combline filter in both the passband and the stopbands. While the coupling matrix method is quite popular today, we will demonstrate how it fails to fully predict the performance of combline filters in several practical situations.

COMBLINE FILTERS

One of the most useful and flexible microwave filter topologies is the combline filter.[1] We can realize these filters as high Qu cavity filters and as thin-film or printed circuit board planar filters. In the case of narrowband filters we can add cross-couplings that realize transmission zeros in the stopbands, which enhance selectivity. Millions of cross-coupled cavity combline filters and diplexers have been deployed around the world to support cellphone networks. Over the years a smaller number of high performance combline filters and multiplexers have also been designed for military and satellite applications.

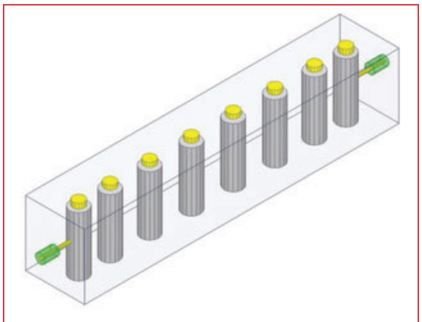

Fig. 1 N = 8, 20 percent bandwidth inline combline filter with lumped loading, modeled in Ansys HFSS.

THE COUPLING MATRIX

The basic concept of cross-coupled filters was demonstrated in the mid-1960s by Johnson[2] and Kurzrok.[3,4] The coupling matrix has become ubiquitous in the filter community since the seminal paper in 1972 by Atia and Williams.[5] Today, many published filter papers include a coupling matrix. Most would agree that the basic coupling matrix concept represents a narrowband, lumped element filter approximation with frequency independent couplings.

It is generally agreed that coupling matrix synthesis should be valid up to about 10 percent relative bandwidth. Some researchers have attempted to enhance the coupling matrix by introducing frequency dependent couplings. One claimed advantage of the coupling matrix is that once the matrix is synthesized, many topologies can be generated, although most of those topologies have very high tuning sensitivity and are not very useful.

INLINE CAVITY COMBLINE FILTERS

In ***Figure 1*** we find a 3D Finite Element Method (FEM) model of an N = 8 inline cavity combline filter. The resonators are typically 30 to 60 degrees long, depending on bandwidth. Capacitive loading brings them to resonance. Three styles of loading are typically used: resonator loading where the tuning screw penetrates the resonator open end, lumped loading with no screw penetration and cover loading where the resonator extends into a pocket in the filter cover. Tapping into the first and last resonators is the most common and flexible input/output scheme. Capacitive coupling with a probe or

disk and inductive coupling with a grounded loop are also possibilities.

If we wanted to develop a design program[6] for the inline combline filter, we could first synthesize a commensurate round rod array[7] and modify the result to be equal diameter. Adding the tuning screw details can only be done through optimization. Adding the input and output taps also requires optimization.[8] At this point, we have a set of dimensions and a network theory model of the filter (see ***Figure 2***).

If we build hardware at this point or make a 3D FEM model of the filter, we find that the filter bandwidth is much larger than predicted. This is the well-known bandwidth expansion problem for inline cavity combline filters.[9] Although the resonators are sitting in a waveguide below cutoff, they can generate evanescent modes in the cavity that modify the assumed transverse electromagnetic (TEM) coupling values.

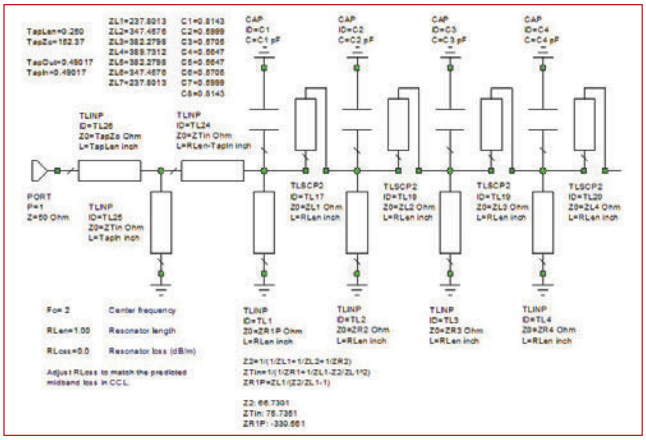

Fig. 2 **Partial schematic for the N = 8 combline filter, modeled in Cadence Microwave Office.**

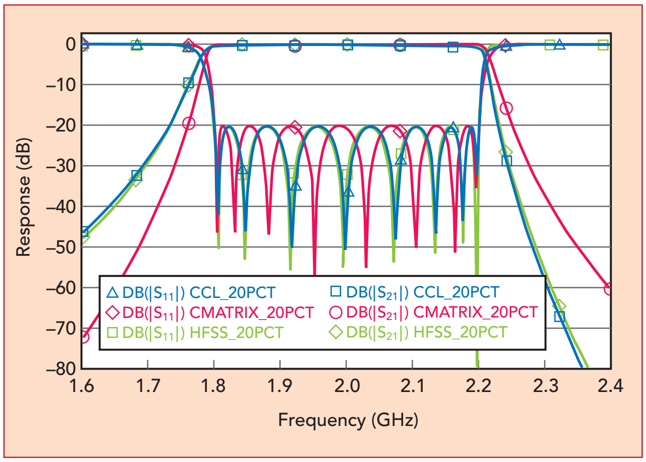

Fig. 3 **Comparing simulation from the circuit model (blue), HFSS model (green) and coupling matrix (red).**

We can correct our design in several ways. We can build a two-resonator 3D FEM model and compare its coupling to a two-resonator network theory model with a correction element added. The result is a correction curve that is a function of the resonator spacing. The approach used in the cavity combline (CCL) software[6] is to modify the desired ground plane spacing (GPS) which modifies the couplings between resonators. This GPS prime (GPS') correction was derived from a large database of measured combline filter results.

In ***Figure 3*** we compare the network theory model from CCL, the HFSS simulation of the CCL generated dimensions and the coupling matrix prediction. At one percent bandwidth these curves lie on top of each other but start to diverge as bandwidth increases. At 10 percent bandwidth the divergence is obvious, and it is even more so at 20 percent bandwidth. Note the network theory model agrees quite well with HFSS, which we take to be the reference, at all practical fractional bandwidths.

The coupling matrix predicts quite different rejection in the stopbands which greatly reduces its value as a fully predictive design tool. Although we are stretching the boundaries of what is typically claimed for the coupling matrix, the uninitiated could clearly be misled as bandwidth increases.

There is at least one TEM cross-section solver for the round or rectangular rod case available in a commercial microwave computer-aided design (CAD) tool.[10] It is tempting to use because we can build a simplified model of a tapped filter and work directly in physical dimensions. If we use our N = 8 combline example, ***Figure 4*** is a simplified schematic using the AWR RCCOAX model.

If we take the dimensions from CCL, which include the GPS' correction and plug them into our simplified model, the predicted bandwidth is much smaller than what we have designed (see ***Figure 5***). If we know about the bandwidth expansion problem in advance, however, we can modify the GPS in our simplified model and come very close to the desired bandwidth (see ***Figure 6***). In this case, the desired physical GPS is 1.00 in. and the GPS' in the model is 1.2 in. We also modified the tap position in the model from 0.573 to 0.557 in.

MICROSTRIP INTERDIGITAL AND COMBLINE FILTERS

Modeling microstrip passive components has always been a challenge. The microstrip interdigital filter[11] has been a very popular topology in integrated microwave assemblies due to its very compact layout. The active area of an N = 5 tapped interdigital filter in thin-film ceramic is roughly λ/4 wide and λ/4 long (see ***Figure 7***). This is in contrast to the popular edge-coupled topology that can be several wavelengths long.

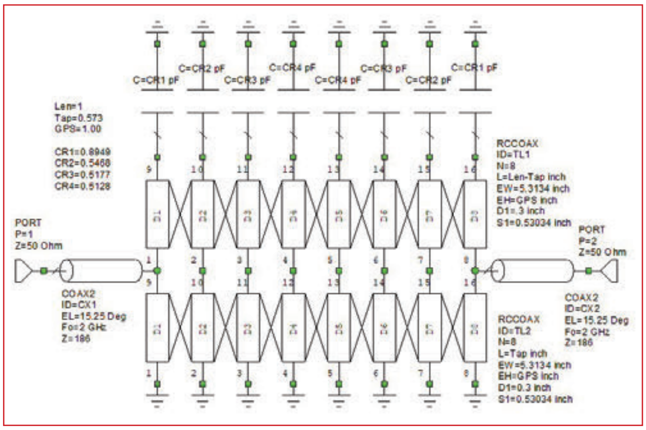

Fig. 4 **Simplified TEM model with the physical GPS = 1.00 in.**

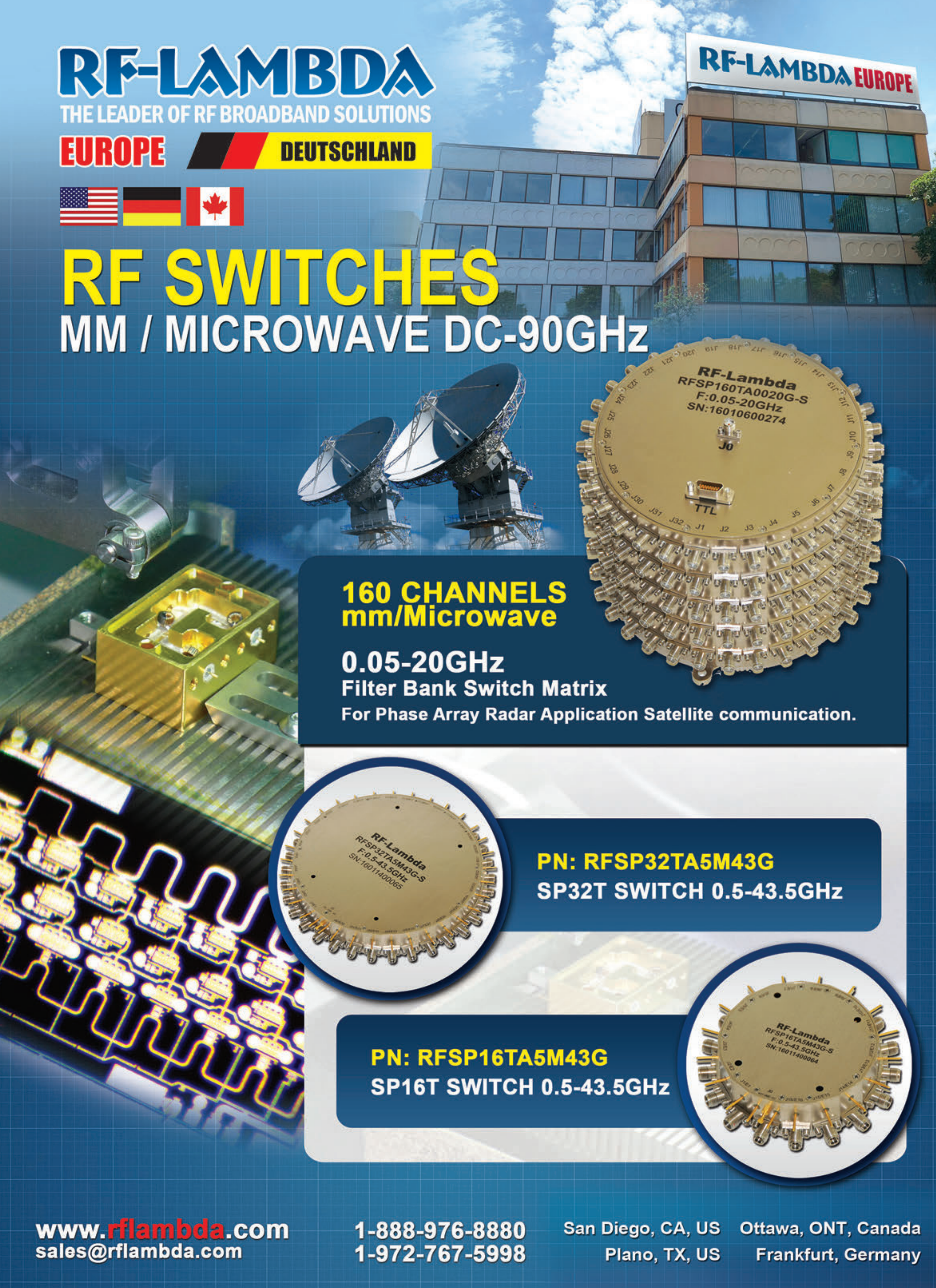
RF-LAMBDA
THE LEADER OF RF BROADBAND SOLUTIONS
EUROPE
DEUTSCHLAND
RF-LAMBDA EUROPE
RF SWITCHES
MM / MICROWAVE DC-90GHz
RF-Lambda
RFSP160TA0020G-S
F:0.05-20GHz
SN:16010600274
160 CHANNELS
mm/Microwave
0.05-20GHz
Filter Bank Switch Matrix
For Phase Array Radar Application Satellite communication.
PN: RFSP32TA5M43G
SP32T SWITCH 0.5-43.5GHz
PN: RFSP16TA5M43G
SP16T SWITCH 0.5-43.5GHz
www.rflambda.com
sales@rflambda.com
1-888-976-8880
1-972-767-5998
San Diego, CA, US
Plano, TX, US
Ottawa, ONT, Canada
Frankfurt, Germany

There are manufacturing issues with the microstrip interdigital filter, however, that can be quite frustrating. The laser drilled vias, often used for grounding, have a finite XY location tolerance in the substrate. The alignment of the metal pattern to the vias also has a finite tolerance. If we consider the resulting electrical length of each resonator, these tolerances can cause every other resonator to be either too long or too short. The resulting passband is then seriously mistuned.

After fighting these issues for many years, we finally seriously considered the microstrip combline. A key development was the understanding that because microstrip is quasi-TEM and we have some inductive loading at the base of the resonators and some capacitive loading at the resonator open ends, we can build useful combline filters without adding discrete loading capacitors and grounding vias at the open ends. This is a significant simplification for manufacturing.

We also adopted a slot to ground, common to all the resonators, rather than individual vias for grounding (see ***Figure 8***), which adds additional flexibility and simplicity. With this topology, if the resonator lengths shift due to tolerances at least they all shift together. The center frequency may shift but the passband tuning is hardly affected.

If we build a microstrip interdigital or combline filter in an open environment or in a waveguide below

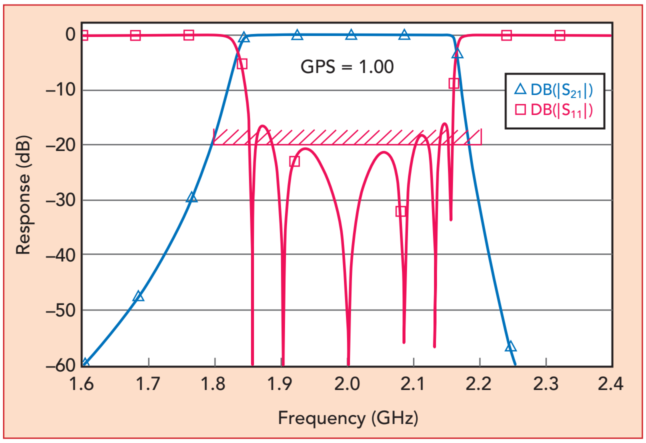

Fig. 5 **Simplified TEM model response with the physical GPS = 1.00 in.**

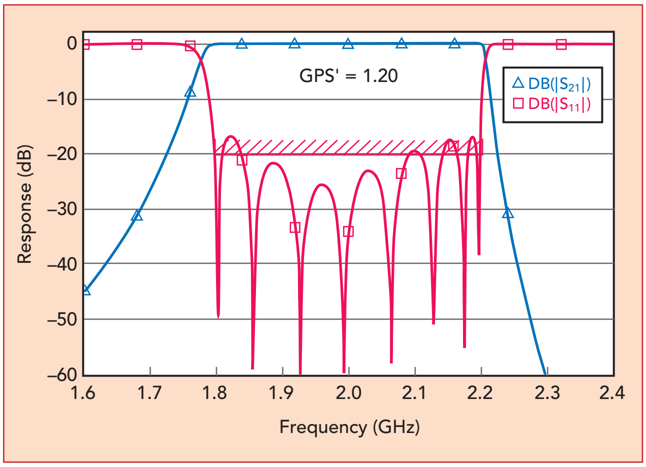

Fig. 6 **Simplified TEM model response with GPS' = 1.20 in. and the modified tap position.**

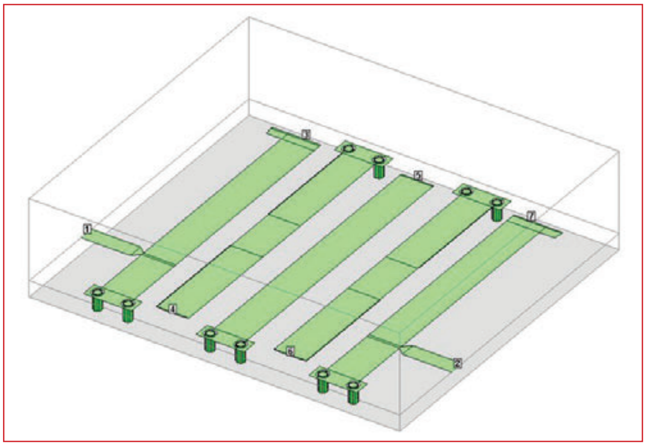

Fig. 7 **Alumina microstrip interdigital filter with N = 5.**[11]

0.3~18GHz
High Power Directional Coupler

- High power handling **600W CW**
- Excellent coupling, flatness and directivity which will significantly improve the signal acquisition accuracy
- Environment conditions meet MIL-STD-202F
- Low VSWR & insertion loss
- Custom-design & narrow band is available
- Arbitrary customization of 30-40dB nominal coupling

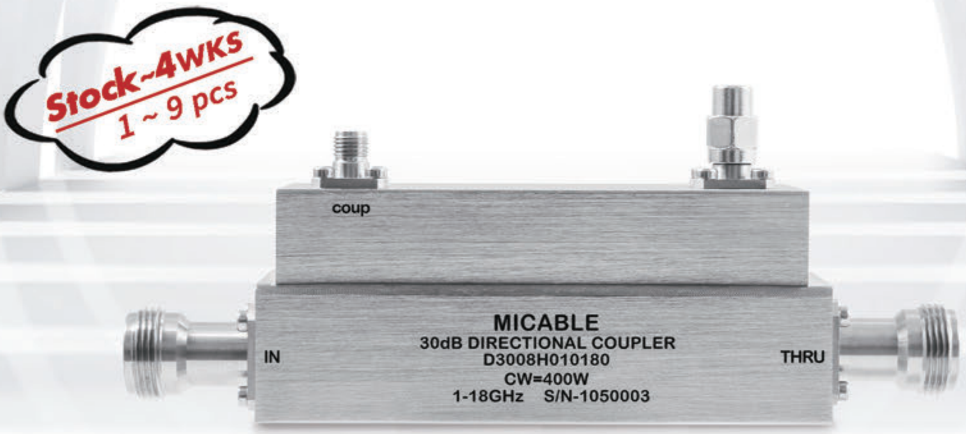

Test Curve of D3008H010180

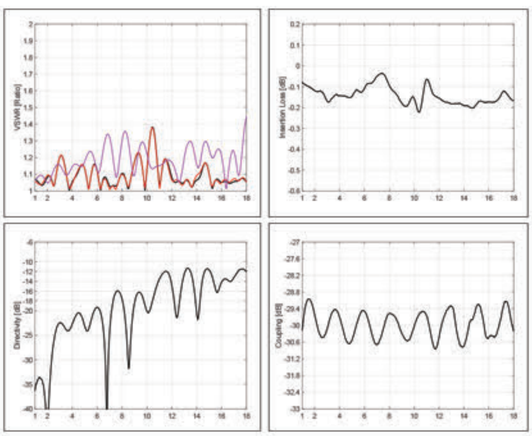

Freq. Range (GHz)	P/N	Coupling Max.(dB)	Main Line VSWR	Coupling VSWR	Insertion Loss*	Flatness	Directivity Min.(dB)	Power Max.(W)	Unit Price** (USD)
			Max.(:1)		Max.(dB)				
0.3-6	D3012H003060	30±0.9	1.4	1.4	0.6	±1.2	15	600	1,678
	D4012H003060	40±1.0	1.4	1.4	0.6	±1.3	15	600	1,678
0.5-6	D3012H005060	30±0.7	1.3	1.3	0.4	±1.0	15	600	1,175
	D4012H005060	40±0.8	1.3	1.3	0.4	±1.1	15	600	1,175
0.5-18	D3008H005180	30±1.2	1.5	1.6	1.0	±1.2	10	400	3,362
	D4008H005180	40±1.2	1.5	1.6	1.0	±1.4	10	400	3,362
0.7-8	D3012H007080	30±0.8	1.4	1.4	0.5	±1.0	14	600	1,265
	D4012H007080	40±0.8	1.4	1.4	0.5	±1.0	14	600	1,265
1-8	D3012H010080	30±0.8	1.4	1.4	0.4	±0.9	14	600	1,076
	D4012H010080	40±0.8	1.4	1.4	0.4	±0.9	14	600	1,076
1-18	D3008H010180	30±1.2	1.5	1.6	0.6	±1.0	10	400	2,475
	D4008H010180	40±1.2	1.5	1.6	0.6	±1.0	10	400	2,475
2-18	D3008H020180	30±1.0	1.5	1.6	0.6	±0.8	10	400	2,178
	D4008H020180	40±1.0	1.5	1.6	0.6	±0.8	10	400	2,178
6-18	D3008H060180	30±1.0	1.5	1.6	0.5	±0.7	10	400	928
	D4008H060180	40±1.0	1.5	1.6	0.5	±0.7	10	400	928

* Theoretical I.L. Included
** FOB FUZHOU FACTORY

More Information-
Scan the QR Code

Fujian MIcable Electronic Technology Group Co.,Ltd
Tel: +86-591-87382856 Email: sales@micable.cn Website: www.micable.cn

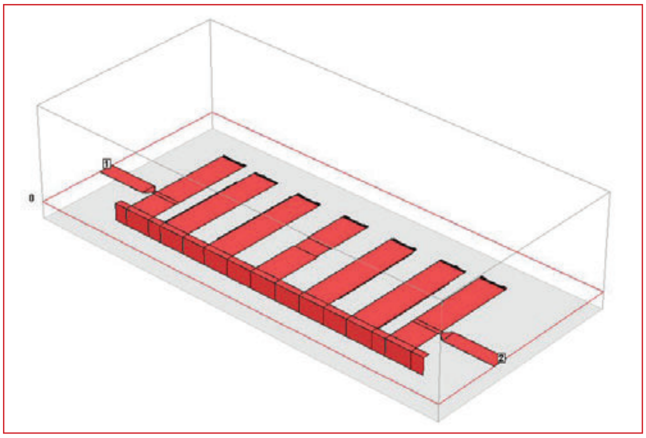

Fig. 8 **X-Band microstrip combline filter with N = 7, modeled with Sonnet. The via to ground is realized as a metalized slot in the substrate.**

cutoff, a transmission zero appears in the upper stopband due to non-adjacent couplings between the resonators (see ***Figure 9***). Using an approximate technique,[12] we proved to ourselves that including couplings between next nearest neighbors was not enough. All the non-adjacent couplings had to be included to come close to measured results.

Later in the mid-1980s, as computer power improved, we had access to more sophisticated 2D cross-section quasi-TEM and Spectral Domain Method models for multiple coupled strips in multilayer dielectrics. The quasi-TEM models generated a capacitance and inductance matrix that could be easily converted into an admittance matrix in a circuit simulator. The Spectral Domain models included energy that went into longitudinal section electric and magnetic (LSE and LSM) modes which had no simple, unambiguous conversion into an admittance matrix. Measured versus modeled results using these 2D cross-section methods can be found in the work of Swanson and Hoeffer.[13]

In late 1989 and early 1990 when the first 3D full wave electromagnet (EM) simulators appeared, they initially could only produce individual discontinuity models that we used to augment our 2D cross-section solver solutions. As EM simulation software became more efficient and computer power continued to increase, we could finally model the complete filter in a 3D EM environment. Like the inline cavity combline, we noticed interesting interactions between the filter and the cutoff waveguide channel that enclosed it. The resonators in any distributed printed filter couple to evanescent modes in the channel, which must be accounted for in the simulation.

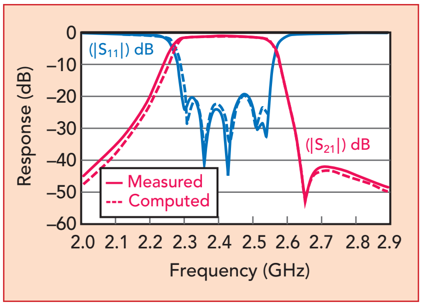

Fig. 9 **Measured vs. computed responses of the microstrip interdigital filter.**[11]

In ***Figure 10*** we see measured results for the interdigital filter in Figure 7 with the cover on and off. The cover is far enough away from the substrate surface to preclude any significant influence on resonator impedances and coupling coefficients. Further proof is that when the cover is replaced by a coarse metal screen or even a metallic paper clip across the channel, the response returns almost exactly to the full cover case.

All this means we must choose the cross-section dimensions of the channel early in the design process. If those dimensions change, a redesign of the filter is often required. In the coupling matrix there is clearly no a priori method to include all the non-adjacent couplings found in microstrip combline and interdigital filters; therefore, it cannot predict the high side transmission zero that results from those couplings.

CROSS-COUPLED CAVITY COMBLINE FILTERS

Before we begin our analysis of specific filter examples, we need to review an important contribution to our understanding of how transmission zeros are realized in cross-coupled cavity combline filters. From Wenzel,[14] three rules for how transmission zeros move in the complex plane are defined and two zero movement types are also defined (see ***Figure 11***). In our filter examples we are primarily concerned with the behavior of a simple quad. To analyze the simple quad, we start with four inductively coupled resonators and add a capacitive cross-coupling from Resonator 1 to Resonator 4.

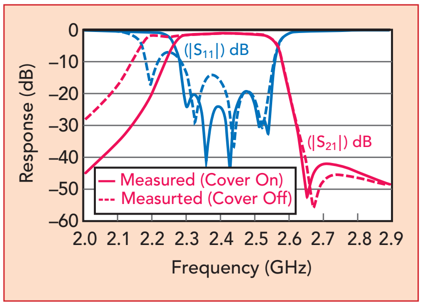

Fig. 10 Measured interdigital filter, comparing the cover on and off.[11]

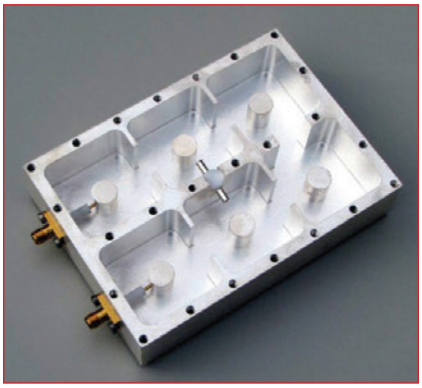

Fig. 12 Folded N = 6 combline filter with two transmission zeros.[15]

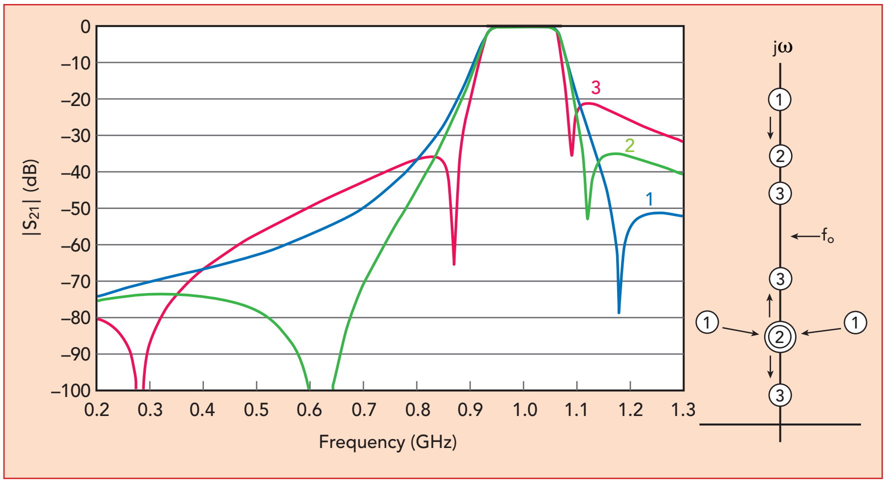

Fig. 11 Movement of transmission zeros in the complex plane for a simple quad.[14]

Using the notation of Wenzel,[14] as the capacitance is increased from zero, first a Type 1 zero appears above the passband and a complex quad of Type 2 zeros break off from infinity. As the capacitance increases further, two of the Type 2 zeros meet on the positive jω axis while the upper stopband zero moves closer to the passband. In the notation of Wenzel,[14] this is the break frequency where the two low side zeros finally split and move in opposite directions.

We observe there are not one but two zeros in the lower stopband. Those zeros may be coincident, or not, depending on the filter bandwidth and tuning. In either case, the result is the asymmetric stopband rejection we will observe in our filter examples. It is this complex zero movement that cannot be reproduced by a coupling matrix. When we introduce a simple quad in conventional coupling matrix software, a single zero appears in the lower and upper stopbands and the two zeros move with almost perfect symmetry for any value of the capacitive cross-coupling.

FOLDED CROSS-COUPLED COMBLINE FILTER EXAMPLES

Our first example is a folded N = 6 combline filter from an excel-

Lowest Noise in the Industry

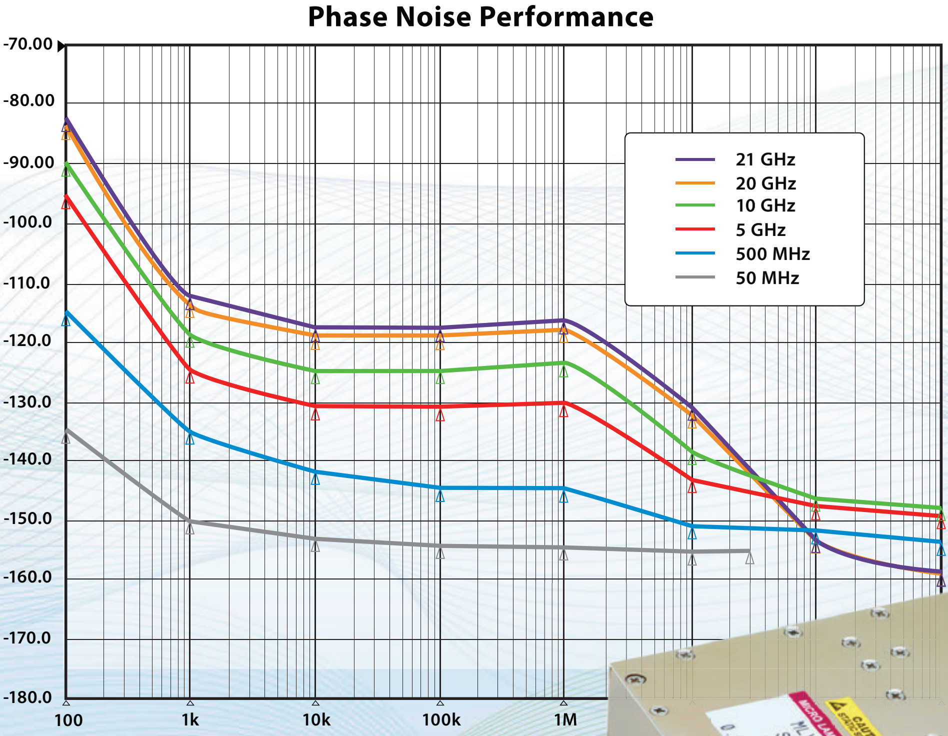

US patents #9,793,904 B1, #9,734,099 B1

Wide Band, Fast Tune Frequency Synthesizers

Industry Leading Performance!

The LUXYN™ MLVS-Series Frequency Synthesizers from Micro Lambda Wireless is one of the fastest and quietest synthesizers on the market. Standard frequency models are available covering 500 MHz to 20 GHz and 500 MHz to 10 GHz with options to cover down to 50 MHz and up to 21 GHz in a single unit.

With the lowest noise in the industry, (phase noise at 5 GHz is -130 dBc/Hz @ 10 kHz offset and at 10 GHz is -125 dBc/Hz @ 10 kHz offset), these synthesizers are designed for low noise & fast tune applications such as Receiving Systems, Frequency Converters and Test & Measurement Equipment.

For more information contact Micro Lambda Wireless.

www.microlambdawireless.com

Micro Lambda is a ISO 9001:2015 Registered Company

MICRO LAMBDA WIRELESS, INC.

"Look to the leader in YIG-Technology"

46515 Landing Parkway, Fremont CA 94538 • (510) 770-9221 • sales@microlambdawireless.com

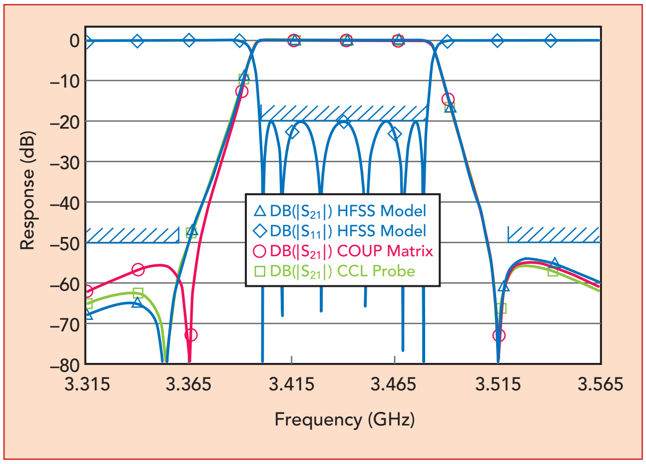

Fig. 13 Simulations with the capacitive probe modeled as a transmission line cascade: HFSS (blue), coupling matrix (red) and CCL (green).

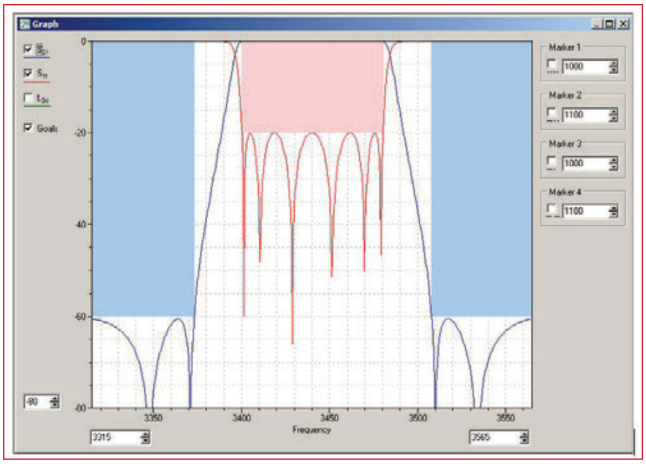

Fig. 14 Coupling matrix prediction for two cross-couplings in the N = 6 folded filter. The stopband rejection stays symmetrical for all cross-coupling values.

lent tutorial paper by Morten Hagensen[15] that includes measured data (see ***Figure 12***). This filter is located in the WiMax band and has 3 percent relative bandwidth, which is well within the acceptable range for the coupling matrix approach.

We generated network theory and EM models to contrast with the coupling matrix prediction for this filter. If we place a capacitive (negative) coupling between Resonator 2 and Resonator 5, the coupling matrix predicts nearly perfect symmetry in the stopbands (see ***Figure 13***). This symmetry is maintained as we increase or decrease the magnitude of the cross-coupling; but, the measured data, the network theory model and the 3D FEM model each present the asymmetric response predicted in the previous section.

After many years of experience with port tuning, we trust the 3D EM model to be correct. Even with a simple lumped capacitor cross-coupling in the network theory model we see the same type of asymmetry predicted by the EM model. As we increase the complexity of the capacitive probe model, correlation with the EM model gets better and better.

In his tutorial paper, Hagensen[15] speculates that the asymmetry observed in the measured hardware is due to a parasitic coupling from Resonator 2 to Resonator 4; however, there are no parasitic couplings in our network theory model, which agrees with the 3D EM simulation.

A more dramatic example can be found when we add a second inductive (positive) cross-coupling from Resonator 1 to Resonator 6. Again, the coupling matrix tells us the rejection in the stopbands will be very symmetrical, no matter what magnitudes we choose for the two cross-couplings (see ***Figure 14***).

When we port tune the EM model we can find a set of tunes that meet the rejection goal in the upper stopband, but the transmission zeros in the lower stopband are not distinct and rejection is compromised (see ***Figure 15***). The low side transmission zeros disappear. If we model the capacitive probe carefully the network theory model agrees with the EM simulation.

Likewise, we can find a different tuning that meets the rejection in the lower stopband, but now the rejection in the upper stopband does not meet the specification (see ***Figure 16***).

iNRCORE
TTE Z1000
BTS-2BG

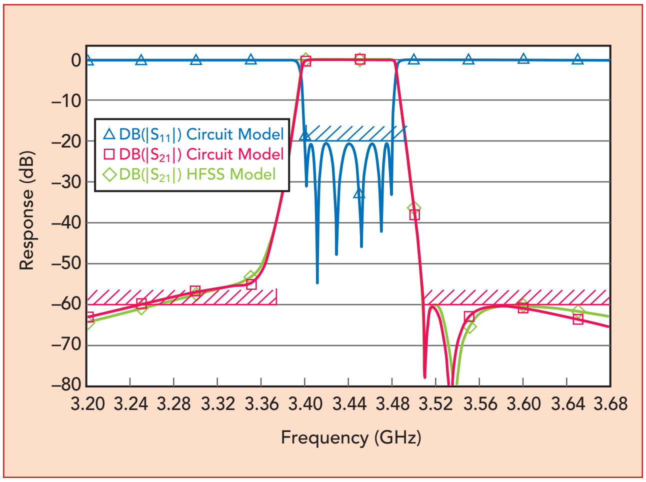

Fig. 15 EM model port tuned to match upper stopband goals. The low side transmission zeros disappear.

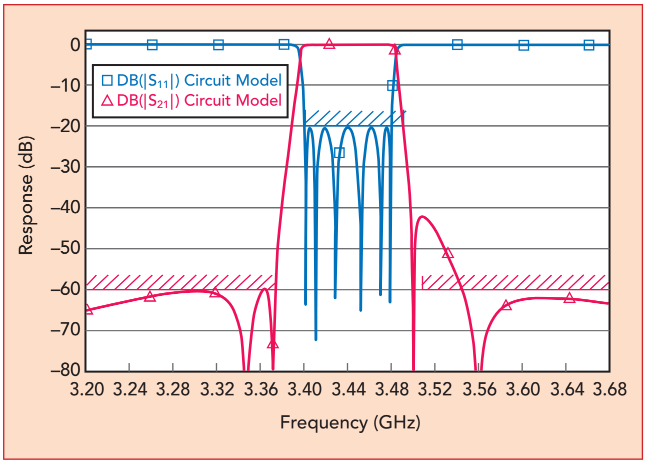

Fig. 16 EM model port tuned to match the lower stopband goals, showing the upper stopband no longer meets the specification.

We conclude that there is no tuning solution that actually meets the symmetrical stopband rejection predicted by the coupling matrix. We can find a more symmetric solution by making the quad complex (adding a capacitive diagonal coupling). As pointed out by Wenzel,[14] however, this simple addition can have a surprising impact on tuning sensitivity.

Finally, we noticed another measured versus modeled result in the literature that supports our analysis. It is another N = 6 folded combline filter. In Zhang et al. (Figure 13),[16] the interior rejection peaks predicted by the coupling matrix are symmetric while the measured filter is asymmetric (see ***Figure 17***).

Although no dimensions are given by Zhang et al.,[16] we constructed a quick network theory model like Figure 2 based on an estimation of their geometry. With only a simple lumped capacitive coupling from resonator two to five and lumped element resonated couplings at the input and output, we produced the plot in ***Figure 18***, which agrees well with the measured asymmetry.

As in Hagensen,[15] the unproved claim is that parasitic couplings are the source of the transmission zero asymmetry. Again, we point out there are no parasitic couplings in the network theory model we derived. Rather, the simple quad is behaving as predicted by Wenzel.[14]

CONCLUSION

We have demonstrated simulation and design methods for practical combline filters using three distinct combinations of topology and technology. The emphasis is on finding methods that fully predict the filter performance in both the passband and stopbands. We have also pointed out where the popular coupling matrix synthesis may fall short in this regard. Our concern is

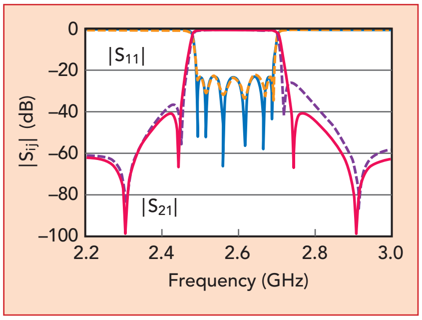

Fig. 17 Measured (dashed lines) vs. synthesized (solid lines) responses.[16]

10 MHz ***Rubidium Frequency Standard***

- 5 MHz and 10 MHz outputs
- Ultra-low phase noise (<–130 dBc/Hz at 10 Hz)
- 0.005 ppm aging over 20 years
- Built-in distribution amplifier (up to 22 outputs)
- 1 pps input and output

The FS725 Benchtop Rubidium Frequency Standard is ideal for metrology labs, R&D facilities, or anywhere a precision frequency standard is required.

It has excellent aging characteristics, extremely low phase noise, and outstanding reliability. A 1 pps input is provided for phase-locking to GPS, providing Stratum 1 performance.

With a built-in 5 MHz and 10 MHz distribution amplifier, the FS725 is the ultimate laboratory frequency standard.

Allan Variance vs. Time

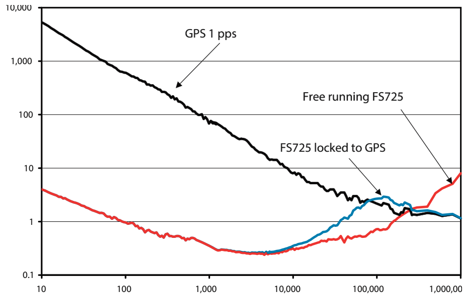

Observation Interval (seconds)

FS725 Rear Panel

FS725... $2,995 (U.S. list)

SRS Stanford Research Systems

www.thinksrs.com/products/FS725.html
Tel: (408)744-9040

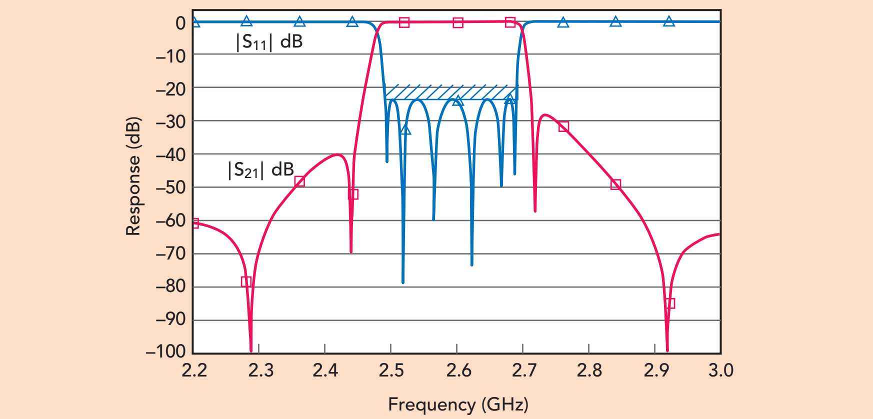

Fig. 18 Estimated network theory model for Zhang et al.,[12] which agrees with the measurement.

that a student or novice engineer might assume that any coupling matrix synthesis result fully predicts the performance of the realized combline filter.

In the end, our own filter design flows rely on an early approximation of filter performance with network theory models and then a quick transition to 3D EM models that can be rapidly optimized using port tuning. The port tuning process can be automated to find exact dimensions, when needed, with a minimum number of EM simulations.[17] The simple linear interpolation scheme described by Swanson[17] is easily understood, far easier to implement and much more efficient than most EM based optimization methods currently available in the literature. ■

References

1. G. L. Matthaei, "Comb-Line Band-Pass Filters of Narrow or Moderate Bandwidth," *Microwave Journal*, Vol. 6, No. 8, August 1963, pp. 82–96.
2. E. C. Johnson, "New Developments in Designing Bandpass Filters," *Electronic Industries*, January 1964, pp. 87–94.
3. R. M. Kurzrok, "General Three-Resonator Filters in Waveguide," *IEEE Transactions on Microwave Theory and Techniques*, Vol. 14, No. 1, January 1966, pp. 46–47.
4. R. M. Kurzrok, "General Four-Resonator Filters at Microwave Frequencies," *IEEE Transactions on Microwave Theory and Techniques*, Vol. 14, No. 6, June 1966, pp. 295–296.
5. A. E. Atia and A. E. Williams, "Narrow Bandpass Waveguide Filters," *IEEE Transactions on Microwave Theory and Techniques*, Vol. 20, No. 4, April 1072, pp. 258–265.
6. "Cavity Combline (CCL)" Design Software, *DGS Associates*, Web: https://www.dgs-boulder.com/cavity-combline-ccl.
7. R. J. Wenzel, "Synthesis of Combline and Capacitively Loaded Interdigital Bandpass Filters of Arbitrary Bandwidth," *IEEE Transactions on Microwave Theory and Techniques*, Vol. 19, No. 8, August 1971, pp. 678–686.
8. E. G. Cristal, "Tapped-Line Coupled Transmission Lines with Applications to Interdigital and Combline Filters," *IEEE Transactions on Microwave Theory and Techniques*, Vol. 23, No. 12, December 1975, pp. 1007–1012.
9. I. Shapir, V. A. Sharir and D. G. Swanson, "TEM Modeling of Parasitic Bandwidth Expansion in Combline Filters," *IEEE Transactions on Microwave Theory Techniques*, Vol. 47, No. 9, September 1999, pp. 1664–1669.
10. "Multiple Coupled Lines in a Rectangular Shield (Dynamic Model) (EM Quasi-Static): RCCOAX Symbol," *Cadence AWR*, Web: https://awrcorp.com/download/faq/english/docs/Elements/rccoax.htm.
11. D. G. Swanson, "Narrow-Band Microwave Filter Design," *IEEE Microwave Magazine*, Vol. 8, No. 5, October 2007, pp. 105–114.
12. D. G. Swanson, "A Novel Method for Modeling Coupling Between Several Microstrip Lines in MIC's and MMIC's," *IEEE Transactions on Microwave Theory and Techniques*, Vol. 39, No. 6, June 1991, pp. 917–923.
13. D. G. Swanson and W. J. R. Hoeffer, *Microwave Circuit Modeling Using Electromagnetic Field Simulation*, Artech House, 2003, pp. 381–383.
14. R. J. Wenzel, "Understanding Transmission Zero Movement in Cross-Coupled Filters," *IEEE MTT-S International Microwave Symposium Digest*, June 2003, pp. 1459–1462.
15. M. Hagensen, "Narrowband Microwave Bandpass Filter Design by Coupling Matrix Synthesis," *Microwave Journal*, Vol. 53, No. 4, April 2009, pp. 219–226.
16. Y. Zhang, F. Seyfert, S. Amari, M. Olivi and K. Wu, "General Synthesis Method for Dispersively Coupled Resonator Filters with Cascaded Topologies," *IEEE Transactions on Microwave Theory and Techniques*, Vol. 69, No. 2, February 2021, pp. 1378–1393.
17. D. G. Swanson, "Port Tuning a Microstrip Folded Hairpin Filter," *IEEE Microwave Magazine*, Vol. 21, No. 4, April 2020, pp. 18–28.

MiCable

NEW

110GHz HIGH PERFORMANCE MILLIMETER WAVE CABLE ASSEMBLIES

DC~110GHz

- **Cable Loss** <15dB/m@110GHz
- **VSWR** <1.45:1@110GHz
- **Shielding Effectiveness** <-90dB
- **Amplitude Stability vs. Flex.** <±0.1dB@110GHz
- **Phase Stability vs. Flex.** <±8°@110GHz
- **Phase Stablity vs.Temp.** 400ppm@-40℃~+70℃
- **Wire Diameter** 3.0mm w/ armor

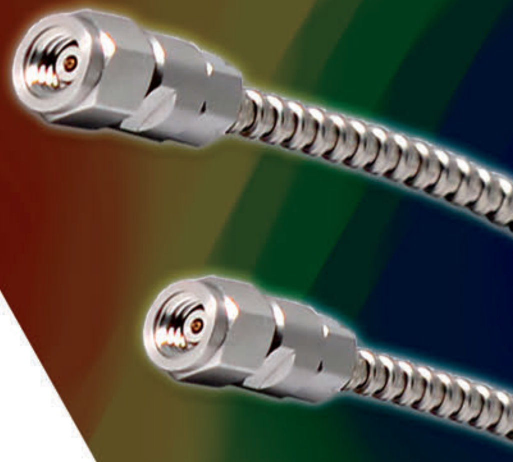

Model	Connector Configure	Length (inches)	Unit Price (1-9pcs)
T110-1Y-1Y-6	1mm male to 1mm male	6	$1,094
T110-1Y-1Y-12	1mm male to 1mm male	12	$1,116
T110-1Y-1Y-24	1mm male to 1mm male	24	$1,161

Applications

- Connections of module to module or rack to rack
- Various test systems
- Temperature cycle test in chamber
- Military & commercial millimeter wave equipment

VSWR

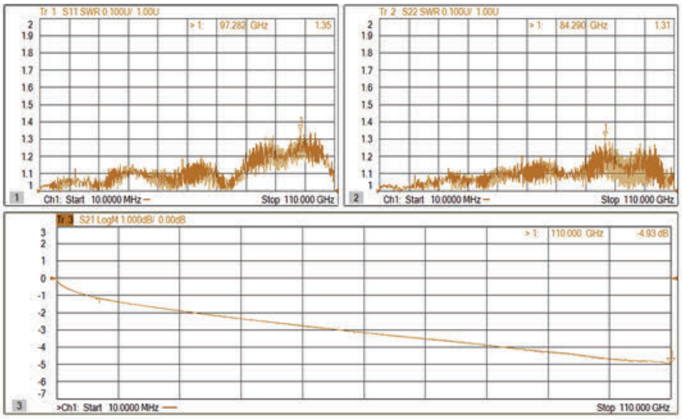

More Information-
Scan the QR Code

Fujian MIcable Electronic Technology Group Co.,Ltd
Tel: +86-591-87382856 Email: sales@micable.cn Website: www.micable.cn

Broadband Power Amplifier Design Method Based on SIR and Multi-Frequency Point Matching

Guohua Liu, Yijun Lin, Cantianci Guo and Zhiqun Cheng
Hangzhou Dianzi University, Hangzhou, China

A broadband power amplifier (PA) design is based on a stepped impedance resonator (SIR). Compared with an open circuit microstrip line resonator, the SIR has a better frequency response. Precise harmonic control of the open microstrip line and the SIR matching circuit has the potential for broadband harmonic suppression as well. A multi-frequency method with four frequency points is used to design the matching structure to improve power and bandwidth performance. A broadband high efficiency 1 to 3.8 GHz PA designed using this method yields an output power of 39.7 to 41 dBm with a gain of 9.7 to 11 dB and efficiency greater than 60 percent.

As important components of wireless communication systems, PAs have been the focus of research for many years. The performance of the PA determines the signal strength and working bandwidth of the system. Therefore, improving PA output power and bandwidth has always been a primary research objective.

Many PA design methods have been derived over years of research. With the Doherty PA using active load modulation technology, a peak PA is controlled by input power to achieve an optimal output impedance for high dynamic range operation.[1]

To improve efficiency, harmonic control PAs have been proposed. The main areas of research employ Class-J[2,3] and Class-F[4] modes, which are characterized by drain current and voltage waveform shaping with harmonic suppression matching circuits. The efficiency of the PA is improved because the drain current and voltage overlap area is reduced.

The Continuous Class-B/J PA[5,6] is an extension of the Class-J mode. The increased factor can be used for broadband matching, and the nonlinear effects of the drain-source capacitor CDS can improve efficiency.[7] The filter may be used as a harmonic suppression matching circuit as well.[8] Higher harmonics are filtered due to the frequency characteristics of the filter. Most filters, however, have narrow working bandwidths and complicated designs, and their characteristics influence the performance of the PA's working sideband.

The work presented here is based on the theory of a harmonic control PA with a combined matching structure of an open circuit microstrip resonator and a SIR. The multi-frequency point design method is adopted to achieve harmonic suppression and increase bandwidth. To verify its effectiveness, a broadband PA is designed and fabricated.

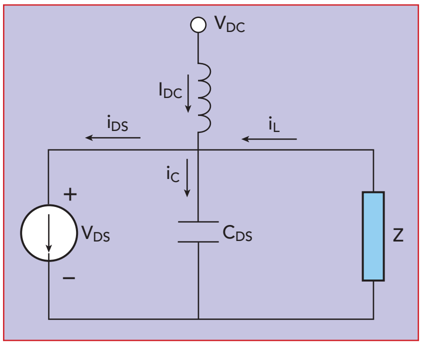

Fig. 1 Harmonic control PA circuit.

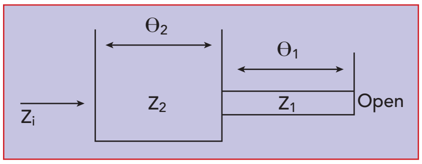

Fig. 2 λ/4 SIR.

THEORETICAL ANALYSIS

Harmonic Control PA

By controlling the output harmonics of the PA and shaping the output voltage and current waveforms, efficiency can be improved. A Class-F PA is a typical harmonic control power amplifier, nevertheless it is narrowband. Steve C. Cripps proposed a new PA with harmonic control (see ***Figure 1***).[9] Its voltage and current waveforms are:

$$I(\theta) = \frac{I_{max}}{\pi} + \frac{I_{max}}{2}\sin(\theta) + \frac{2I_{max}}{3\pi}\cos(2\theta) \quad (1)$$

$$V(\theta) = (1-\cos\theta)(1-\sin\theta) \quad (2)$$

where I_{max} is the maximum drain current. When only the fundamental and second harmonic are retained, the voltage and current waveforms are approximately half sine waves.[10] In Equations (1) and (2), the fundamental and second harmonic impedances are:

$$Z(f_0) = R_{opt} + jR_{opt} \quad (3)$$

$$Z(2f_0) = -j\frac{3\pi}{8}R_{opt} \quad (4)$$

where $R_{opt}=2(V_{DC}-V_k)/I_{max}$, which is the optimal load impedance. V_{DC} is the drain power supply, V_k is the knee voltage and I_{max} is the maximum drain current. In Equation (4), unlike for a Class-F PA, the second harmonic impedance is reactive, which means that the matching impedance can move around the Smith chart, and so it has the potential to be broadband.

SIR

In this design, a λ/4 SIR[11] comprises two transmission lines with different characteristic impedances (see ***Figure 2***). Z_i is the input impedance, Z_1 and Z_2 are the characteristic impedances of the two transmission lines and θ_1 and θ_2 are the electrical lengths of Z_1 and Z_2, respectively. Therefore, Z_i is:

$$Z_i = Z_2\frac{Z_1 - Z_2\tan\theta_2\tan\theta_1}{jZ_2\tan\theta_1 + jZ_1\tan\theta_2} \quad (5)$$

When Z_i is equal to zero, the relationship between characteristic impedance and electrical length is:

$$Z_2Z_1 - Z_2^2\tan\theta_1\tan\theta_2 = 0 \quad (6)$$

$$\tan\theta_1\tan\theta_2 = \frac{Z_1}{Z_2} = R_Z \quad (7)$$

where R_Z is a free design parameter.

The input impedance of a λ/4 open-ended stub is determined by its characteristic impedance and electrical length. By comparison, the SIR structure has more free design parameters. Although the SIR structure provides better harmonic suppression, its increased length results in greater signal loss. The combination of a λ/4 open circuit microstrip line and SIR offers higher harmonic suppression while minimizing signal loss.

MATCHING NETWORK CIRCUITS DESIGN

Based on the above theoretical analysis of a harmonic control PA and SIR structure, a multi-frequency point design method is used to realize the combined open circuit microstrip line resonator and SIR matching structure. Four frequency points (f_1, f_2, f_3, f_4) are selected.

The influence of higher harmonics in the PA becomes larger as frequency increases, so the SIR provides a wider harmonic suppression bandwidth, but at the cost of increased signal loss. To improve harmonic suppression while minimizing loss, a hybrid circuit structure is used for output matching.

Open circuit microstrip line resonator matching is used at frequencies f_1 and f_2, while the SIR is designed for matching at frequencies f_3 and f_4 to further expand the harmonic suppression bandwidth. A center frequency f = 2.4 GHz is selected. To keep low frequency second harmonics from overlapping with the high frequency fundamental and to avoid wide spacing between the four frequencies, the frequency points $f_1 = 2$, $f_2 = 2.6$, $f_3 = 3.2$ and $f_4 = 3.8$ GHz are selected.

The harmonic control matching network is shown in ***Figure 3a***. Z_{IN} is

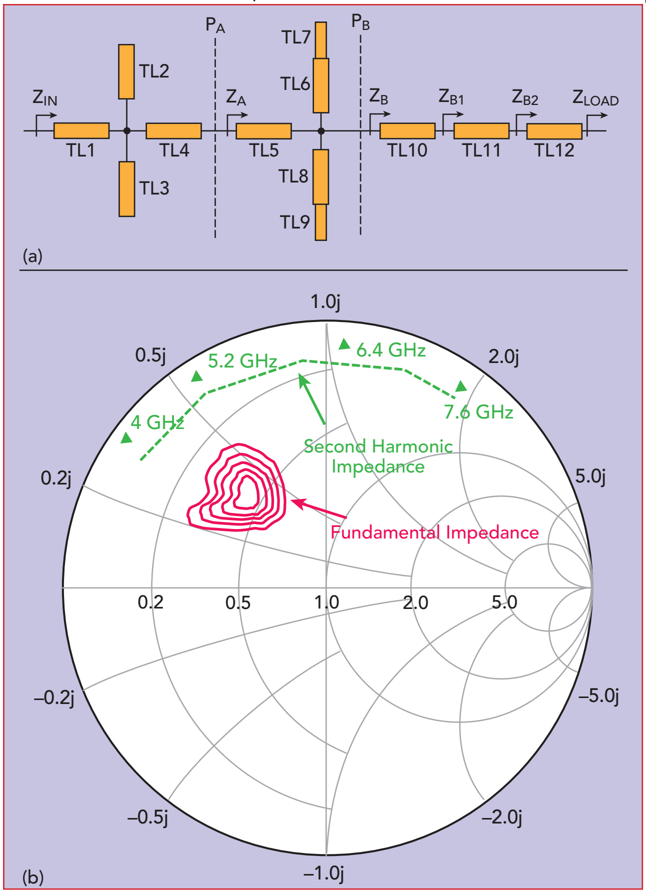

Fig. 3 Harmonic control matching circuit (a) and simulated fundamental and second harmonic impedances (b).

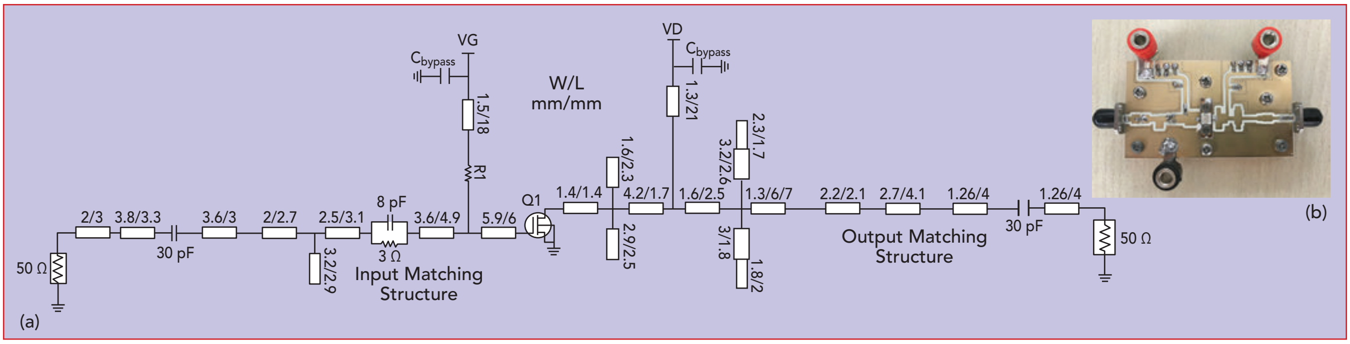

Fig. 4 Schematic (a) and fabricated (b) PA.

the transistor drain impedance; TL2 and TL3 are open circuit microstrip line resonators; TL6, TL7 and TL8, TL9 are SIRs; TL1, TL4 and TL5 are impedance transformation lines and TL10 is a tuned line.

In this design, only the second harmonic is suppressed. The harmonic suppression circuit design includes two parts. One matches a specific frequency from an open circuit impedance to a short circuit impedance, and the other matches a short circuit impedance to the drain impedance. The open circuit microstrip line resonators are designed at f_1 and f_2, respectively. TL2 and TL3 match the second harmonic impedance from an open circuit impedance to a short circuit impedance. The electrical lengths of the microstrip lines meet the following requirements:

$$\theta_2^{2f_1} = 90° \quad (8)$$

$$\theta_3^{2f_2} = 90° \quad (9)$$

The electrical lengths of θ_2 and θ_3 are set to λ/4 at frequencies $2f_1$ and $2f_2$, respectively. The characteristic impedances Z_2 and Z_3 of TL2 and TL3 can be designed freely. In this design, Z_2 = 39 Ω and Z_3 = 25.5 Ω. A terminal short circuit impedance transformation line, TL1, must be added to match the short circuit impedance to the transistor drain impedance. The relationship between the electrical length and impedance of TL1 is:

$$Z_{IN}(2f_1) = jZ_1 \tan\left(\theta_1^{2f_1}\right) \quad (10)$$

$$Z_{IN}(2f_2) = jZ_1 \tan\left(\theta_1^{2f_2}\right) \quad (11)$$

$$\theta_1^{2f_2} = k_1\theta_1^{2f_1} \quad (12)$$

where k_1 is defined as f_2/f_1 in Equation (12) and Z_1 is the characteristic impedance of TL1 in Equations (10) and (11).

Impedances $Z_{OMN(2f1)}$ and $Z_{OMN(2f2)}$ are the optimal impedances at $2f_1$ and $2f_2$ of the transistor and can be obtained by second harmonic load-pull. To ensure that the second harmonic impedances of f_1 and f_2 are purely reactive, it is necessary to freely tune Z_1 and θ_1. In this design, Z_1 = 42.4 Ω and θ_1= 7.4 degrees at $2f_1$.

The SIR is used to suppress harmonic effects caused by high frequencies and is designed at f_3 and f_4. According to the above theory, the electrical length and characteristic impedance of the SIR must satisfy Equations (5) through (7) and the relationships are:

$$\tan\theta_6^{2f_3} \tan\theta_7^{2f_3} = \frac{Z_7}{Z_6} \quad (13)$$

$$\tan\theta_8^{2f_4} \tan\theta_9^{2f_4} = \frac{Z_9}{Z_8} \quad (14)$$

where θ_6 and θ_7 are the TL6 and TL7 electrical lengths corresponding to $2f_3$, and where θ_8 and θ_9 are the TL8 and TL9 electrical lengths corresponding to $2f_4$. Z_6, Z_7, Z_8 and Z_9 are the characteristic impedances of TL6 through TL9 of the two SIRs, respectively. With the impedances Z_6 = 24, Z_7 = 29, Z_8 = 30 and Z_9 = 35 Ω, the electrical lengths are determined by Equations (13) and (14).

To simplify the calculation, two impedance planes PA and PB are defined. Then the second harmonic impedances of f_3 and f_4 can be obtained by load-pull simulation. The short circuit impedance transformation line matches the second harmonic impedances of f_3 and f_4 to the short circuit plane PB. The relationship between electrical length and characteristic impedance is:

$$Z_A(2f_3) = jZ_5 \tan\left(\theta_5^{2f_3}\right) \quad (15)$$

$$Z_A(2f_4) = jZ_5 \tan\left(\theta_5^{2f_4}\right) \quad (16)$$

$$\theta_5^{2f_4} = k_2\theta_5^{2f_3} \quad (17)$$

where $Z_A(2f_3)$ and $Z_A(2f_4)$ are the drain second harmonic impedances matched to plane PA after calculation, k_2 is defined as f_4/f_3, and θ_5 and Z_5 are the electrical length and characteristic impedance of TL5. Similarly, Z_5 can be adjusted to reduce the interaction between the two SIRs on the second harmonic impedance. TL4 is microstrip line connecting the previous circuit and the bias circuit.

To match the impedance $Z_{LOAD(f0)}$ to the optimal fundamental impedance of plane P_B (obtained by load-pull simulation), the fundamental matching circuit can be designed by:

$$Z_B = Z_{10}\frac{Z_{B1} + jZ_{10}\tan(\theta_{10})}{Z_{10} + jZ_{B1}\tan(\theta_{10})} \quad (18)$$

$$Z_{B1} = Z_{11}\frac{Z_{B2} + jZ_{11}\tan(\theta_{11})}{Z_{11} + jZ_{B2}\tan(\theta_{11})} \quad (19)$$

$$Z_{B2} = Z_{12}\frac{Z_{LOAD} + jZ_{12}\tan(\theta_{12})}{Z_{12} + jZ_{LOAD}\tan(\theta_{12})} \quad (20)$$

where Z_B is the equivalent fundamental impedance in plane P_B.

To implement this circuit, six circuit parameters Z_{10}, Z_{11}, Z_{12}, θ_{10}, θ_{11} and θ_{12} must be determined. Three equations (18 through 20) are obtained for each frequency point condition. When f_2 and f_3 are selected, the above six parameters are calculated. The output har-

Ultra Low Phase Noise Phase Locked Clock Translators

Up to 27.5 GHz

Features
- Cost Effective
- Eliminates Noisy Multipliers
- Patented Technology

Applications
- Scanning & Radar Systems
- High Frequency Network Clocking (A/D & D/A)
- Test & Measurement Equipment
- High Performance Frequency Converters
- Base Station Applications
- Agile LO Frequency Synthesis

New!

Model	Frequency (Mhz)	Typical Phase Noise		Package
		@10 kHz	@100 kHz	
VFCTS100-10	100	-156	-165	
VFCTS105-10	105	-156	-165	
VFCTS120-10	120	-156	-165	
VFCTS125-10	125	-156	-165	
VFCTS128-10	128	-155	-160	
FCTS800-10-5	800	-144	-158	
FCTS1000-10-5	1000	-141	-158	
FCTS1000-100-5	1000	-141	-158	
FSA1000-100	1000	-145	-160	
FXLNS-1000	1000	-149	-154	
KFCTS1000-10-5	1000	-141	-158	
KFCTS1000-100-5	1000	-141	-158	
KFSA1000-100	1000	-145	-160	
KFXLNS-1000	1000	-149	-154	
FCTS2000-10-5	2000	-135	-158	
FCTS2000-100-5	2000	-135	-158	
KFCTS2000-100-5	2000	-135	-158	
KSFLOD12800-12-1280	12800	-122	-123	
KSFLOD25600-12-1280	25600	-118	-118	
KSFLO27R5-100-12	27500	-88	-98	

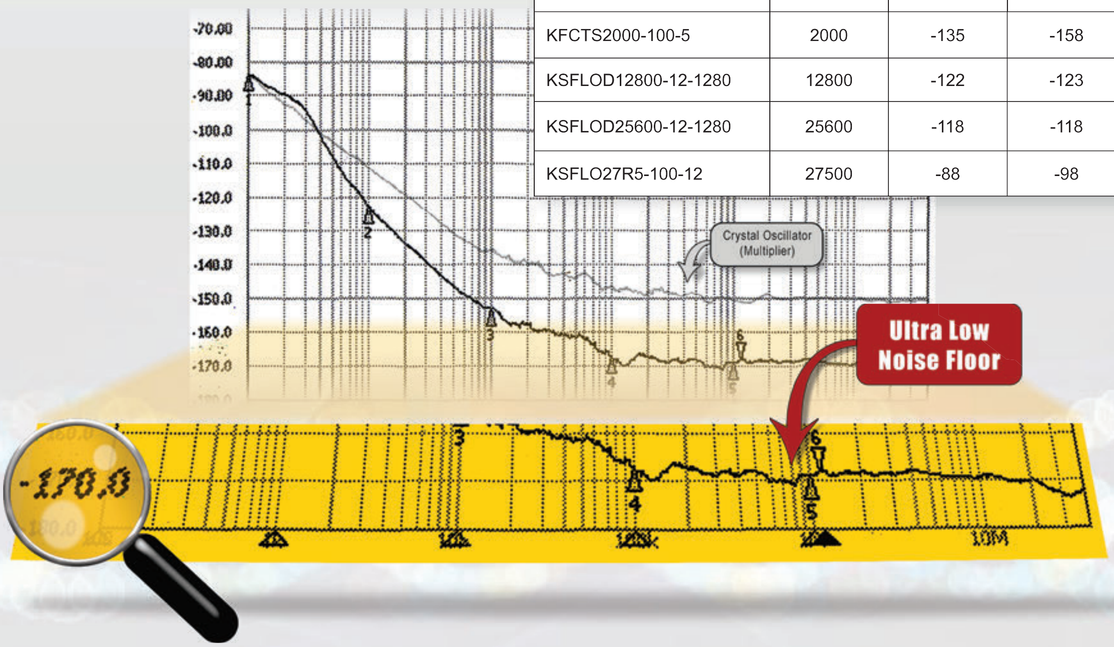

Talk To Us About Your Custom Requirements.

SYNERGY® MICROWAVE CORPORATION
Phone: (973) 881-8800 | Fax: (973) 881-8361
E-mail: sales@synergymwave.com | Web: www.synergymwave.com
Mail: 201 McLean Boulevard, Paterson, NJ 07504

monic suppression circuit consists of TL1 through TL12. The simulated impedances of the transistor are shown in ***Figure 3b***.

CIRCUIT SIMULATION AND MEASUREMENT

To validate the design method, a broadband PA (see ***Figure 4***) is designed with a CGH40010F GaN transistor. The amplifier is mounted on a 0.508 mm thick Rogers RO4350B substrate with an ε_r of 3.66. The Gate supply V_{GS} = -2.7 V and the drain supply V_{DS} = 28 V.

The second harmonic is suppressed by the multi-frequency method. From 1 to 1.9 GHz, four frequency points of 1, 1.3, 1.6 and 1.9 GHz are selected for testing. From the test results, second harmonic suppression is -18.2, -32.9, -21.3 and -23 dBc, respectively. From 2 to 3.8 GHz, because the second harmonic is outside the working band, suppression is greater. Voltage and current waveforms are shown in ***Figure 5***.

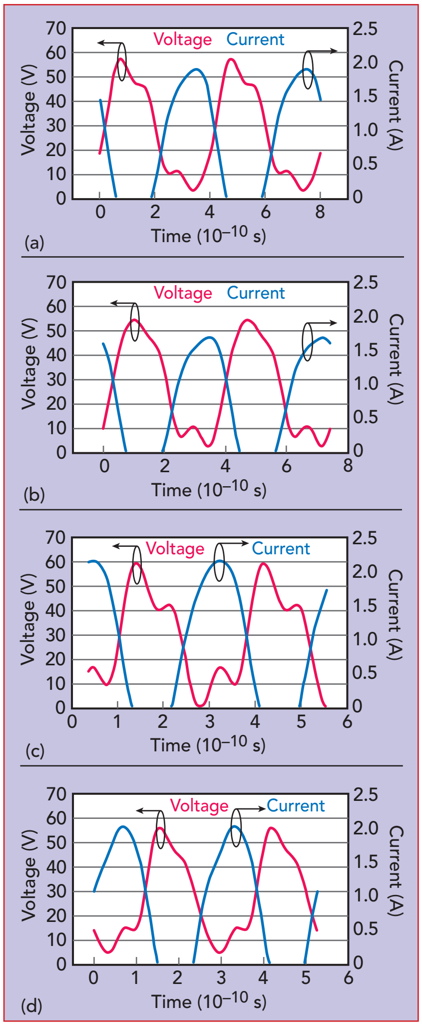

Fig. 5 Simulated drain voltage and current waveforms at 2 (a), 2.6 (b), 3.2 (c) and 3.8 (d) GHz.

Single-tone continuous wave signal measurements are performed over the designed operating band from 1 to 3.8 GHz (see ***Figure 6***). Measured and simulated results of drain efficiency (DE), output power and gain are shown in Figure 6a. DE and gain changing with the input power are shown in Figure 6b. The saturated output power is 39.7 to 41 dBm, the gain exceeds 10 dB over the band and the DE is between 60 and 68 percent from 1 to 3.8 GHz. The relative bandwidth is greater than 116 percent.

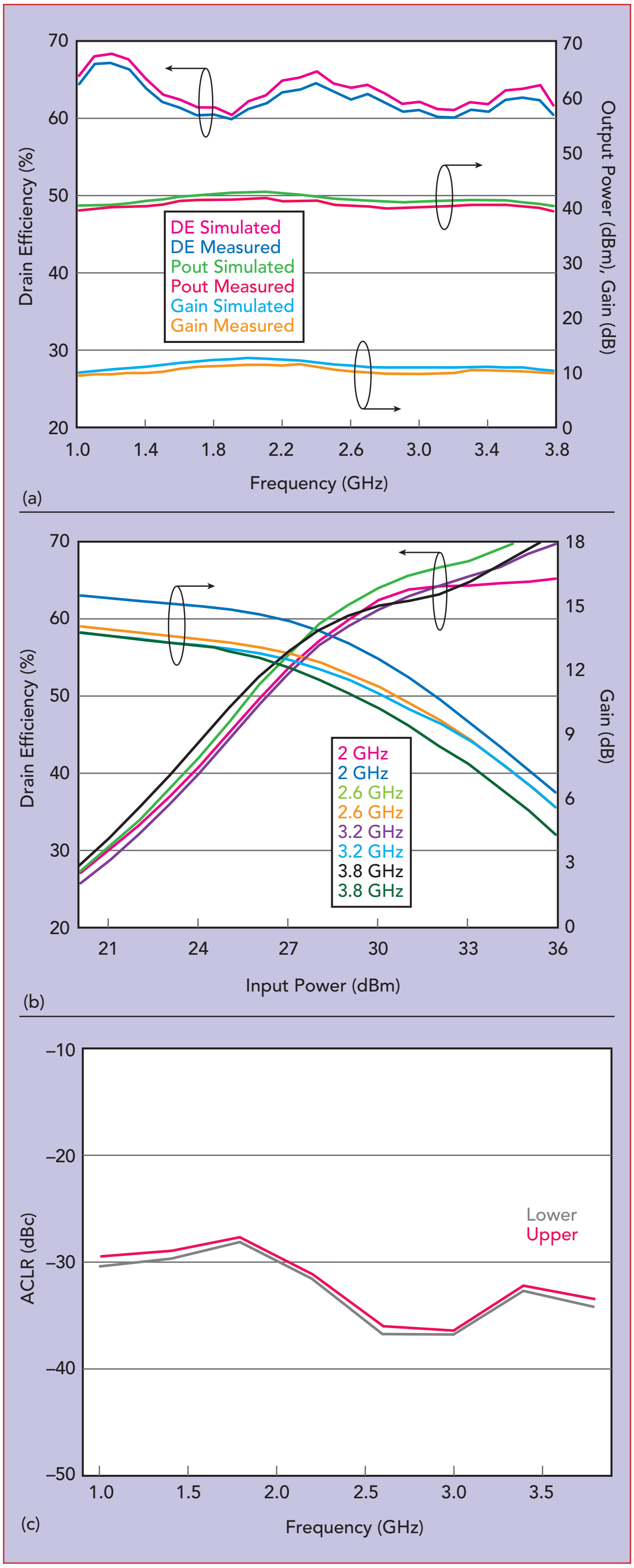

Fig. 6 Measured vs. simulated DE, output power and gain (a), measured vs. simulated output power and DE (b) and measured ACLR (c).

To demonstrate linearity, the PA is driven by a 10 MHz W-CDMA signal with peak-to-average power ratio of 6.5 dB. The adjacent channel leakage ratio (ACLR) is shown in Figure 6c. The average output power is about 36 dBm. An ACLR of less than -27.8 dBc is obtained within the 1.0 to 3.8 GHz band.

Some published broadband PA results are shown in ***Table 1***. The PA described here has better efficiency and output power for approximately the same bandwidth.

CONCLUSION

A broadband PA based on SIR and multi-frequency points matching reduces the impact of high frequency harmonics to enhance PA performance. A prototype PA achieves an output

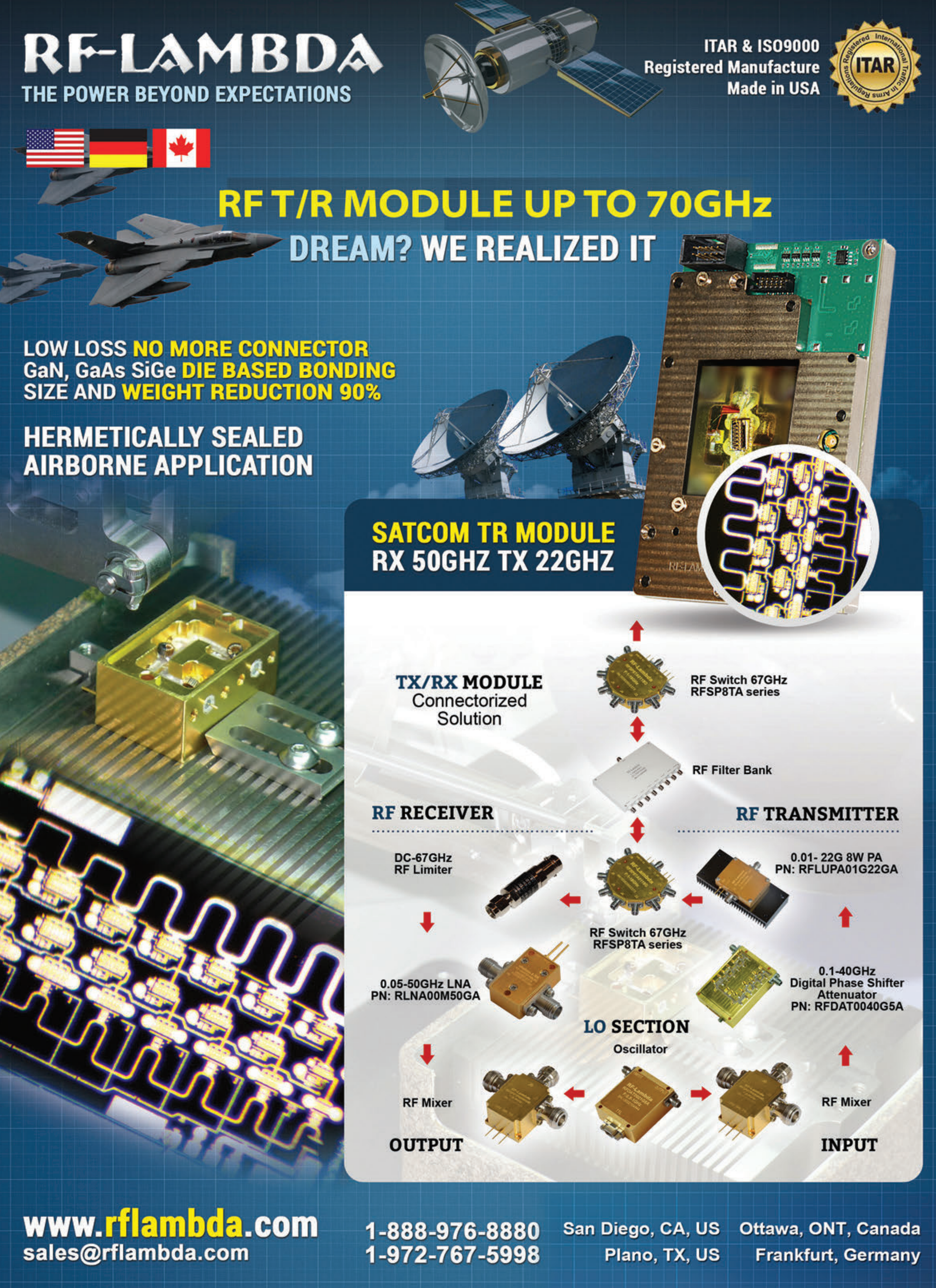

RF-LAMBDA
THE POWER BEYOND EXPECTATIONS
ITAR & ISO9000
Registered Manufacture
Made in USA
ITAR
RF T/R MODULE UP TO 70GHz
DREAM? WE REALIZED IT
LOW LOSS NO MORE CONNECTOR
GaN, GaAs SiGe DIE BASED BONDING
SIZE AND WEIGHT REDUCTION 90%
HERMETICALLY SEALED
AIRBORNE APPLICATION
SATCOM TR MODULE
RX 50GHZ TX 22GHZ
TX/RX MODULE
Connectorized
Solution
RF Switch 67GHz
RFSP8TA series
RF Filter Bank
RF RECEIVER
RF TRANSMITTER
DC-67GHz
RF Limiter
0.01- 22G 8W PA
PN: RFLUPA01G22GA
RF Switch 67GHz
RFSP8TA series
0.05-50GHz LNA
PN: RLNA00M50GA
0.1-40GHz
Digital Phase Shifter
Attenuator
PN: RFDAT0040G5A
LO SECTION
Oscillator
RF Mixer
RF Mixer
OUTPUT
INPUT
www.rflambda.com
sales@rflambda.com
1-888-976-8880
1-972-767-5998
San Diego, CA, US
Plano, TX, US
Ottawa, ONT, Canada
Frankfurt, Germany

TABLE 1

BROADBAND PA COMPARISON

Reference	Frequency (GHz)	Bandwidth (%)	DE (%)	Pout (dBm)
2	2.8 to 4.2	40	58 to 78	40.6 to 42
3	1.4 to 2.4	52	63 to 68	39.8 to 40.3
5	1.5 to 2.5	50	60 to 75	39.5 to 41.5
6	1.3 to 2.4	59	63 to 72	40.1 to 41.2
8	1.9 to 3.1	48	48 to 56	39.3 to 40.5
This Work	1 to 3.8	116	60 to 68	39.7 to 41

power of 40 dBm with a DE of 60 to 68 percent from 1 to 3.8 GHz over a relative bandwidth of 116 percent. Its performance verifies the hybrid matching method for the design of a broadband PA.

ACKNOWLEDGMENT

This work is supported by Zhejiang Provincial Public Technology Research Project of China Grant LGG21F010006. ■

References

1. C. Shen, S. He, X. Zhu, J. Peng and T. Cao, "A 3.3–4.3-GHz High-Efficiency Broadband Doherty Power Amplifier," *IEEE Microwave and Wireless Components Letters*, Vol. 30, No. 11, November 2020, pp. 1081–1084.
2. Q. Li, S. He, W. Shi, Z. Dai and T. Qi, "Extend the Class-B to Class-J Continuum Mode by Adding Arbitrary Harmonic Voltage Elements," *IEEE Microwave and Wireless Components Letters*, Vol. 26, No. 7, July 2016, pp. 522–524.
3. C. Liu and Q. -F. Cheng, "Highly Efficient Broadband Class-J Power Amplifier Using Modified Multisection Quarter-Wave Lines and Short-Circuited Stubs," *IET Microwaves Antennas & Propagation*, Vol. 13, No. 11, May 2019, pp. 1860–1865.
4. E. Aggrawal, K. Rawat and P. Roblin, "Investigating Continuous Class-F Power Amplifier Using Nonlinear Embedding Model," *IEEE Microwave and Wireless Components Letters*, Vol. 27, No. 6, June 2017, pp. 593–595.
5. H. Huang, C. Yu, Y. Wu, Q. Jin, C. Fan, J. Gao and Y. Liu, "Analysis and Design of a Novel Concurrent Class B/J Continuum Power Amplifier," *International Journal of RF and Microwave Computer-Aided Engineering*, Vol. 30, No. 8, May 2020.
6. S. Saxena, K. Rawat and P. Roblin, "Continuous Class-B/J Power Amplifier Using a Nonlinear Embedding Technique," *IEEE Transactions on Circuits and Systems II-Express Briefs*, Vol. 64, No. 7, July 2017, pp. 837–841.
7. Z. A. Mokhti, J. Lees, C. Cassan and A. Alt, "The Nonlinear Drain–Source Capacitance Effect on Continuous-Mode Class-B/J Power Amplifiers," *IEEE Transactions on Microwave Theory and Techniques*, Vol. 67, No. 7, July 2019, pp. 2741–2747.
8. M. F. Haider, F. You, W. Shi, S. Ahmad and T. Qi, "Broadband Power Amplifier Using Hairpin Bandpass Filter Matching Network," *Electronics Letters*, Vol. 56, No. 4, February 2020, pp. 182–184.
9. S. C. Cripps, P. J. Tasker, A. L. Clarke, J. Lees and J. Benedikt, "On the Continuity of High Efficiency Modes in Linear RF Power Amplifiers," *IEEE Microwave and Wireless Components Letters*, Vol. 19, No. 10, October 2009, pp. 665–667.
10. A. Alizadeh, M. Frounchi and A. Medi, "Dual-Band Design of Integrated Class-J Power Amplifiers in GaAs pHEMT Technology," *IEEE Transactions on Microwave Theory and Techniques*, Vol. 65, No. 8, August 2017, pp. 3034–3045.
11. L. Zhang, X. -Z. Li, M. -J. Xing, Q. Chen and X. -D. Yang, "Research of SIR Filter Based on Integrated Passive Device Technology," *International Conference on Electronic Packaging Technology*, August 2017.

INVITED PAPER

Challenges for Successful Device Testing at 50 GHz

Ryan Benech
Roos Instruments, Santa Clara, Calif.

Manufacturing and testing of devices at microwave and mmWave frequencies have many inherent challenges. These devices have traditionally been built in small quantities and sold for high average selling prices. The next area of communications growth, however, is expanding into frequencies beyond 50 GHz and will require greater optimization and efficiency of manufacturing operations for high accuracy and measurement speed to meet cost and volume objectives.

Uncertainties in the signal path that were insignificant at lower frequencies, now become dominant factors with up to 20× the magnitudes (see ***Table 1***). Some examples include: socket and/or probe card losses and repeatability, connection cable losses, mismatch errors, connector repeatability, modulation accuracy and repeatability, signal dynamic range and low signal measurement sensitivity. To put this into perspective, the estimated total path loss at 2 GHz is 0.55 to 0.75 dB including 0.2 dB peak-to-peak mismatch ripple:

$$\text{Estimated Total Path Loss} = 0.2\ \text{dB} + (2\ \text{ft} \times 0.2\ \text{dB}) + 0.05\ \text{dB} = 0.65 \pm 0.1\ \text{dB} \quad (1)$$

When making a return loss (RL) measurement the round-trip loss must be overcome and removed to calculate the actual RL of the device under test. At 2 GHz, that could be as much as 1.5 dB, with 0.75 dB to the device and 0.75 dB reflected. A well-matched device and test setup will typically have a 25 dB RL or better.

Contrast this with the estimated total path loss at 50 GHz. It is significantly larger at 6.7 dB to 7.5 dB, including 0.8 dB mismatch ripple:

$$\text{Estimated Total Path Loss} = 4\ \text{dB} + (2\ \text{ft} \times 1.45\ \text{dB}) + 0.2\ \text{dB} = 7.1 \pm 0.4\ \text{dB} \quad (2)$$

When making RL measurements, the round-trip loss at 50 GHz could be as much as 15 dB, 20× higher than at 2 GHz. That must be overcome and removed to de-embed the actual RL of the device.

A typical well-matched device and test setup at 50 GHz has 20 dB RL or better. When the median 14 dB round-trip loss is added, however, a dead short at the device will look like 14 dB RL, which is equivalent to a VSWR of 1.5. The variance in measurements over frequency will be almost as high as 1 dB.

A signal into a well-matched device of 18 dB RL will first see 7 dB loss, then the device's 18 dB RL, then 7 dB loss on the return trip, returning a signal that is 32 dB down from the original test signal level. This reduces the effective measurement dynamic range by about 15 dB. In linear terms, this means that the measurement system must measure a 39.8× smaller voltage signal and still maintain the usable accuracy and repeatability required to test the device.

Losses have a logarithmic effect on the ability to make accurate and repeatable measurements. If the total losses to the device were only 2 to 3 dB greater, the round-trip loss in the system would approach 20 dB. In linear voltage terms that is 100× smaller, which approaches the limit of what can be error corrected.

Since loss in the device connection path has a logarithmic effect on the ability to make accurate and repeatable measurements within reasonable testing times, the biggest impact and the first place to direct improvement efforts is in reducing loss in the socket and connection.

This example illustrates why scalar measurements are not sufficient when testing at 50 GHz and why vector measurement techniques

TABLE 1
TYPICAL ATE UNCERTAINTIES

Description	At 2 GHz	At 10 GHz	At 25 GHz	At 50 GHz
Socket and/or probe card losses (dB)	0.2	0.5	1.5	4
Connection cable losses (dB/ft)	0.2	0.6	1	1.45
Mismatch errors (dB)	±0.1	±0.2	±0.3	±0.4
Connector repeatability (dB)	0.05	0.1	0.15	0.2
Modulation accuracy (%)	1	4	5	6
Low signal measurement sensitivity (dBm)	-116	-110	-90	-80

are required. Vector measurements are more precise when used with de-embedding algorithms to characterize and compensate for physical parasitic elements present at 50 GHz; however, there are two significant challenges when using vector de-embedding:

1. With losses between the measurement instrument and the device approaching 7 to 10 dB, the error vectors are often greater than the device's measurement vectors. While it is possible to remove large error vectors to see the smaller device vectors, it requires a measurement system that is repeatable.
2. Since most of the communications devices in this frequency range are also frequency translation devices, the fact that there are different input, local oscillator (LO) and output frequencies further complicates the measurement process when attempting to use traditional S-parameter testing methods to achieve these accurate results.

Either one of these challenges would make bringing these devices into production difficult but combining them could make it seem insurmountable.

Much work has been done to address these issues by embracing new methods to determine the linearity and distortion introduced by the devices that meets optimization and efficiency goals for building cost-competitive mmWave devices at high volumes. Some of these alternate methodologies are:

1. Power measurements with vector error correction to overcome mismatch losses inherent in typical scalar power measurement methods using traditional spectrum analyzers and power meters.
2. Generating multiple signals and combining these sources with mmWave power amplifiers for enough power to overcome high losses and still cause the devices to produce measurable nonlinearity effects for intermodulation distortion (IMD), second order intercept point (IP2) and third order intercept point (IP3) measurements.
3. S-parameter measurements with indirect phase reference methodology that uses multiple one-port models at different input and output frequencies with accurate calibration processes to characterize and de-embed the measurements.
4. Using vector voltage averaging to measure signals below the noise floor to increase measurement sensitivity.
5. Model-based distortion measurements to overcome modulation inaccuracies at millimeter frequencies for accurate adjacent channel power ratio (ACPR) and error vector magnitude (EVM) measurements with direct amplitude (AM-to-AM) and amplitude frequency (AM-to-FM) measurements for providing accurate phase and amplitude information to the design team for model and process compensation and alignment.

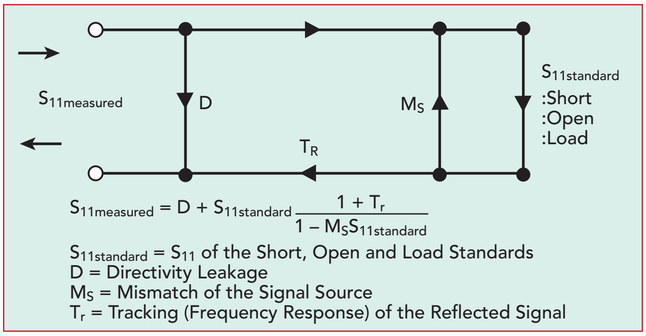

▲ Fig. 1 **Simplified one-port error model.**

POWER MEASUREMENTS

Typical scalar power meters have good 50 Ω matches. If used in well-matched systems, they provide good power references or power transfer standards. When measuring devices directly with a scalar power meter, however, the devices typically do not have 50 Ω matches, therefore frequency dependent mismatch uncertainty can become quite large. This can be problematic even when making P_{out} and P_{1dB} compression measurements at 2 GHz. At 50 GHz with the added overall socket and connection mismatch uncertainty approaching 1 dB, this approach is untenable.

Only with a vector corrected power measurement technique can a P_{1dB} measurement in this environment have credibility. Traditional vector network analyzers (VNAs) measure only ratios such as gain and RL, but recently many of the new breed of VNAs now incorporate power accuracy calibrations to address this need.

MULTI-SIGNAL GENERATION

Since RF source power at 50 GHz is harder to come by and is degraded rapidly by transmission losses, amplifying and then combining signals close to the device under test is the only way to effectively source clean two-tone signals for testing. This is not typically available in commercial VNAs; therefore, a custom network analyzer test set must be assembled and the calibration necessary to characterize and compensate for inherent system losses, such as directivity and crosstalk, must be created. Some vendors are starting to offer more customizable network analyzer tools sets to address this need.

ONE-PORT S-PARAMETER ERROR CORRECTION

National Institute of Standards and Technology (NIST) articles have been published with the rigors of six-port power and implied phase reference approaches of network analysis for addressing the challenges of S-parameter measurements of frequency translation devices with multiple ports and frequencies. These are especially relevant when testing at higher frequencies up to 50 GHz. Employing these methods (see ***Figure 1***) greatly simplifies the measurement of S-parameters needed to error-correct the mismatch and loss effects more prevalent at 50 GHz.

The trade-off is the loss of absolute phase measurement capability through the device. Relative phase can still be measured accurately; however, providing the ability to make all the ratio S-parameter measurements needed for error correction. Some new VNAs incorporate frequency transitional device testing methods using these approaches.

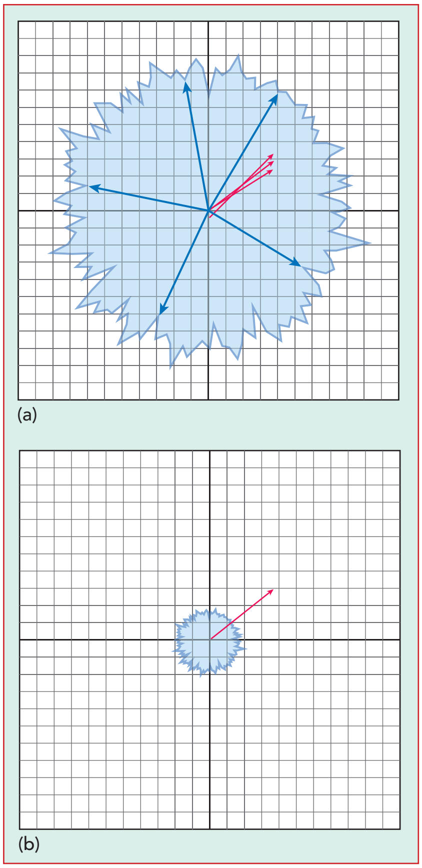

▲ Fig. 2 **Signals below the noise floor (a) while the vector average of the coherent signals is above the noise floor (b).**

VECTOR VOLTAGE AVERAGING

Measuring phase and amplitude of signals (vectors) enables signal processing techniques to be used in measurements at 50 GHz that extends the dynamic range and sensitivity in high frequency and high bandwidth systems. This is effectively a spectrum analyzer but with a vector receiver.

As frequency becomes higher, like bandwidth increasing, the signal-to-noise ratio begins to decline because more noise is present along with the desired signals. ***Figure 2*** shows how vector measurements with random noise (shown in blue) average to a much smaller magnitude since opposite phases effectively cancel. A coherent signal (shown in red), however, averages to a stable version of itself that may be smaller in magnitude than the original noise floor, but much larger than the level of the noise vector average.

MODEL-BASED TESTING

Modulating signals such as WCDMA at 2 to 6 GHz is challenging with significant errors in both the modulation and demodulation measurement systems, meaning that effectively testing any device with less than 6 to 8 percent EVM is an exercise in futility to maintain any type of accuracy.

NIST typically recommends measurement equipment be 10x more capable than what is measured for best accuracy and anything under 2× more capable is effectively useless. This leaves many RF components unmeasurable when their individual specs are as little as 0.7 to as much as 6 percent EVM. When moving to 50 GHz, the ability to modulate these signals is further reduced, in part because the signals must be up-converted, effectively increasing errors dependent on the additive effect of linearity and phase noise characteristics in the upconversion process.

For high volume production testing, an error model approach like the way RF simulation systems predict EVM based on intrinsic device performance is much better, especially at 50 GHz. For power amplifiers, it is the AM-to-AM and AM-to-PM effects of the devices, and how they perturb the symbol constellation from the ideal, that leads to the EVM and ACPR calculation.

Error model EVM can provide measurement times approaching 30 msec with repeatability less than 0.1 percent. For I/Q modulators and demodulators, the DC offsets as well as the magnitude and phase errors of the devices are easily measured and characterized with traditional swept measurement methodologies.

Seven different measurements, four different RF carrier measurements at different DC offsets and three RF image measurements at different magnitude and phase balances, solve for the DC and AC intrinsic errors. This method minimizes baseband stimulus error, eliminates test system phase noise errors, minimizes waveform capture errors, is very fast at less than 100 msec and improves standard deviations.

Contributions by Roos Instruments engineers in the field of RF/microwave and mmWave device production test techniques regarding these novel production-proven approaches have been documented.[1-5]

COMMERCIALLY AVAILABLE IMPLEMENTATION

One of the currently available RF/microwave automated test equipment (ATE) systems that addresses these issues at 50 GHz is Cassini by Roos Instruments. Cassini is a modular architecture where test instrument modules (TIMs) provide the building blocks for a configurable microwave system from DC to 110 GHz (see ***Figure 3***). This enables an enhanced measurement capability and frequency extension as well as instant multi-site expansion. TIMs are air-cooled, shielded instruments that provide all the source, receive, measurement and signal processing capability for a broad range of DC, digital, mixed-signal, RF and mmWave applications. Fixtures carry the modular architecture of Cassini into the device interface environment providing seamless integration with Cassini's software, extending and enhancing the capabilities of the test instruments with an integrated calibration layer that guarantees signal accuracy to the device pin.

Designed to address the previously described challenges is the newly released System RF Core (SyRF Core) 25 GHz TIMs with support test set TIMs in contiguous bands to 50, 70, 86 and 110 GHz.

The focus of this article is the 50 GHz test set TIM paired with the new 25 GHz source and receiver TIMs. This synergistic design is one that optimizes the latest available technology to build the best performing measurement architecture on the market.

The key features of the new TIMs are:

- Fundamental mixing up to 25 GHz and complimentary low harmonic double balanced mixers for all frequencies up to 110 GHz
- Broadband compact high speed frequency synthesized source
- Excellent impedance match up through 50 GHz in coax using integrated 60 GHz blind mate connections to the device interface board

- Direct frequency domain high speed vector measurement receiver with a built-in fundamental LO
- Production-proven modulated measurements techniques.

The 50 GHz test set TIM can produce three simultaneous RF signals with independent frequency multipliers to provide the device with two-tone stimulus and mixer LO sources at the same time, which are required to test any up- or down-converting device at mmWave frequencies. It can down-convert and route both incident and reflected signals for each of these signal paths to the high speed vector receiver. Power measurements at mmWave frequencies are performed through the vector receiver and take advantage of vector error correction to compensate for mismatch issues.

CONCLUSION

The Roos Instruments Cassini ATE is the premier microwave/mmWave test system available on the market with the lowest risk and highest throughput for handling high volume millimeter frequency devices. ■

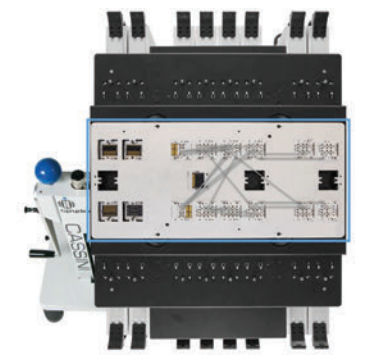

(a)

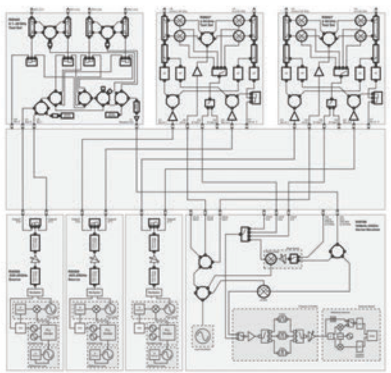

(b)

Fig. 3 Cassini ATE (a) and block diagram (b).

References

1. M. S. Heutmake, "The Error Vector and Amplifier Distortion," *Proceedings of Wireless Communications Conference*, August 1997.
2. A. Nassery, S. Ozev, M. Verhelst and M. Slamani, "Extraction of EVM from Transmitter System Parameters," *Sixteenth IEEE European Test Symposium*, May 2011.
3. S. Yamanouchi, K. Kunihiro and H. Hid, "An Efficient Algorithm for Simulating Error Vector Magnitude in Nonlinear OFDM Amplifiers," *Proceedings of the IEEE Custom Integrated Circuits Conference*, October 2004.
4. D. Morris, W. R. Eisenstadt, A. Paganini, M. Slamani, T. Platt and J. Ferrario "Synthetic DSP Approach for Novel FPGA-Based Measurement of Error Vector Magnitude," *International Test Conference*, November 2010.
5. A. Nassery, S. Ozev and M. Slamani, "Analytical Modeling for EVM in OFDM Transmitters Including the Effects of IIP3, I/Q Imbalance, Noise, AM/AM and AM/PM Distortion," *18th IEEE European Test Symposium*, May 2013.

RFIC 2023: IEEE Radio Frequency Integrated Circuits Symposium

San Diego, CA, USA

June 11-13, 2023

RFIC IMS IEEE

RFIC 2023 Call for Papers

The **2023 IEEE Radio Frequency Integrated Circuits Symposium (RFIC 2023)** is the premier forum focused exclusively on presenting the latest research results in RF, millimeter-wave, and wireless integrated circuits.

Continuing in 2023: RFIC has expanded its focus to include systems, applications, and *interactive demonstrations*, including mobile systems for 5G and beyond, radar, terahertz, biomedical, and optoelectronic systems.

Technical Areas: The symposium solicits papers describing original work in all areas related to RF, mm-Wave, THz, and wireless systems and ICs. Work must be demonstrated through IC hardware results and measurements.

- **Wireless Radios and Systems-on-Chip**: innovative circuit and system-on-chip concepts related to software-defined radio, cognitive radio, interference cancellation, full-duplex, advanced SOCs for cellular/WiFi, GPS, low-power radio circuits for sensors, IoT, Zigbee, biomedical applications, radio architectures suitable for energy harvesting, wake-up receivers, *etc*.
- **mm-Wave Communication Circuits and Systems-on-Chip:** >20GHz (*i.e.*, mm-Wave through THz) circuits and SOCs for wireless communication, including phase shifters, phased arrays, beamformers, MIMO transceivers and other systems for 5G and 6G applications.
- **Radar, Imager, and Sensor Systems-on-Chip**: integrated radar, imaging, spectroscopy, and sensing circuits at microwave through THz frequencies, including vehicular radar SOCs.
- **Transmitters and Power Amplifiers:** for RF through mm-Wave frequencies and higher, power amplifiers, drivers, modulators, digital transmitters, advanced TX circuits, linearization and efficiency enhancement techniques, *etc*.
- **Front-End Circuits:** LNAs, mixers, VGAs, T/R switches, integrated FEM, amplifiers, filters, demodulators.
- **Analog and Mixed-Signal Circuits:** RF and baseband converters (ADC/DAC), sub-sampling/over-sampling circuits, converters for digital beamforming, converters for emerging TX and RX architectures, power (DC-DC) converters for RF applications, I/O transceivers and CDRs for wireline and optical connectivity.
- **Oscillators and Frequency Synthesizers:** VCOs, injection-locking frequency dividers/multipliers, PLLs, DLLs, MDLLS, DDS, LO drivers, frequency dividers.
- **Device/Packaging/Modeling and Testing Technologies:** RF device technology (both silicon and compound semiconductors), MEMs, integrated passives, photonic, reliability, packaging, modeling and testing, EM modeling/co-simulation, built-in-self-test (BIST).
- **Emerging Circuit Technologies:** MEMs-based sensors and actuators, 3D ICs, silicon photonics, quantum computing ICs, hardware security, novel terahertz solutions, and AI/machine learning applied to RF circuits.
- **RFIC System Applications**: system level innovations in RFICs with application to communication, biomedical, radar and imaging. May include *interactive demonstration* and presentation. Additional details can be found on the RFIC website.

Format and Location: The 2023 symposium is currently planned as an in-person conference. More details to follow. In person events will be held at the San Diego Convention Center in San Diego, CA. RFIC 2023 starts on Sunday, June 11, 2023 with a large selection of workshops followed by two plenary talks and a reception featuring our top industry and student papers. Monday and Tuesday, June 12-13 will be comprised of oral presentations, and panel sessions.

Microwave Week 2023: RFIC 2023 kicks off *Microwave Week*. The week continues with the International Microwave Symposium and then the ARFTG Microwave Measurement Conference. This week, with more than 9000 participants, is the world's largest and most important gathering of RF and microwave professionals in the field.

Industry Exhibition: A three-day Exhibition typically showcases more than 900 Exhibitors who represent the state-of-the-art of the industry covering everything needed for RF and microwave design. More on the format of the 2023 Exhibition is found on both RFIC and IMS websites

Electronic Submission Deadlines

Manuscript in PDF format:	**January 15, 2023**
Final Manuscripts for the RFIC Digest:	**March 22, 2023**

All submissions must be made at rfic-ieee.org in pdf form. Hard copies are not accepted.

MTT-S®

Sponsored by the IEEE MTT-S, EDS, and SSCS

rfic-ieee.org

SSCS EDS

Author Registration and Paper Submission Steps:

1. All papers must be submitted via the website: **rfic-ieee.org**.
2. Author registration form: title, author(s) and affiliation(s), and statement of exclusivity. This form also includes an abstract of 30-50 words (description of the subject, its importance, and how the work contributes to the field). This information is required and must be submitted via the website: **rfic-ieee.org**.
3. Authors must use the template provided on the website to format their manuscript. **The manuscript may not exceed 4 pages total and the file size must be less than 2 MB. For PDF files, use Distiller and select "embed all fonts". Please note that we do not accept "*.doc" or "*.docx" files.**
4. Authors must adhere to specific guidelines to ensure that the submission complies with our **DOUBLE-BLIND REVIEW PROCESS**. Details are provided on **rfic-ieee.org**. Pay close attention to how authors should cite their previous work.
5. Submission deadline: **15 January 2023.** *Submissions will be acknowledged instantly.* Late submissions will not be considered.

Authors of accepted papers will be required to submit a final manuscript for publication, including a clear die photo of the work described in the manuscript.

Paper Selection Criteria: All submissions must be in **English.** Papers will be selected based on the following factors:

- **Originality**: The paper must be unique, significant, and state-of-the-art. Are references to existing literature included?
- **Quantitative content**: The papers should give an explicit description of the work with supporting data.
- **Quality:** Clarity of the writing and figures. What is the context of the contribution to previous work?
- **Interest to attendees**: Why should this work be reported at the RFIC Symposium?

Clearances: Authors must obtain all required company and government clearances prior to submitting a paper. A statement of clearance, signed by the submitting author, must accompany the final manuscript for the paper to be considered for publication.

Double Submission: Authors who do not properly cite their previous work, including concurrent IMS or other conference submissions, or who submit an RFIC manuscript to two or more publications without informing the editor/TPC chair that the paper is concurrently under review by another publication will be reported to IEEE and may be banned from future publications.

Notification: Authors will be notified of decisions on 8 March 2023. Authors of accepted papers will receive copyright release forms and instructions for publication and presentation. Final manuscripts for publication must be received by **22 March 2023.**

Presentation Format:

- ***Oral Presentation Papers:*** Authors will be given 20 minutes to describe novel circuit and system techniques, measurement results, and potential impact to the RFIC community.
- ***Interactive Demonstration Papers:*** Select papers from the RFIC System Applications area will be presented in poster format along with functional hardware demonstration.

All Authors must provide a PDF version of the presentation material for registered attendees to download during and after the symposium.

Visa Requirements: *Due to the short timeframe between paper acceptance and RFIC, contact authors should provide their name as it shows on their passport and correct mailing address.*

Student SUPERPASS: RFIC enthusiastically invites participation from students at all levels to attend Microwave Week. All students will be offered the opportunity to purchase a SUPERPASS allowing access to RFIC, IMS, ARFTG, all workshops, technical lectures, panels, and more. SUPERPASS prices are significantly discounted to encourage participation.

Best Student Paper Award: A student paper award contest will be held as part of RFIC. Student papers will be reviewed in the same manner as all other papers. To be considered, the author must have been a full-time student (9 hours/term graduate, 12 hours/term undergraduate) during the time the work was performed **and** be the lead author and presenter of the paper. *The email address of the student's advisor must be supplied during submission time and will be used to verify student eligibility.* Complimentary registration will be given to the student finalists. *Finalists will present a poster or a demo at the Sunday's Symposium Showcase.*

Industry Best Paper Award: An industry paper award contest will be held as part of RFIC. Industry papers will be reviewed in the same manner as all other conference papers. Only papers with an industrial first author **and** presenter will be qualified for the Industry Best Paper Award. *Selected finalists will also present a poster or a demo at the Sunday's Symposium Showcase.*

Invited Journal Articles: Select authors will be invited to submit an expanded manuscript to the RFIC special issue in *IEEE Journal of Solid-State Circuits*. In addition, all authors are invited to submit an expanded version of their papers to a special issue of *IEEE Transactions of Microwave Theory & Techniques*.

Photos Courtesy of the San Diego Convention Center.

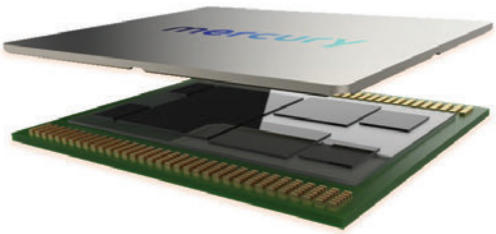

Trusted Onshore Facility Brings Latest Technology to Mission-Critical Applications

Mercury Systems
Andover, Mass.

Most silicon (Si) used in defense applications is designed by domestic chipmakers but fabricated in overseas foundries, which introduces vulnerabilities to the microelectronics supply chain—from weather catastrophes to geo-political disruption. To reduce these risks, technology organizations with expertise building products for aerospace and defense are expanding onshore microelectronics facilities to enhance their design and manufacturing capabilities.

One of the early initiatives in the industry is the Mercury Systems microelectronics manufacturing facility in Phoenix. The company made a $15 million investment in 2019 to upgrade the facility and enhance its 2.5D and 3D custom microelectronics capabilities, followed by another facility expansion in 2022. Mercury's manufacturing facility is recognized as a trusted U.S. defense microelectronics supplier, DMEA accredited. Having a trusted onshore supplier enables military customers, including the Department of Defense (DOD), to access the leading commercial Si technologies, and using the trusted open system architecture addresses the DOD requirement for onshore manufacturing of critical microelectronics.

▲ Fig. 1 To maintain superiority, radar and EW systems require adaptable, intelligent processing at the sensor edge.

As a proof point of this capability, Mercury Systems has developed an RF system in package (RF SiP) that integrates high speed data converters, digital processing, memory and power management in a single package. The RFS1140 is the first to combine data converters operating at 64 GSPS with powerful AI core FPGA processing and power management.

Heterogeneous integration of these circuit functions reduces system cost, size and complexity. Perhaps more important, it reduces latency because the SiP can be placed close to an antenna, enabling new sensor processing applications for defense platforms and programs (see ***Figure 1***). Countering the latest radar and electronic warfare threats requires extremely low latency responses driven by an intelligent, adaptive strategy. Addressing this rapidly evolving need requires innovation from chip to system, which defined the powerful functionality integrated in the RFS1140.

DATA PROCESSING

The RSF1140 uses the AMD Xilinx Versal AI Edge adaptive compute acceleration platform (ACAP), a heterogeneous processor incorporating three types of compute engines and fabricated in 7 nm CMOS technology. Complemented with high speed direct digitization up to 32 GHz and four channels each of analog-to-digital and digital-to-analog data conversion at 64 GSPS per channel, the RFS1140 provides ultra-low latency processing. Integrating on-chip memory and power management in the SiP completes the processing system and contributes to overall system longevity (see ***Figure 2***).

Versal devices are the industry's first ACAP, combining adaptable processing and acceleration engines with programmable logic and configurable connectivity. The customized heterogeneous hardware enables applications such as data center, automotive, 5G and wired telecom, as well as defense. With transformational technologies like intelligent engines, adaptable engines and scalar engines with an integrated Si host interconnect shell, the Versal device provides superior performance per watt compared to conventional FPGAs, CPUs and GPUs.

To track potential targets, including those moving at hypersonic speeds, the RF SiP uses high speed data converters to provide the massive processing required. Two 10-bit Jariet Electra-MA transceivers in each RFS1140 directly digitize waveforms, from 40 to 64 GSPS per channel and analog frequencies as high as 36 GHz, with instantaneous bandwidth exceeding 4 GHz. Designed and fabricated in the U.S., the converters are fabricated on a 14 nm CMOS process, which provides high DC power efficiency.

Each transceiver channel in the RF SiP uses interleaved analog-to-digital and digital-to-analog converters followed by programmable digital up- and down-conversion; linear equalization, decimation and interpolation; and a 16-bit SerDes baseband data interface.

TRUSTED AND SECURE

The RFS1140 enables edge processing by maximizing performance through a highly customizable architecture developed, designed and manufactured from a source trusted for DOD programs. The RF SiP offers direct digitization and massive processing, minimizing SWaP-C by eliminating multiple boards required in a traditional system.

By using this SiP architecture, future generations of semiconductors created by continuous commercial R&D investments can be used to rapidly upgrade military systems. Systems using the RF SiP will be able to add new capabilities in the same physical form factor, saving development cost and speeding system upgrades, while decreasing the complexity of upgrade cycles.

More than ever, critical military systems such as EW, phased array radar and C5ISR need trusted onshore microelectronics from a company with expertise in secure, heterogeneous packaging. The advanced SiP technology from Mercury Systems' onshore design and manufacturing capability brings commercial technology to mission-critical applications, enabling sensor processing at the edge.

Mercury Systems
Andover, Mass.
www.mrcy.com

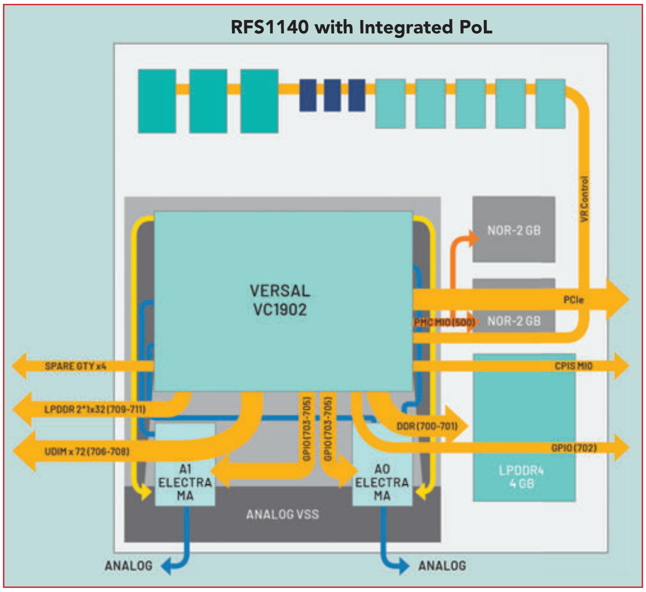

Fig. 2 The RFS1140 integrates high speed data converters, an advanced heterogeneous ACAP processor, memory and power conversion.

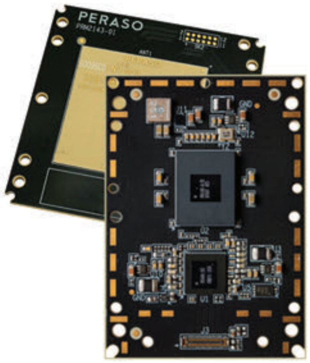

Antenna to Baseband Modules for 60 GHz FWA Networks

Peraso Inc.
San Jose, Calif.

Peraso, a supplier of mmWave semiconductors and modules, has introduced the Perspectus line of 60 GHz modules for the fixed wireless access (FWA) market. These three high reliability modules can be used in point-to-point or point-to-multipoint networks and provide multi-Gbps throughput with low latency (see ***Figure 1***). The Perspectus modules combine RFICs and baseband Si, developed by Peraso, with printed circuit board (PCB) antenna arrays (see ***Figure 2***).

Providing a complete transceiver from antenna to baseband eliminates the design challenges of mmWave antenna design—a fine art—and matching components from different suppliers. With a USB 3.0 interface, they are straightforward to integrate with host processors. The modules are fully tested, do not require factory calibration and have FCC modular certification.

All Perspectus modules use Peraso's PRS1165 transceiver IC, which integrates 16 high-power beamformer chains. The transceiver supports all six of the 802.11ad/ay channels from 57 to 71 GHz, and the frequency synthesizer and selectable RF filters support half-bandwidth channels and half-channel frequency steps. Longer link ranges can be achieved using channels 5 and 6, which are outside the oxygen absorption band. Peraso's MAC PHY baseband processor, the PRS4601 B2E, provides the functionality for 802.11ad operation and supports point-to-point and point-to-multipoint capability. Peraso provides Linux drivers and offers various software/firmware versions optimized for FWA applications.

The three modules in the Perspectus line offer different antenna arrays, which provide various gain and fields of view (see ***Table 1***). The arrays are integrated into the PCB to improve matching, reduce cost and increase reliability. One of the three modules, the PRM2141X, can connect to a high gain parabolic reflector, which enables Gbps data rates over links exceeding 20 km when using the upper channels.

Each module may be used as

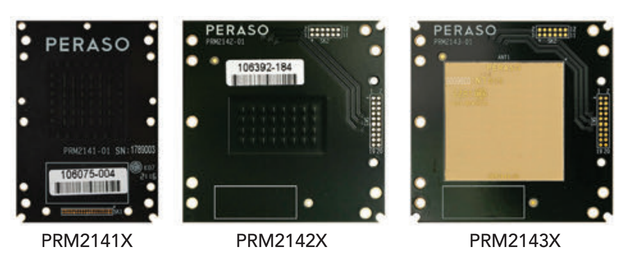

Fig. 1 **The three modules currently in the Perspectus 60 GHz family.**

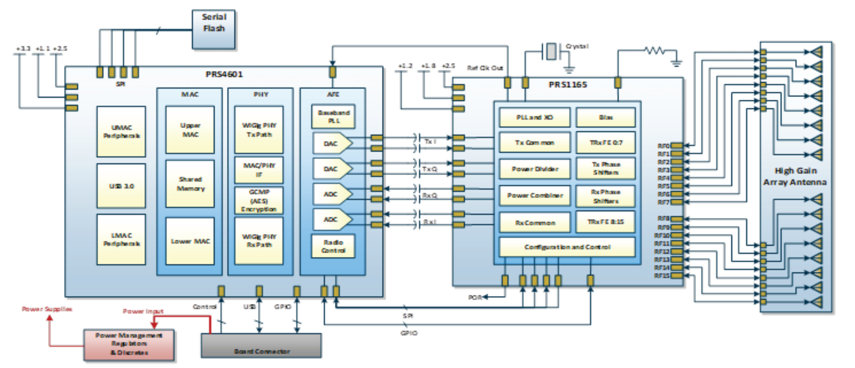

Fig. 2 **Block diagram of the 16-element array module.**

TABLE 1

PERSPECTUS 60 GHZ MODULE PERFORMANCE

	PRM 2141X	PRM 2142X	PRM 2143X
Antenna Array • Number of Elements • Polarization	 16 Vertical	 32 Vertical	 64 Vertical
Maximum EIRP (dBm)	37	40 (Reg. Limit)	40 (Reg. Limit)
Antenna Gain (dBi)	15	18	22
Scan Range (±°) • Azimuth • Elevation	 45 45	 45 20	 20 15
Digital Interface	USB 3.0 for Data and Control, 2.5 V CMOS 1 PPS Sync and GPIO		
Power Consumption (W) • Tx • Rx	 7–11.5 4.5	 11.5 4.5	 11.5 4.5
Size (mm)	35 x 50	50 x 50	50 x 50
Range at 1 Gbps Throughput (km)	0.7 with Array >20 with Dish	1	1.5

an access point (AP), station (STA) or in a peer-to-peer (P2P) configuration. Typically, the modules with wider fields of view (the PRM2141X or PRM2142X) will be used as APs, with the PRM2143X employed as the STA. For longer links, the PRM2141X with a dish can be used as the STA.

Peraso's infrastructure software package enables point-to-multipoint networks with up to 32 STAs. Enhancements to the 802.11ad protocol such as directional beam scan and connect and STA focus can enhance beamforming performance over the extended distances supported by the hardware. The software also provides an aiming mode, to aid installation and link monitoring statistics, which are required to manage the network.

Perspectus modules are in production and have been adopted by wireless service providers as their primary solution for multi-Gbps service in urban and suburban networks. Evaluation kits and modules are available from Peraso and Richardson RFPD.

Peraso Inc.
San Jose, Calif.
www.perasoinc.com
www.richardsonrfpd.com/Supplier/Index/Peraso

Feedthrough Adapters For Thermal Vacuum Test Systems

Thermal vacuum (TVAC) testing is a critical step in qualifying components and systems for spaceflight. Major investments in time and materials are required to develop instrumented vacuum chambers that enable accurate and reliable testing of devices and systems as though they were in space.

Eravant has developed a line of TVAC-safe components constructed with low outgassing materials and adhesives that withstand cryogenic temperatures and repeated exposure to large temperature gradients. These include a series of hermetically sealed coaxial bulkhead feedthroughs with 1.0, 1.35, 1.85, 2.4 and 2.92 mm and SMA connectors.

For the highest frequency mmWave systems, the model SCT-1F1F-UB-B-V is a 1.0 mm female-to-female bulkhead coaxial adapter that uses a glass bead and an O-ring seal to provide a hermetically sealed RF interface between the vacuum and atmosphere environments. At 110 GHz, insertion loss is 2 dB with return loss of 13 dB. Leakage from the atmosphere to the vacuum is less than 1 x 10^{-8}cc/s of helium at 1 atmosphere. In addition to TVAC testing, the adapter is well-suited for cryostats used in imaging systems, wafer probe stations, spectrometers, bolometers and radio telescopes operating at mmWave frequencies.

Eravant's TVAC-safe components also include waveguide-to-coaxial adapters, directional couplers, waveguide attenuators, compact isolators and waveguide terminations. The waveguide-to-coaxial adapters cover the waveguide bands from WR28 through WR10, including end-launch and right-angle configurations. TVAC-capable waveguide attenuators are offered with standard and custom attenuation levels. Compact waveguide isolators suitable for TVAC testing typically provide 0.5 dB insertion loss and 18 dB isolation.

VENDORVIEW

Eravant
Torrance, Calif.
www.eravant.com/products/by-application/space

18–26.5 GHz Solid-State Power Amplifier Delivers 1 kW Pulsed

Exodus Advanced Communications has developed a solid-state high-power amplifier (HPA) for mmWave pulsed radar, electronic warfare and radiated susceptibility testing, such as EMI-Lab/RS103. The instantaneous bandwidth of the AMP4065P-1KW amplifier covers the full K-Band, from 18 to 26.5 GHz, and provides at least 1 kW pulsed output power within a 3 dB peak-to-peak power flatness. The AMP4065P-1KW is unique: providing this level of power at mmWave frequencies from a solid-state HPA.

The HPA's pulse capability supports radar systems with narrow or wide RF pulses and duty cycles to 5 percent; it has an 80 dB on/off ratio. The HPA uses a class AB design to achieve better than –20 dBc harmonics and –60 dBc spurious at rated output power. Gain can be controlled over greater than a 20 dB range.

The AMP4065P-1KW has extensive control and monitoring functions, including the gain control and optional calibrated power monitoring, using either the large 7 in. color display or via remote control. The color touchscreen shows the forward and reflected power, VSWR in real time, system voltages and currents and the internal system temperature and operating temperatures of the HPA module heat sinks. These performance parameters are also available via the remote interface.

Rack integrated, the AMP4065P-1KW uses type K (2.92 mm) female connectors for the RF input and optional RF sampling ports. To handle the high output power, the output connector is a WR42 waveguide flange.

Exodus Advanced Communications' products use LDMOS, GaN HEMT and GaAs technology, with a good share of the devices manufactured by the company. In addition to HPAs, Exodus designs low noise amplifiers, modules and multi-band systems for applications operating from 10 kHz to > 51 GHz.

VENDORVIEW

Exodus Advanced Communications
Las Vegas, Nev.
www.exoduscomm.com

5G Repeater for C-Band Integrates With Existing and New Repeater Systems

Wilson Electronics' Enterprise 1337R is the company's first C-Band 5G cellular repeater, developed to maximize coverage within any facility. The Enterprise 1337R amplifies the mid-band frequencies between 3.7 and 3.8 GHz with automatic time-division duplex synchronization and software defined filtering to target the preferred carrier's network. Because the repeater operates in licensed 5G bands, it does require carrier approval to operate. The Enterprise 1337R works well with existing and new cellular repeater systems, such as the WilsonPro 1300 and 4300 systems, to add C-Band 5G coverage with no additional backhaul, data plan or recurring fees required.

Two indoor and outdoor ports are designed to provide maximum coverage, and the dual amplification paths support either 2 x 2 MIMO or multiple towers, providing setup versatility. The repeater requires both indoor and outdoor C-Band antennas connected to the repeater with 50 Ω coaxial cables with N-type connectors, which are available from WilsonPro. Maximum uplink and downlink power is 26 dBm per path. Each amplification path has a noise figure of 5 dB and provides up to 90 dB of gain.

The Enterprise 1337R fits a standard 2U rack and has a touchscreen display. For remote monitoring and management, it connects to the WilsonPro Cloud.

Wilson Electronics
Salt Lake City, Utah
www.wilsonelectronics.com

Keysight & Cisco Validate Characteristics of ORAN WG9 xHaul Transport

In this video, Keysight and Cisco demonstrate the SRv6 uSID based xHaul transport and validate the latency characteristics as per ORAN WG9 test specification.

Keysight Technologies
www.youtube.com/watch?v=JwKUDMoAMug

MMIC Technologies: Integrated Passive Devices (IPD)

IPD brings all the advantages of continuously evolving MMIC technology developed for high volume applications like computers and cell phones to passive devices which were traditionally implemented with larger, more expensive technologies such as thin film. Learn more in the blog post.

Mini-Circuits
https://blog.minicircuits.com/mmic-technologies-integrated-passive-devices-ipd

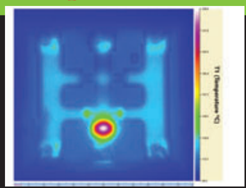

Nxbeam 5G/6G Wireless Communications Solutions

Nxbeam's products answer the demand for high throughput real-time data. Visit the 5G/6G Wireless Communications webpage to learn more about their mmWave front-ends and radio products.

Nxbeam
www.nxbeam.com/product/5g/

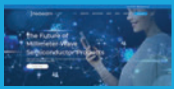

Qorvo Highlights Market & Tech Portfolio Expansion

This video underscores Qorvo's technology leadership in new and emerging markets for wireless and wired connectivity, power management, UWB, MEMS, GaN, BAW filters and SiC power.

Qorvo
www.qorvo.com/design-hub/videos/qorvo-corporate-overview

Updated Cable Builder Is Now Live!

SV Micro added ten new .047" and .085" cable connector options to their Cable Builder. Precisely build the cable assembly you need in any length and instantly see pricing, datasheets and more.

SV Microwave
https://svmicrowave.com/cable-builder

Datasheets Now on Swift Bridge Technologies' Website!

Swift Bridge Technologies has updated its website to include datasheets for the FastEdge and DuraWave product lines. These provide detailed performance specifications and much more.

Swift Bridge Technologies
www.swiftbridgetechnologies.com/fdata-sheets

NEW PRODUCTS

FOR MORE NEW PRODUCTS, VISIT WWW.MWJOURNAL.COM/BUYERSGUIDE FEATURING VENDORVIEW STOREFRONTS

DEVICES/ COMPONENTS/MODULES

Multi-Channel FMCW Radar Transceiver

VENDORVIEW

With four transmit and four receive channels, model SSC-7337331202-1212-B1 is an E-Band FMCW transceiver sub-assembly that operates from 70 to 75 GHz. The transceiver includes a digitally controlled synthesizer, frequency multipliers for transmitters and receivers, a single side-band modulator, a four-way switch for the transmit channels and four I/Q mixers for the receivers. The transmitted power is +2 dBm for each channel and receiver conversion loss is 12 dB. The subsystem requires +6 VDC at 2.3 Amps.

Eravant

www.eravant.com

Gelled Tantalum Capacitors

Exxelia now offers the reliability level R, in addition to level M and P for the specifications MIL-PRF-39006/22 and MIL-PRF-39006/25, equivalent to CLR79 and CLR81 series. Available in all package sizes (T1 to T4), these fully sealed products cover voltages from 6 to 125 V, deliver capacitance values ranging from 1.7 to 1200 μF and are designed to operate at temperatures ranging from -55°C to +125°C and withstand the harshest environmental conditions.

Exxelia

www.exxelia.com

Ultra-Broadband Resistive Power Dividers

VENDORVIEW

HYPERLABS INC. has expanded its line of ultra-broadband resistive power dividers by adding a four-way, 12 dB power divider (HL957X series) and a two-way, two-resistor power splitter (HL948X series). Both additions offer bandwidths from DC to over 67 GHz. The four-way power divider is a lower-cost and smaller-sized option over implementing multiple two-way dividers. The newly released power splitters are suitable for making power ratio measurements as the accuracy of the divided outputs is extremely well tracked. Demos available upon request.

HYPERLABS INC.

www.hyperlabsinc.com

Coaxial Mixer

VENDORVIEW

Mini-Circuits' model ZMDB-653H-E+ coaxial frequency mixer features RF and LO frequency range of 20 to 65 GHz and IF range of DC to 20 GHz. Well suited for frequency up-/down-conversion in defense radar, communications and test systems, the level 15 (+15 dBm LO power) mixer is 0.56 × 0.56 × 0.34 in. (14.22 × 14.22 × 8.64 mm) with female 1.85 mm connectors. Typical LO-RF isolation is 45 dB with typical conversion loss of 11 dB from 20 to 65 GHz.

Mini-Circuits

www.minicircuits.com

Broadband Capacitors

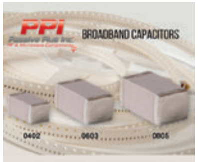

Passive Plus Inc. (PPI) has developed larger broadband capacitors in three larger case sizes: 0402BB, 0603BB and 0805BB. Values available are 10 nF (10,000 pF) and 100 nF (100,000 pF), depending on case size. These capacitors are intended primarily for coupling RF signals or, occasionally, for bypassing them to ground, while blocking DC. The applications for which they are intended require small, surface-mountable devices that provide low RF impedances, i.e., low insertion losses and reflections, across extremely large RF bandwidths and temperatures typically ranging from -55°C to +125°C.

Passive Plus Inc.

www.passiveplus.com

SP3T Switch

VENDORVIEW

Qorvo's QPC1006 is a single pole, triple throw (SP3T) switch fabricated on Qorvo's QGaN25 0.25 μm GaN on SiC production process. Operating from 0.15 to 2.8 GHz, the QPC1006 typically supports 50 W input power handling at control voltages of 0/-40 V for both CW and pulsed RF operations. This switch maintains low insertion loss less than 1.0 dB and greater than 30 dB isolation, making it ideal for high-power switching applications across both defense and commercial platforms.

Qorvo

www.qorvo.com

Single Pole, Four Throw, Absorptive Switch

VENDORVIEW

Quantic PMI Model P4T-100M18G-80-T-515-SFF-4W-IND is a single pole, four throw, absorptive switch that operates over the 0.1 to 18.0 GHz frequency range. This model has a maximum insertion loss of 6.0 dB, a minimum isolation of 80 dB, a maximum VSWR of 2.0:1 and a maximum switching speed of 200 ns. It has SMA female connectors and a size of 1.25" × 1.25" × 0.40".

Quantic PMI

www.pmi-rf.com

NewProducts

Termination Resistors

Richardson RFPD Inc., an Arrow Electronics company, announced the availability and full design support capabilities for three new termination resistors from TTM Technologies' Radio Frequency & Specialty Components business unit. The new terminations are optimized for 5G wireless infrastructure applications, as well as GPS/GNSS, Wi-Fi including Wi-Fi 6, and legacy 4G/LTE. The devices are currently in-stock at Richardson RFPD.
Richardson RFPD Inc.
www.richardsonrfpd.com

High-Power High Directivity Directional Couplers

RLC Electronics' high-power high directivity directional couplers offer accurate coupling (± 1.0 dB), low insertion loss (0.1 to 0.35 dB maximum) and > 35 dB directivity in both directions. These high-power couplers are offered with 500 to 1000 W average power handling up to 18 GHz, as well as 100 W versions up to 40 GHz. Couplers are provided in both single and dual directional construction, typically over a two-octave bandwidth or less. RLC can utilize SC or 7/16 connectors on the main line, should this be needed to meet customer designs.
RLC Electronics
www.rlcelectronics.com

Cellular Module for IoT Applications

VENDORVIEW

Würth Elektronik presents the Adrastea-I, its high performance, ultra-low power consumption, multi-band LTE-M and NB-IoT module. This cellular module, measuring only 13.4 × 14.6 × 1.85 mm, comes with integrated GNSS, integrated ARM Cortex M4 and 1 MB Flash reserved for user application development. The module is based on the high performance Sony Altair ALT1250 chipset. Certified by Deutsche Telekom, the Adrastea-I module enables a quick integration to end-products without additional labels, industry-specific certifications (GCF) and operator approvals needed, whenever Deutsche Telekom IoT connectivity (SIM card) is used.
Würth Elektronik
www.we-online.com

CABLES & CONNECTORS

50 W 90-Degree Hybrid

VENDORVIEW

MIcable introduces 0.1 to 0.605 GHz 400 W/50 W cost-effective 90-degree hybrid with low insertion loss, low VSWR in a small package (drop-in/surface mount). Since the excellent stability and heat dissipation ability, it is ideal for power amplifiers, power combination network, antenna feed network, modulators and phase shifter applications.
Fujian MIcable Electronic Technology Group Co. Ltd.
www.micable.cn

RF Cables

VENDORVIEW

DuraWave™ PS43 was developed by Swift Bridge Technologies to exceed OEM performance through 43.5 GHz. These ruggedized, phase and magnitude stable RF cables are well suited for on-site field testing, manufacturing environments and the testing laboratory. Insertion losses at 43.5 GHz are typically 30 to 40 percent lower than the OEM's test port cables with VSWR < 1.25 (< -18 dB S11 and S22). These assemblies are available on DigiKey with precision 2.92 and 2.4 mm connectors in various gender combinations.
Swift Bridge Technologies
www.swiftbridgetechnologies.com

AMPLIFIERS

Digital Variable Gain Amplifiers

BeRex announced the release of four new products; the BVA1761, BVA1762, BVA2761 and BVA2762 are digital variable gain amplifiers (DVGAs) which are designed for glitch-safe attenuation state transitions, highly accurate 7-bit digitally controlled attenuation over a 31.75 dB range, with 0.25 dB steps, while maintaining high linearity. Designed with outstanding RF characteristics, the DVGAs are primarily intended for 5G/4G/3G wireless infrastructure equipment, satellite radio and other high-end wireless applications.

BeRex
www.berex.com

Amplifiers

VENDORVIEW

Pasternack, an Infinite Electronics brand, has released a new line of temperature compensated amplifiers covering broadband and ultra-broadband frequencies ranging from 0.5 to 40 GHz. These high reliability temperature compensated amplifiers are available with and without

heat sinks to address multiple precision performance and test and measurement applications. Designs feature integrated voltage regulators covering a DC voltage ranging from +12 to +15 Vdc and power levels ranging from 15 to 20 dBm.
Pasternack
www.pasternack.com

SOFTWARE

Version 22.3 of the Modelithics COMPLETE Library™

VENDORVIEW

Modelithics® announced that version 22.3 of the Modelithics COMPLETE Library™ for Keysight PathWave RF Synthesis (Genesys)

is now available and includes compatibility with Keysight Genesys 2022. It supports the Vendor Parts Synthesis (VPS) capability in Genesys to automate the selection of discrete parts from the Modelithics COMPLETE Library. It accounts for the parasitics of the parts, substrates and bond pads to enable one-pass hardware realization to meet the original optimized design specs.
Modelithics Inc.
www.Modelithics.com

Cascade Analysis Platform

The simulation platform is hosted in a secure cloud, has full featured components and produces stunning graphics that can be shared or used for presentations. It calculates compression-aware gain, noise figure, independent splitter and combiner branches and other parameters necessary for RF system design. RF Graph is offering a 30-day free trial and is initially priced less than $9 per month.
RF Graph
www.rfgraph.com

ANTENNAS

Standard Gain Horn Antennas

VENDORVIEW

HASCO's gain horn antennas offer 23 dBi typical gain, precisely electroformed over a mandrel and gold-plated. These horns have a pyramidal shape with a rectangular aperture. The standard gain horn antenna is used for antenna range calibration and general-purpose system setups. HASCO's gain horns are used in many applications, such as antenna testing and RF radiation pattern measurement. HASCO's gain horns function as a calibration standard or as reference for antenna gain measurement.
HASCO
www.hasco-inc.com

TEST & MEASUREMENT

Amplitude and Control Module

Designed specifically for high performance simulator and ATE systems, General Microwave's amplitude control module provides precise amplitude control of signal amplitude and pulse modulation over a high dynamic range with fine resolution. With 10 BIT TTL control, modules provide up to 100 dB attenuation, harmonics < -60 dB and pulse modulation 80 dB, 25 ns control. Available in bands from 0.5 to 40 GHz and can be upgraded to include optional phase control.
Kratos General Microwave Corp.
www.kratosmed.com

Programmable Linear DC Power Supplies

RIGOL Technologies announced their next generation of programmable linear DC power supplies, the DP2000. This completely new benchtop power supply features three fully isolated channels with automatic internal series and parallel connections and an intuitive 4.3" touch screen. The DP2000 delivers high-resolution for measuring low-range currents down to 1 µA, a high speed sampling mode, an arbitrary output mode with a 1 ms dwell time and low output noise and ripple < 350 µVrms.
RIGOL Technologies
www.rigolna.com

MICRO-ADS

Reviewed by Gary Lerude

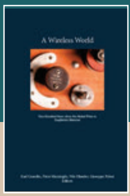

Bookend

A Wireless World: One Hundred Years since the Nobel Prize to Guglielmo Marconi

Edited by Karl Grandin, Piero Mazzinghi, Nils Olander and Giuseppe Pelosi

In 1909, the Nobel Prize in Physics was awarded jointly to Guglielmo Marconi and Karl Ferdinand Braun "in recognition of their contributions to the development of wireless telegraphy." A century later, in 2009, the Royal Swedish Academy of Sciences organized an international symposium and subsequent exhibition to commemorate the Nobel Prize recognition of the two wireless pioneers. The events expanded the circle to acknowledge the contributions of Antonio Meucci. Meucci, an Italian who emigrated to the U.S., developed a way to carry voice via electric signals over wires—the first telephone—in 1856/1857. In the 1990s, those wires yielded to wireless, which transformed the "land line" telephone into the mobile phone, which virtually every human on the planet carries.

The 2009 commemoration in Sweden led to the book, "A Wireless World," which documents some of the historic elements of the Nobel Prize presented at the conference and exhibition. The book has four sections, beginning with a compilation of documents from 1909, including a reproduction of the typescript of Marconi's Nobel Prize lecture with his handwritten notes. The second section discusses Marconi's background, education and the achievements leading to his nomination for the Nobel Prize. The third section provides context for the era, covering Marconi's contemporaries in the field, such as Karl Ferdinand Braun, and the researchers who followed. The final section and perhaps the most interesting shows images and photos of the devices and equipment from that early wireless era.

Today, those of us who are so embedded in wireless can find ourselves insensitive to the mystery of the unknown and the awe of discovery when electromagnetic principles were gradually transformed into the products we rely upon today. "A Wireless World" provides an opportunity to revisit and reimagine those early days, even marveling at the fruits of that work.

ISBN Print Edition: 978-91-7190-178-1
ISBN PDF Edition: 978-91-7190-179-8
Hardcover: $169
Digital download: $126
To order this book, contact:
Firenze University Press
www.fupress.com

Advertising**Index**

Sales Representatives

Microwave Journal

Eastern and Central Time Zones
Michael Hallman
Associate Publisher
(NJ, Mid-Atlantic, Southeast, Midwest, TX)
Tel: (301) 371-8830
Cell: (781) 363-0338
mhallman@mwjournal.com

Shannon Alo-Mendosa
Northeastern Reg. Sales Mgr.
(New England, New York, Eastern Canada)
Tel: (781) 619-1942
Cell: (978) 501-9116
salomendosa@horizonhouse.com

Submitting ad material?
Visit: www.adshuttle.com/mwj
(866) 774-5784
outside the U.S. call +1-414-566-6940

Pacific and Mountain Time Zones
Brian Landy
Western Reg. Sales Mgr.
(CA, AZ, OR, WA, ID, NV, UT, NM, CO, WY, MT, ND, SD, NE & Western Canada)
Tel: (831) 426-4143
Cell: (831) 713-9085
blandy@mwjournal.com

International Sales
Richard Vaughan
International Sales Manager
Tel: +44 207 596 8742
rvaughan@horizonhouse.co.uk

Ed Kiessling
(781) 619-1963
ekiessling@mwjournal.com

Germany, Austria, and Switzerland (German-speaking)
WMS.Werbe- und Media Service
Brigitte Beranek
Tel: +49 7125 407 31 18
bberanek@horizonhouse.com

France
Gaston Traboulsi
Tel: +44 207 596 8742
gtraboulsi@horizonhouse.com

Israel
Dan Aronovic
Tel: +972 50 799 1121
aronovic@actcom.co.il

Korea
Young-Seoh Chinn
JES MEDIA, INC.
Tel: +82 2 481-3411
corres1@jesmedia.com

China
Shenzhen
Annie Liu
ACT International
Tel: 86-755-83211818 [sic: see below]

Shanghai
Linda Li
ACT International
Tel: 86-021-62511200
lindal@actintl.com.hk

Wuhan
Phoebe Yin
ACT International
phoebey@actintl.com.hk

Beijing
Cecily Bian
ACT International
Tel: +86 135 5262 1310
cecilyb@actintl.com.hk

Hong Kong, Taiwan, Singapore
Floyd Chun
ACT International
Tel: +86-13724298335
floydc@actintl.com.hk

Japan
Katsuhiro Ishii
Ace Media Service Inc.
Tel: +81 3 5691 3335
amskatsu@dream.com

Corporate Headquarters: 685 Canton Street, Norwood, MA 02062 • Tel: (781) 769-9750

DC TO 50 GHZ

Hi-Rel Screening

For the Toughest Environments

- 50+ years of design and manufacturing experience
- Supply chain security—no EOL target
- Ceramic, plastic and bare die packaging formats
- Broad selection off-the-shelf + custom designs
- In-house upscreening for MMIC, core and wire, and LTCC components

Capable of meeting MIL requirements for:

Acceleration, fine leak, gross leak, HAST, HTOL, mechanical shock, thermal shock, and vibration. Additional screening available on request.

Mini-Circuits®

FABS and LABS

Quantic PMI Begins New Era Serving Mission-Critical Programs

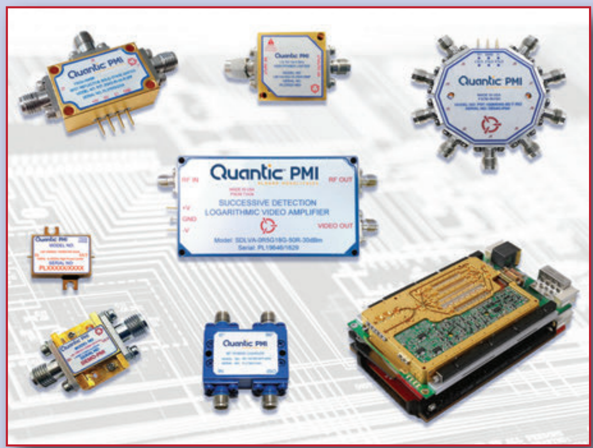

Quantic PMI (Planar Monolithics) is entering a new era of opportunity, combining the technology, products and market respect PMI has built over 33 years with the strategy, investment and culture of Quantic Electronics and its portfolio of companies. Formed in 1989 by Dr. Ashok Gorwara, PMI grew to become the classic RF/microwave business serving the defense market, supplying most any single-function component and multi-function module designed with planar microwave integrated circuits and MMICs. Quantic acquired the business from Gorwara in March 2021, adding PMI to its portfolio of RF/microwave companies (Corry, Croven, MWD (Microwave Dynamics), TRM, Wenzel and X-Microwave).

During its long history, PMI developed an extensive portfolio of solid-state products, creating a catalog of more than 4000 off-the-shelf items available from Quantic PMI or one of its distributors. PMI's core products are logarithmic amplifiers in various configurations, solid-state switches, low noise amplifiers, filters and switch-filter banks, limiters, attenuators and phase shifters, covering applications from DC to 67 GHz. As most of its business supports aerospace and defense, both U.S. and allies, all products are designed and built to perform and survive on mission-critical platforms. The company is certified to ISO9001:2015, ITAR registered and can work on sensitive U.S. Department of Defense contracts.

Quantic PMI has two design and manufacturing locations. Headquartered in Frederick, Maryland, PMI recently consolidated operations into a new 20,000 square foot facility that includes: 4000 square feet dedicated to R&D; a 7500-square-foot class clean room with ESD flooring for hybrid assembly and RF testing; and space for in-house environmental stress screening, a machine shop and painting. Each test bench within the facility has liquid CO_2 for testing over temperature. A secondary component manufacturing facility located in El Dorado Hills, California, has machining, assembly, testing and engineering in a 5100-square-foot facility.

Although Quantic PMI operates as an independent business, being part of Quantic's portfolio brings synergies and additional opportunities to grow. Sales teams across Quantic's companies are collaborating to cross-pollinate their respective customer relationships and offer more products to fill a program's block diagram.

Another benefit of being a Quantic company has been the change in culture, conveyed in Quantic's three maxims: dream big, have fun and get "stuff" done. Quantic encourages an informal, "no ego" environment where team members are empowered and accountable. Although backed by private equity, Quantic is transparent about business goals and results. Every employee is a shareholder and receives financial rewards tied to company performance. This reinforces the emphasis on empowerment and accountability.

With a long list of opportunities in the sales funnel, Quantic PMI is positioned for growth. New programs tap its portfolio of RF/microwave components, whether single-function or integrated into complex subsystems. Other Quantic company products can be added when needed. In addition to its efficient layout, optimized for the manufacturing flow, the new facility in Frederick will support doubling production capacity.

Reflecting the expertise developed over decades, Quantic PMI will continue to build on its strong reputation, whether helping military programs solve product obsolescence challenges or designing products for new markets, like the constellations of satellites flying in low or medium Earth orbit. Indeed, it's a new era for Quantic PMI.

www.quanticpmi.com

HIGH POWER DIRECTIONAL COUPLERS

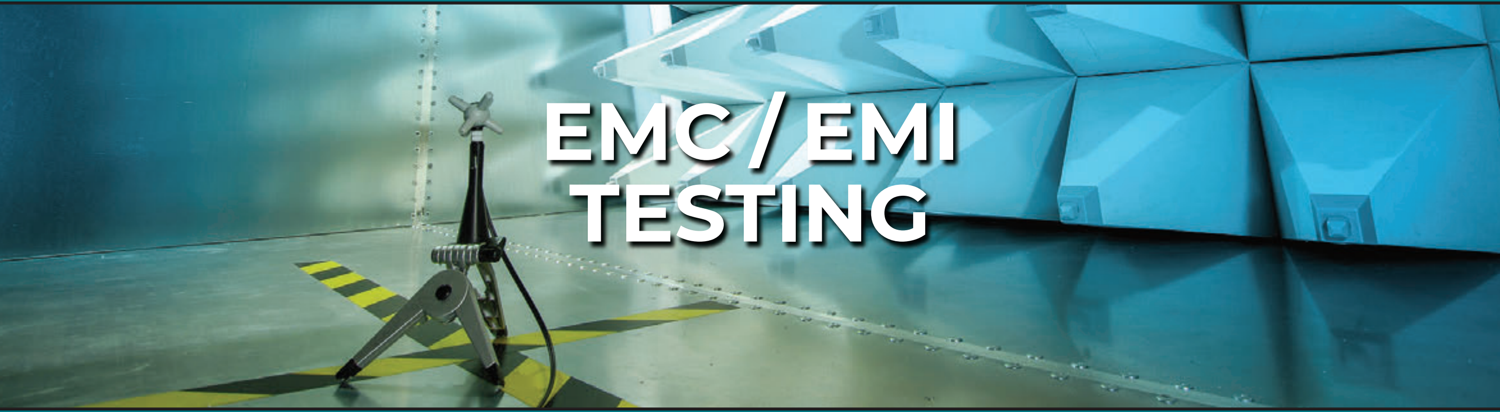

Up to 1000:1 Bandwidth ✦ Low Insertion Loss ✦ *Mismatch Tolerant*® Designs

Model	Type	Frequency (MHz)	Power (W CW)	Coupling (dB)	Insertion Loss (dB)	Connectors	Size (inches)
C8730	Dual	0.009-250	500	40	0.40	N-Female	10.5 x 3.0 x 2.0
C8731	Dual	0.009-250	1000	40	0.40	N-Female	10.5 x 3.0 x 2.0
C11462	Dual	0.009-400	500	40	0.45	N-Female	6.7 x 2.28 x 1.69
C8510	Dual	0.009-1000	500	40	0.45	N-Female	6.7 x 2.28 x 1.69
C5047	Dual	0.01-100	4,000	50	0.15	7/16-Female	10.0 x 4.16 x 3.5
C1979	Dual	0.01-100	10,000	60	0.10	LC-Female	2.0 x 6.0 x 4.5
C5086	Dual	0.01-250	250	40	0.50	N-Female	5.2 x 2.67 x 1.69
C5100	Dual	0.01-250	500	40	0.40	N-Female	10.5 x 3.0 x 2.0
C5960	Dual	0.01-250	1,000	50	0.40	N-Female	10.5 x 3.0 x 2.0
C1460	Dual	0.01-250	2,000	50	0.15	N-Female	10.0 x 3.0 x 2.0
C4080	Dual	0.01-250	3,500	50	0.20	N-Female	10.0 x 4.6 x 3.5
C11026	Dual	0.01-220	5,000	60	0.10	LC-Female	12.0 x 6.0 x 4.5
C8390	Dual	0.01-250	10,000	60	0.10	LC-Female	12.0 x 6.0 x 4.5
C5339	Dual	0.01-400	200	40	0.50	N-Female	5.2 x 2.67 x 1.69
C6047	Dual	0.01-400	500	40	0.50	N-Female	5.2 x 2.67 x 1.69
C2630	Dual	0.01-1000	100	40	0.60	N-Female	5.0 x 2.0 x 1.51
C6021	Dual	0.01-1000	500	40	0.45	N-Female	6.7 x 2.28 x 1.69
C6277	Dual	0.01-1000	500	50	0.45	N-Female	6.7 x 2.28 x 1.69
C11146	Dual	0.01-1000	500	43	0.45	SC-Female	6.7 x 2.63 x 2.20
C11047	Dual	0.01-1000	1,000	43	0.45	SC-Female	6.7 x 2.63 x 2.20
C11161	Dual	0.01-1000	1,000	50	0.45	SC-Female	6.7 x 2.63 x 2.20
C1795	Dual	0.1-1000	100	40	0.50	N-Female	5.0 x 2.0 x 1.51
C5725	Dual	0.1-1000	500	40	0.50	N-Female	5.2 x 2.28 x 1.69
C11077	Dual	0.1-1000	1,000	43	0.45	SC-Female	6.7 x 2.28 x 1.69
C3910	Dual	80-1000	200	40	0.20	N-Female	3.0 x 3.0 x 1.09
C5982	Dual	80-1000	500	40	0.20	N-Female	3.0 x 3.0 x 1.09
C3908	Dual	80-1000	1,500	50	0.10	7/16-Female	3.0 x 3.0 x 1.59
C6796	Dual	80-1000	5,000	60	0.20	1 5/8" EIA	6.0" Line Section
C8060	Bi	200-6000	200	20	0.40	SMA-Female	1.8 x 1.0 x 0.56
C8000	Bi	600-6000	100	30	1.10	SMA-Female	4.8 x 0.88 x 0.50
C10117	Dual	700-6000	250	40	0.20	N-Female	2.0 x 2.0 x 1.06
C10364	Dual	700-6000	500	50	0.20	7/16-Female	2.15 x 2.0 x 1.36
C10996	Dual	700-6000	700	50	0.20	7/16-Female	2.15 x 2.0 x 1.36
C11555	Dual	700-6000	1,000	50	0.20	7/16-Female	2.15 x 2.0 x 1.36
C10695	Dual	700-6500	500	50	0.20	7/16-Female	2.15 x 2.0 x 1.36

Werlatone, Inc. 17 Jon Barrett Road Patterson, NY 12563 845-278-2220 sales@werlatone.com www.werlatone.com